Hg Model Development in CE-QUAL-W2 for the Hells Canyon Complex

Scott Wells, Zhong Zhang, Bernadel Garstecki, Chris Berger, Jesse Naymik

Prepared for Idaho Power

Department of Civil and Environmental Engineering
Portland State University
Portland, OR

January 2025

Contents

List of Figures

List of Tables

Acknowledgements

This project was funded by Idaho Power to address issues with Hg in the Hells Canyon Complex on the Snake River. Our project manager was Jesse Naymik. Dr. Zhong Zhang wrote the first code iteration and provided the basic background and write-up of the equations including the non-equilibrium section which is Appendix B. Dr. Reed Harris provided useful comments and feedback during the preparation of the original equations. Bernadel Garstecki worked on developing the Hg boundary conditions and implementing them in the CE-QUAL-W2 Hg model. Chris Berger ran the model and provided updated model statistics and graphics. Jesse Naymik worked on the Hg boundary conditions using analyses from Austin Baldwin from the USGS.

Introduction

Idaho Power Company is developing strategies for improving water quality in the Hells Canyon Complex (HCC) on the Snake River (see Figure 1). The HCC includes Brownlee, Oxbow, and Hells Canyon Reservoirs. The objective of this study was to develop a computer simulation model of the HCC incorporating Hg dynamics. This modeling tool would then be used to assess strategies for water quality improvement.

FIGURE 1. THE HELLS CANYON COMPLEX ALONG THE SNAKE RIVER INCLUDING BROWNLEE RESERVOIR, OXBOW RESERVOIR, AND HELLS CANYON RESERVOIR ALONG THE IDAHO-OREGON BORDER.

This document describes the Hg model used in the water quality and hydrodynamic model developed for the HCC Snake River system. Wells et al. (2025) documented the eutrophication model for Brownlee, Oxbow, and Hells Canyon Reservoirs, including model set-up and calibration over the period 2014-2018. This hydrodynamic and eutrophication model was a critical component of the Hg model since it relied on many internal processes, such as temperature, dissolved oxygen, organic and inorganic solids, and dissolved organic carbon.

The following topics are discussed in this report:

- The Hg module in CE-QUAL-W2
- Field data used in the HCC as Boundary Conditions to the HCC model
- Implementation of the Hg Module in CE-QUAL-W2
- Summary

Hg Module in CE-QUAL-W2

The model domain is conceptualized as a multi-layer water column underlain by an active sediment layer (Figure 2). The active sediment layer is envisioned as a single well-mixed layer with a fixed thickness of ≈ 2-5 cm. The conceptualization is based on two important features in surface sediments. First, most methylmercury production in surface sediments typically occurs primarily within the top few cm. This is evident in vertical profiles of methylmercury concentrations in surface sediments, which typically peak near or at the surface. As sediments accumulate over time, the vertical profile continues to exhibit higher concentrations near the surface, indicating that the processes governing the location of peak concentrations (methylation and demethylation) operate on a time scale faster than the rate of sedimentation. Averaging methylmercury concentrations over deeper depths would typically underestimate the concentrations near the surface. The second reason for using a surface layer on the order of a few cm thick is that this is a typical depth for surface mixing driven by physical mixing associated with shear stress, bioturbation, and possibly gas formation and ebullition. Thus, the top few cm of the sediment bed is the primary zone interacting with overlying waters and the food web, unless strong erosion occurs. The single well-mixed layer forms the basis for the earliest toxic models like WASP (EPA, 2001). The Dynamic Mercury Cycling Mode (D-MCM), as described in Harris et al. (2020), typically uses a scheme with a well-mixed surface sediment layer and an underlying layer, with a water boundary layer. Hence, this conceptual model is currently not adapted to areas of strong erosion since resuspension is not currently included in the formulation at this time.

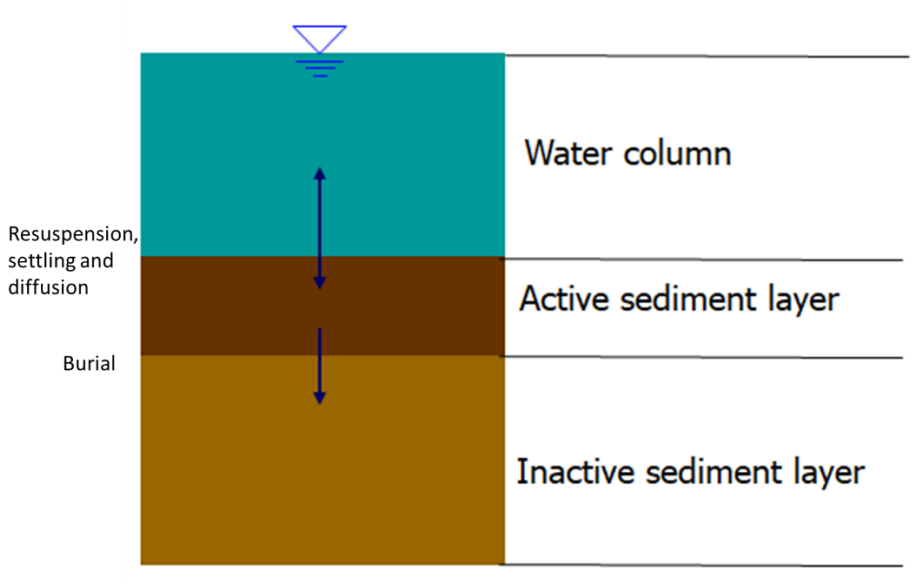

FIGURE 2. CONCEPTUAL MODEL FOR THE WATER COLUMN AND BED SEDIMENT. THE INACTIVE SEDIMENT LAYER IS WHERE BURIAL TAKES PLACE.

Hence, instead of incorporating the Hg model within the sediment diagenesis module of CE-QUAL-W2, the Hg sediment module would exist "alongside" the sediment diagenesis model and use model predictions from the sediment diagenesis model as needed, in a manner maintaining internal consistency between the behavior and properties of the mercury sediment layer and the diagenesis model.

The Hg module simulates elemental mercury, *Hg0*, inorganic mercury, *HgII*, and methylmercury, *MeHg,* in the water column and *HgII* and *MeHg* in the active sediment layer (Figure 3). In the water column, *Hg0* is simulated only in the dissolved phase, while *HgII* and *MeHg* are partitioned among particles and two dissolved components: that portion bound to dissolved organic carbon (DOC) and that considered "freely dissolved", or not bound to DOC. Particle types in the water column competing for HgII and MeHg include refractory and labile organic solids (particulate organic matter, POM), multiple types of inorganic solids (based on particle size), multiple types of algae, and multiple types of zooplankton. Some sediment HgII and MeHg can partition into lower trophic level benthic organisms, but that feature may be added at a later time. This assumes in the interim that mercury allocated to benthic organisms does not have an appreciable effect on concentrations on sediment solids or porewater. Even though HgII and MeHg partitioning can have fast and slow exchanging components, this model is using fast exchange or equilibrium, instantaneous exchange. The slow component, if included would include adsorption and desorption kinetics and would be applied to non-living solids (organic and inorganic) and possibly DOC-bound HgII and MeHg. Besides adding more complexity and model coefficients to the algorithm, using non-equilibrium partitioning would increase the number of state variables in the model. These new state variables would be the

HgII and MeHg sorbed components of all the solid fractions and dissolved fractions. A summary of a similar model is shown in prior work by Zhong and Johnson (2016).

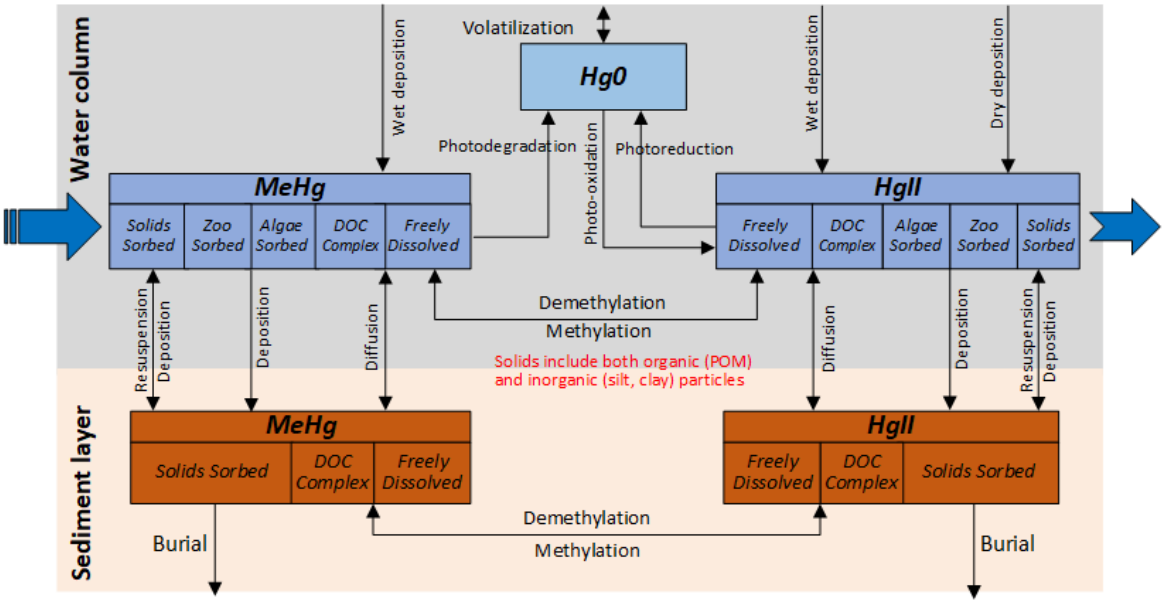

FIGURE 3. CONCEPTUAL MODEL OF HG BIOGEOCHEMICAL PROCESSES. ZOO SORBED IS ZOOPLANKTON SORBED FRACTION. THE SOLIDS SORBED INCLUDE BOTH INORGANIC SUSPENDED SOLIDS GROUPS AND ORGANIC SOLIDS GROUPS.

Water Column Processes

As conceptualized in Figure 3, three Hg species in the water column are modeled in CE-QUAL-W2: *Hg0*, *HgII*, and *MeHg*.

- *[Hg0]*, concentration of dissolved elemental Hg in water (ng L^{-1}) or (µg m^{-3})
- *[HgII]*, concentration of total (unfiltered) inorganic HgII in water (ng L^{-1})
- *[MeHg]*, concentration of total (unfiltered) MeHg in water (ng L^{-1})

The governing equation for all water column constituents is the laterally averaged 3-D advective-diffusion equation:

$$\frac{\partial B\Phi}{\partial t}+\frac{\partial UB\Phi}{\partial x}+\frac{\partial WB\Phi}{\partial z}-\frac{\partial}{\partial x}\left[BD_x\frac{\partial \Phi}{\partial x}\right]-\frac{\partial}{\partial z}\left[BD_z\frac{\partial \Phi}{\partial z}\right]=q_\Phi B+S_\Phi B$$

where:

Φ = laterally averaged Hg constituent concentration, µg m^{-3}

D_x = longitudinal temperature and constituent dispersion coefficient, m^2 sec^{-1}

D_z = vertical temperature and constituent dispersion coefficient, m^2 sec^{-1}

q_Φ = lateral inflow or outflow mass flow rate of constituent per unit volume, µg m^{-3} sec^{-1}

S_Φ = laterally averaged source/sink term, µg m^{-3} sec^{-1}.

The CE-QUAL-W2 User Manual (Wells, 2024) describes how the velocity field and dispersion coefficients are computed and solved numerically.

The concentrations of Hg species in the model are expressed in terms of nanograms per volumetric units of liter (ng L^{-1}). Dissolved *HgII* and *MeHg* are each grouped into two components, those bound to DOC and those freely dissolved. In addition, *HgII* and *MeHg* are found in multiple solids types: refractory particulate organic matter (RPOM), labile particulate matter (LPOM), inorganic suspended solids groups, algae groups, and zooplankton groups. The model also computes distributed concentrations of total (unfiltered) HgII and MeHg in the water column as derived variables in the CE-QUAL-W2. In the current model application, we have assumed only two inorganic suspended solids groups: fine and coarse, but the current model framework is not limited to only two components.

The *HgII* and *MeHg* components computed in the water column include:

- $HgII_d$, concentration of freely dissolved HgII in water(ng L^{-1})
- $HgII_{doc}$, concentration of DOC complexed HgII in water (ng L^{-1})
- $HgII_{totdiss}$, total dissolved HgII concentration (DOC-bound plus other) (ng L^{-1})
- $HgII_{apt}$, total concentration of algae (phytoplankton) adsorbed HgII in water (ng L^{-1})
- $HgII_{Lpom}$, concentration of labile organic solid adsorbed HgII in water (ng L^{-1})
- $HgII_{Rpom}$, concentration of refractory organic solid adsorbed HgII in water (ng L^{-1})
- $HgII_{pt}$, total concentration of TSS (inorganic and organic solids) adsorbed HgII in water (ng L^{-1})
- $HgII_{pts}$, total concentration of TSS (inorganic and organic solids) adsorbed HgII in water (ng g^{-1})
- $MeHg_d$, concentration of dissolved MeHg in water (ng L^{-1})
- $MeHg_{doc}$, concentration of DOC complexed MeHg in water (ng L^{-1})
- $MeHg_{apt}$, total concentration of algae (phytoplankton) adsorbed MeHg in water (ng L^{-1})
- $MeHg_{pom}$, concentration of organic solid adsorbed MeHg in water (ng L^{-1})
- $MeHg_{pt}$, total concentration of TSS (inorganic and organic solids) adsorbed MeHg in water (ng L^{-1})
- $MeHg_{pts}$, total concentration of TSS (inorganic and organic solids) adsorbed MeHg in water (ng g^{-1})

The Hg module simulates the following transformation processes among three Hg species in the water column:

- Photo-degradation: MeHg → Hg0
- Photo-Reduction: HgII → Hg0
- Photo-Oxidation: Hg0 → HgII

- Biological methylation: HgII → MeHg
- Biological demethylation: MeHg → HgII

Additionally, the model accounts for atmospheric boundary fluxes of HgII and MeHg. These fluxes could include the following processes, even though they are lumped together in the model:

- Wet deposition of MeHg
- Wet deposition of HgII
- Dry deposition of HgII
- Reactive gaseous mercury (RGM) deposition of HgII

Equilibrium Partitioning and Distribution of HgII and MeHg in the Water Column

HgII and *MeHg* may be partitioned between the freely dissolved phase and DOC, and the solid adsorbed phases. Solids can be assigned to mineral abiotic solids, detrital (particulate organic matter), or various classes or size categories of solids. Under an equilibrium partitioning, all *HgII* and *MeHg* are assumed to be instantly exchangeable between the freely dissolved, DOC complexed, algae (1 to NAL, where NAL is the number of algal groups), organic solids (two groups), and inorganic solids (1 to NSS, where NSS is the number of inorganic suspended solids groups) adsorbed phases. The linear partitioning fractions of *HgII and MeHg* in the water column are computed as:

$$f_d = \frac{10^6}{R} \quad (1a)$$

$$f_{doc} = \frac{K_{doc}[DOC]}{R} \quad (1b)$$

$$f_{apn} = \frac{K_{apn}[A_{pn}]}{R} \quad (1c)$$

$$f_{pom} = \frac{K_{pom}[POM]}{R} \quad (1d)$$

$$f_{pn} = \frac{K_{pn}[ISS_n]}{R} \quad (1e)$$

$$f_{zpn} = \frac{K_{zpn}[Zoo_{pn}]}{R} \quad (1f)$$

$$R = 10^6 + K_{doc}[DOC] + K_{pom}[POM] + \sum_{n=1}^{NAL} K_{apn}[A_{pn}] + \sum_{n=1}^{N} K_{pn}[ISS_n]] + \sum_{n=1}^{NZOO} K_{zpn}[ZOO_{pn}] \quad (1g)$$

and

$$f_d + f_{doc} + f_{pom} + \sum_{n=1}^{NAL} f_{apn} + \sum_{n=1}^{NSS} f_{pn} + \sum_{n=1}^{NZOO} f_{zpn} = 1 \quad (1h)$$

where subscript i represents either *HgII* or *MeHg* in the water column.

f_d = fraction of freely dissolved HgII or MeHg in water

f_{doc} = fraction of DOC complexed HgII or MeHg in water

f_{pom} = fraction of organic solids adsorbed HgII or MeHg in water

f_{apn} = fraction of algae (phytoplankton) group n adsorbed HgII or MeHg in water

f_{zpn} = fraction of zooplankton group n adsorbed HgII or MeHg in water

f_{pn} = fraction of inorganic solid group n adsorbed HgII or MeHg in water

K_{doc} = HgII or MeHg equilibrium partition coefficient for DOC in water (L kg^{-1})

K_{pom} = HgII or MeHg equilibrium partition coefficient for POM in water (L kg^{-1})

K_{apn} = HgII or MeHg equilibrium partition coefficient for algae (phytoplankton) group n in water (L kg^{-1})

K_{zpn} = HgII or MeHg equilibrium partition coefficient for zooplankton group n in water (L kg^{-1})

K_{pn} = HgII or MeHg equilibrium partition coefficient for solid group *n* in water (L kg^{-1})

DOC = concentration of dissolved organic carbon in water (mg L^{-1})

A_{pn} = concentration of algae (phytoplankton) group *n* in water (mg L^{-1})

ZOO_{pn} = concentration of zooplankton group *n* in water (mg L^{-1})

POM = concentration of particulate organic matter, including labile and refractory fractions (mg L^{-1})

ISS_n = concentration of inorganic solid group *n* in water (mg L^{-1})

NSS = total number of inorganic solid groups in water (mg L^{-1})

NAL = total number of algae (phytoplankton) groups in water (mg L^{-1})

NZOO = total number of zooplankton groups in water (mg L^{-1})

Distributed concentrations of *HgII* and *MeHg* for individual phases can be directly calculated from their partitioning fractions and total concentrations in water:

$$HgII_d = f_{d\text{-}HgII}[HgII] \quad (2a)$$

$$HgII_{doc} = f_{doc\text{-}HgII}[HgII] \quad (2b)$$

$$HgII_{apt} = \sum_{n=1}^{NAL} f_{apn\text{-}HgII}[HgII] \quad (2c)$$

$$HgII_{apts} = 10^3 \frac{\sum_{n=1}^{NAL} f_{apn\text{-}HgII}[HgII]}{\sum_{n=1}^{NAL} A_{pn}} \quad (2c)$$

$$HgII_{pom} = f_{pom\text{-}HgII}[HgII] \quad (2d)$$

$$HgII_{pt} = \sum_{n=1}^{NSS} f_{pn\text{-}HgII}[HgII] \quad (2e)$$

$$HgII_{pts} = 10^3 \frac{\sum_{n=1}^{NSS} f_{pn\text{-}HgII}[HgII]}{\sum_{n=1}^{NSS} ISS_n} \quad (2f)$$

$$HgII_{zoopt} = \sum_{n=1}^{NZOO} f_{zpn\text{-}HgII}[HgII] \quad (2g)$$

$$HgII_{zoopts} = 10^3 \frac{\sum_{n=1}^{NZOO} f_{zpn\text{-}HgII}[HgII]}{\sum_{n=1}^{NZOO} ZOO_{pn}} \quad (2h)$$

and

$$MeHg_{d} = f_{d\text{-}MeHg}[MeHg] \quad (3a)$$

$$MeHg_{pom} = f_{pom\text{-}MeHg}[MeHg] \quad (3b)$$

$$MeHg_{apt} = \sum_{n=1}^{NAL} f_{apn\text{-}MeHg}[MeHg] \quad (3c)$$

$$MeHg_{apts} = 10^3 \frac{\sum_{n=1}^{NAL} f_{apn\text{-}MeHg}[MeHg]}{\sum_{n=1}^{NAL} A_{pn}} \quad (3c)$$

$$MeHg_{doc} = f_{doc\text{-}MeHg}[MeHg] \quad (3d)$$

$$MeHg_{pt} = \sum_{n=1}^{NSS} f_{pn\text{-}MeHg}[MeHg] \quad (3e)$$

$$MeHg_{pts} = 10^3 \frac{\sum_{n=1}^{NSS} f_{pn\text{-}MeHg}[MeHg]}{\sum_{n=1}^{NSS} ISS_n} \quad (3f)$$

$$MeHg_{zoopt} = \sum_{n=1}^{NZOO} f_{zpn\text{-}MeHg}[MeHg] \quad (3g)$$

$$MeHg_{zoopts} = 10^3 \frac{\sum_{n=1}^{NZOO} f_{zpn\text{-}MeHg}[MeHg]}{\sum_{n=1}^{NZOO} ZOO_{pn}} \quad (3h)$$

where

$HgII_d$ = concentration of freely dissolved HgII in water (ng L^{-1})

$HgII_{doc}$ = concentration of DOC complexed HgII in water (ng L^{-1})

$HgII_{pom}$ = concentration of organic solid adsorbed HgII in water (ng L^{-1})

$HgII_{apt}$ = total concentration of algae (phytoplankton) adsorbed HgII in water (ng L^{-1})

$HgII_{zpt}$ = total concentration of zooplankton adsorbed HgII in water (ng L^{-1})

$HgII_{apts}$ = total concentration of algae (phytoplankton) adsorbed HgII in water (ng g^{-1})

$HgII_{zoopts}$ = total concentration of zooplankton adsorbed HgII in water (ng g^{-1})

$HgII_{pt}$ = total concentration of inorganic solids adsorbed HgII in water (ng L^{-1})

$HgII_{pts}$ = total concentration of inorganic solids adsorbed HgII in water (ng g^{-1})

$MeHg_d$ = concentration of dissolved MeHg in water (ng L^{-1})

$MeHg_{doc}$ = concentration of DOC complexed MeHg in water (ng L^{-1})

$MeHg_{pom}$ = concentration of organic solid adsorbed MeHg in water (ng L^{-1})

$MeHg_{apt}$ = total concentration of algae (phytoplankton) adsorbed MeHg in water (ng L^{-1})

$MeHg_{apts}$ = total concentration of algae (phytoplankton) adsorbed MeHg in water (ng g^{-1})

$MeHg_{pt}$ = total concentration of inorganic solids adsorbed MeHg in water (ng L^{-1})

$MeHg_{pts}$ = total concentration of inorganic solids adsorbed MeHg in water (ng g^{-1})

$MeHg_{zpt}$ = total concentration of zooplankton adsorbed MeHg in water (ng L^{-1})

$MeHg_{zpts}$ = total concentration of zooplankton adsorbed MeHg in water (ng g^{-1})

Water Column Internal Source/Sink Rate Equations for Hg0, HgII, MeHg

Components of the mass balance of Hg species (*Hg0*, *HgII* and *MeHg*) for a control volume compartment include: first, changes by physical transport; second, changes by forcing functions to or from the compartment; and third, changes by physical, chemical and biological

(or biochemical) processes occurring within the compartment. Physical, chemical and biological (or biogeochemical) processes occurring within the compartment are lumped into internal source and sink kinetic rates and described below.

Elemental Hg (Hg0):

The following four processes are simulated for *Hg0*:

- *Hg0 photo*-oxidation
- *HgII photo*-reduction
- *MeHg photo*-degradation
- *Hg0* volatilization

Transformations of *HgII* and *MeHg* act on all dissolved HgII and MeHg (DOC-bound and freely dissolved). The internal source and sink rate equation for the concentration of *Hg0* in the water column is stated as

$$\frac{d[Hg0]}{dt} = -\underbrace{Hg0 \rightarrow HgII}_{\text{photo-oxidation}} + \underbrace{HgII \rightarrow Hg0}_{\text{photoreduction}} + \underbrace{MeHg \rightarrow Hg0}_{\text{photodegradation}} + \underbrace{\frac{dHg0}{dt}}_{evasion} \qquad (4)$$

Advective and dispersive fluxes within the water column are included as part of the CE-QUAL-W2 hydrodynamic modeling framework.

1) Photoreduction (HgII → Hg0)

The photoreduction rate from *HgII* to *Hg0* is computed as:

$$\underbrace{HgII \rightarrow Hg0}_{\text{photoreduction}} = K_{reductionPAR}\, \bar{I}_{PAR}\left(f_{d\text{-}HgII} + f_{doc\text{-}HgII}\right)[HgII] \qquad (5)$$

where

I_{PAR} = PAR light intensity in the model layer (W/m^2)

$K_{reductionPAR}$ = photoreduction constant for PAR ($\frac{m^2}{\mathrm{Wd}}$) converted to m^2 $W^{-1}s^{-1}$ internally in the model

The light in the layer (K) and segment (I) is computed from the following for each layer:

$$\bar{I}_{PAR} = I_{in} - I_{out}$$

where

$$I_{in} = I(z_1) = (1-\beta)\varphi_{sn} e^{-\eta z_1}$$

$$I_{out} = I(z_2) = (1-\beta)\varphi_{sn} e^{-\eta z_2}$$

β: fraction of short-wave solar absorbed on surface (0.45 typical value) which is about the PAR fraction of the solar radiation

φ_{sn}: net short wave solar at water surface including effect of shading and reflection and clouds (W/m^2)

η: light extinction coefficient (1/m)

z_1: Depth from surface of top of layer K (m)

z_2: depth from surface to bottom of layer K (m)

2) Photo-oxidation (Hg0 → HgII)

Calculate a target DGM (dissolved gaseous Hg) ratio based on DOC and pH:

$$DGM_{ratio\_target} = k\_oxid\_1\ DOC^{\,k\_oxid\_2}\ pH^{\,k\_oxid\_3}$$

Calculate the current DGM ratio in the simulation:

$$DGM_{ratio} = \frac{[Hg0]}{(f_{d\text{-}HgII} + f_{doc\text{-}HgII})[HgII]}$$

The photo-oxidation rate from *Hg0* to *HgII* is computed as a function of the reduction rate:

$$k_{oxid\_red} = \frac{DGM_{ratio}}{DGM_{ratio\_target}}$$

$$\underbrace{Hg0 \rightarrow HgII}_{\text{photo-oxidation}} = k_{oxid\_red} * \underbrace{HgII \rightarrow Hg0}_{\text{photoreduction}}, \qquad DGM_{ratio} > DGM_{ratio\_target}$$

$$\underbrace{Hg0 \rightarrow HgII}_{\text{photo-oxidation}} = 0, \qquad DGM_{ratio} \leq DGM_{ratio\_target}$$

Alternatively, oxidation could scale with the DGM ratio rather than shut off when the DGM ratio is below the target:

Use the k_{oxid_red} ratio where the target DGM_{ratio} exceeds the simulated DGM_{ratio}:

$$\underbrace{Hg0 \rightarrow HgII}_{\text{photo-oxidation}} = k_{oxid\_red} * \underbrace{HgII \rightarrow Hg0}_{\text{photoreduction}}, \qquad DGM_{ratio} \leq DGM_{ratio\_target} \quad (6)$$

3) Photodegradation (MeHg → Hg0)

The degradation rate from *MeHg* into *Hg0* is computed as:

$$\underbrace{MeHg \rightarrow Hg0}_{\text{photodegradation}} = K_{photoDegPAR}\ \bar{I}_{PAR}\ (f_{d\text{-}MeHg} + f_{doc\text{-}MeHg})[MeHg] \qquad (7)$$

where

$K_{photoDegPAR}$ = MeHg photodegedation rate constant for PAR ($m^2/(Wd)$) converted to $m^2\ W^{-1}s^{-1}$ internally in the model

4) Volatilization of Hg0

The volatilization rate of *Hg0* across the air-water interface is computed as (Mills et al., 1982):

$$Hg0_{volatilization} rate = \underbrace{\frac{dHg0}{dt}}_{evasion} = k_{Hg0} \frac{\left([Hg0] - \frac{[Hg0]_{atm}}{H_{Hg0}}\right)}{h_{cell}} \quad (8)$$

where $k_{Hg0} = \frac{1.0}{\frac{1.0}{k_{Hg0\_wat}} + \frac{1.0}{k_{Hg0\_air}\, H_{Hg0}}}$

$$k_{Hg0\_wat} = 0.632 k_a$$

$$k_{Hg0\_air} = 91.949 u_w$$

The Hg0 volatilization rate is based on the 2-resistance model of gas transfer where both the liquid and gas layer control the overall transfer rate.

H_{Hg0} is a function of water temperature calculated using the equation of Sanemasa (1975).

$$H_{Hg0}(T) = 10^{\frac{-1078}{T_{wk}} - log(T_{wk}) + 5.592} \quad (9)$$

where

DGM_{ratio_target} = calculated target ratio for $\left(\frac{[\mathrm{Hg0}]}{[\mathrm{HgII}]_{\mathrm{dissolved}}}\right)$ $(dimensionless)$

h_{cell} = surface layer depth or thickness (m)

$[Hg0]_{atm}$ = atmospheric concentration of Hg0 $(\mu g/m^3)$

H_{Hg0} = Henry's law constant for Hg0 (dimensionless)

$K_{\_oxid\_1}$ = Constant in eqn to assign target DGMratio

$K_{\_oxid\_2}$ = Constant in eqn to assign target DGMratio $(dimensionless)$

$K_{\_oxid\_3}$ = Constant in eqn to assign target DGMratio $(dimensionless)$

k_a = oxygen reaeration rate (m d^{-1}) computed from CE-QUAL-W2 model

k_{Hg0} = *overall Hg0* gas transfer rate (m d^{-1})

k_{Hg0_water} = *liquid film Hg0* gas transfer rate (m d^{-1})

k_{Hg0_air} = *gas film Hg0* gas transfer rate (m d^{-1})

u_w = wind speed (m s^{-1})

T_{wk} = water temperature in °K

Inorganic Hg (HgII)

The following six processes are simulated for the water column *HgII*:

- *Hg0 photo*-oxidation
- Biological demethylation
- Photo-reduction
- Methylation
- Settling of sorbed fractions
- Diffusion across the sediment-water interface

Partitioning of HgII and MeHg onto solids in the water column will result in associated settling fluxes as solids settle. Dissolved phases of HgII and MeHg on the streambed also exchange across the sediment-water interface through diffusion process. The internal source and sink rate equation for the total concentration of *HgII* in the water column is stated as

$$\frac{d[HgII]}{dt} = -\underbrace{HgII \rightarrow Hg0}_{\text{photoreduction}} + \underbrace{Hg0 \rightarrow HgII}_{\text{photo-oxidation}} - \underbrace{HgII \rightarrow MeHg}_{\text{methylation}} + \underbrace{MeHg \rightarrow HgII}_{\text{demethyation}} - \underbrace{HgII \rightarrow Bed}_{settling} + \underbrace{HgII \leftrightarrow Bed}_{\text{diffusion}} + S_{atm\_dep\_HgII} \quad (10)$$

Where $S_{atm\_dep\_HgII}$ is the atmospheric deposition source term for the surface layer only. Advective and dispersive fluxes in x and z within the water column are part of the CE-QUAL-W2 hydrodynamic modeling framework. Photo-oxidation is described in the section on elemental Hg (Hg0).

1) Methylation (HgII → MeHg)

There are 2 options to compute methylation: one based on carbon turnover rate and another decoupled from carbon turnover.

<u>Carbon Turnover Rate Method</u>

The methylation rate from *HgII* to *MeHg* is computed from the concentration of dissolved and DOC complexed phases of HgII in the water column.

$$\underbrace{HgII \rightarrow MeHg}_{\text{methylation}} = \left(K_{meth-wat} f_{d-HgII} + K_{meth-doc} f_{doc-HgII}\right)[JOC][HgII] \quad (11)$$

where JOC is the anoxic fraction of the total C turnover rate in units of g C/m^3/s. In the Ce-QUAL-W2 model this is computed from the following equation:

$$JOC = (LPOMCD + LRPOMCD + RPOMCD + LDOMCD + LRDOMCD + RDOMCD)\ ANOX\ \frac{KDO}{KDO+O2}$$

where

$LPOMCD = \mu_{LPOM} C_{LPOMC}$ rate of decay of LPOM C in g C/m^3/s

$LRPOMCD = \mu_{LRPOM} C_{LPOMC}$ rate of decay of labile to refractory POM C in g C/m^3/s

$RPOMCD = \mu_{RPOM} C_{RPOMC}$ rate of decay of RPOM C in g C/m^3/s

$LDOMCD = \mu_{LDOM} C_{LDOMC}$ rate of decay of LDOM C in g C/m^3/s

$RDOMCD = \mu_{RDOM} C_{RDOMC}$ rate of decay of RDOM C in g C/m^3/s

$LRDOMCD = \mu_{LRDOM} C_{LDOMC}$ rate of decay of labile to refractory DOM C in g C/m^3/s

μ_{LPOM}: decay rate for LPOM, corrected for temperature in s^{-1}

μ_{LRPOM}: decay rate for LPOM to RPOM, corrected for temperature in s^{-1}

μ_{RPOM}: decay rate for RPOM, corrected for temperature in s^{-1}

μ_{LDOM}: decay rate for LDOM, corrected for temperature in s^{-1}

μ_{RDOM}: decay rate for RDOM, corrected for temperature in s^{-1}

μ_{LRDOM}: decay rate for LDOM to RDOM, corrected for temperature in s^{-1}

C_{RPOMC} : concentration of refractory particulate organic matter C in g/m^3

C_{LPOMC} : concentration of labile particulate organic matter C in g/m^3

C_{RDOMC} : concentration of refractory dissolved organic matter C in g/m^3

C_{LDOMC} : concentration of labile dissolved organic matter C in g/m^3

ANOX: fraction of anoxic to oxic carbon (or organic matter) decomposition between 0 and 1

KDO: dissolved oxygen concentration half-saturation limit in g/m^3

O2: concentration of dissolved oxygen in g/m^3

$K_{meth-wat}$ = methylation rate constant for HgII dissolved $\left(\frac{m^3}{g\ C}\right)$

$K_{meth-doc}$ = methylation rate constant for HgII bound to DOC $\left(\frac{m^3}{g\ C}\right)$

Note that ANOX multiplied by the oxic organic matter decay rates is the anoxic portion of the organic matter decay. Usually, ANOX is much less than 1. The term $\frac{KDO}{KDO+O2}$ provides a smooth transition from oxic to anoxic conditions and is equal to 1 when there is no dissolved oxygen. KDO is the DO concentration when anoxic metabolism is 50% of its maximum (maximum is when DO=0 mg/l).

Methylation Not Based on Carbon Turnover

Another option in the CE-QUAL-W2 model is to compute methylation and demethylation as only dependent on degree of anoxia and a rate constant that is a function of temperature. In this case methylation can be computed as

$$\underbrace{HgII \rightarrow MeHg}_{\text{methylation}} = \left(K_{meth-wat} f_{d\text{-}HgII} + K_{meth-doc} f_{doc\text{-}HgII}\right) \frac{KDO}{KDO+O2} [HgII] \quad (12)$$

where

$K_{meth-wat}$ = methylation rate constant for HgII dissolved $\left(\frac{1}{s}\right)$ adjusted by temperature.

$K_{meth-doc}$ = methylation rate constant for HgII bound to DOC $\left(\frac{1}{s}\right)$ adjusted by temperature.

Earlier the temperature dependence was based on carbon turnover rate dependencies, but in this approach the model user must specify the temperature dependence for the rate constants. An Arrhenius formulation is used to be compatible with earlier Hg studies. Hence, for demethylation the formula for adjusting temperature of the coefficient is

$k_T = k_{20}\theta^{T-20}$ where k_T is the kinetic coefficient adjusted to a temperature T, k_{20} is the coefficient at 20°C, and theta is an empirical parameter. In the model the value of Q10 is specified, which is $Q10 = \theta^{20-10}$ which allows the computation of theta as $\theta = Q10^{1/(20-10)}$.

2) Demethylation (MeHg → HgII)

Carbon turnover method

The demethylation rate from *MeHg* to *HgII* is computed from the concentration of dissolved and DOC complexed phases of MeHg in the water column.

$$\underbrace{MeHg \rightarrow HgII}_{\text{demethylation}} = \left(K_{demeth-wat} f_{d\text{-}MeHg} + K_{demeth-doc} f_{doc\text{-}MeHg}\right)[JOC][MeHg] \quad (13)$$

where

$K_{demeth-wat}$ = demethylation rate constant for dissolved MeHg $\left(\frac{m^3}{g\ C}\right)$

$K_{demeth-doc}$ = demethylation rate constant for MeHg bound to DOC $\left(\frac{m^3}{g\ C}\right)$

Demethylation Not Based on Carbon Turnover

Another option in CE-QUAL-W2 is to compute demethylation as a function of the degree of anoxia and demethylatyion rates adjusted by temperature such as

$$\underbrace{MeHg \rightarrow HgII}_{\text{demethylation}} = \left(K_{demeth-wat} f_{d\text{-}MeHg} + K_{demeth-doc} f_{doc\text{-}MeHg}\right) \frac{KDO}{KDO+O2} [MeHg] \qquad (14)$$

where

$K_{demeth-wat}$ = demethylation rate constant for dissolved MeHg $\left(\frac{1}{s}\right)$ adjusted by temperature

$K_{demeth-doc}$ = demethylation rate constant for MeHg bound to DOC $\left(\frac{1}{s}\right)$ adjusted by temperature

The temperature adjustment is similar to the methylation temperature rate adjustment when it is not based on C turnover.

3) Diffusion across the sediment-water interface

Dissolved Hg species in the bed sediment can transfer across the sediment-water interface, or vice versa. The total porewater concentration of HgII is the sum of the freely-dissolved and DOC-complexed HgII. Therefore, the diffusion mass transfer of HgII across the sediment-water interface is computed as:

$$\underbrace{HgII \leftrightarrow Bed}_{\text{diffusion}} = \frac{v_m}{h}\left[\left(f_{d-HgII2} + f_{doc-HgII2}\right)\frac{HgII_2}{\varphi} - \left(f_{d-HgII} + f_{doc-HgII}\right) HgII\right] \qquad (15)$$

where

v_m : sediment-water transfer coefficient (velocity) (m s^{-1}).

h : layer thickness.

The mass transfer velocity (v_m) of *HgII* and *MeHg* across the sediment-water interface can be either a user specified parameter (constant over time and space) or determined from the sediment diagenesis model which computes the diffusion velocity from the water to the aerobic layer and from the aerobic to the anaerobic layer. To compute an average velocity from the bed to the water column, an overall velocity based on resistance model in series to compute the average velocity. The model user can scale that velocity for use in the Hg model. From the sediment diagenesis model, we use the sediment transfer velocity from the aerobic layer to the water, the porewater diffusion velocity (from anaerobic layer to aerobic layer) and the particle mixing velocity (accounting for bioturbation) to compute an average sediment-water transfer velocity.

Hence, v_m is computed from the following equation:

$$\frac{1}{v_m} = \frac{1}{v_{KL12} + v_{W12}} + \frac{1}{v_S}$$

- Where v_m is the Hg transfer velocity in m/d, v_{KL12} is the porewater diffusion velocity between layer 1 and 2 in m/d, v_{W12} is the particle mixing velocity between layer 1 and 2 in m/d, and v_S is the transfer velocity between the water and layer 1 as shown in Figure 4.

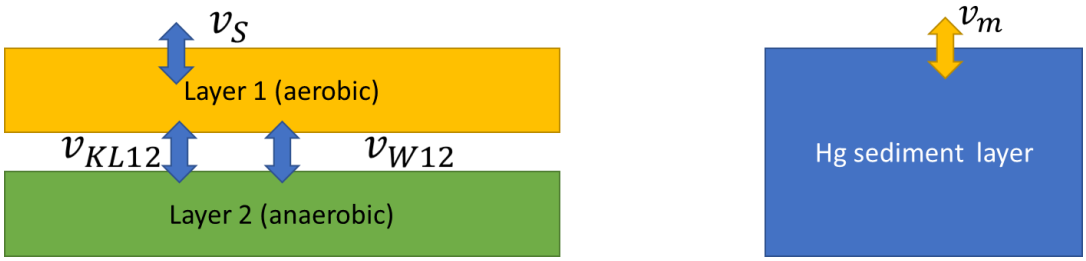

FIGURE 4. COMPARISON OF DIFFUSION VELOCITIES IN THE SEDIMENT DIAGENESIS MODEL AND THAT IN THE HG SEDIMENT MODEL.

As an example of the transfer velocities computed by the CE-QUAL-W2 model, Figure 5 shows the sediment diagenesis components for one segment in Brownlee reservoir showing the rate limiting flux is the transfer from the anaerobic to the aerobic layer (KL12).

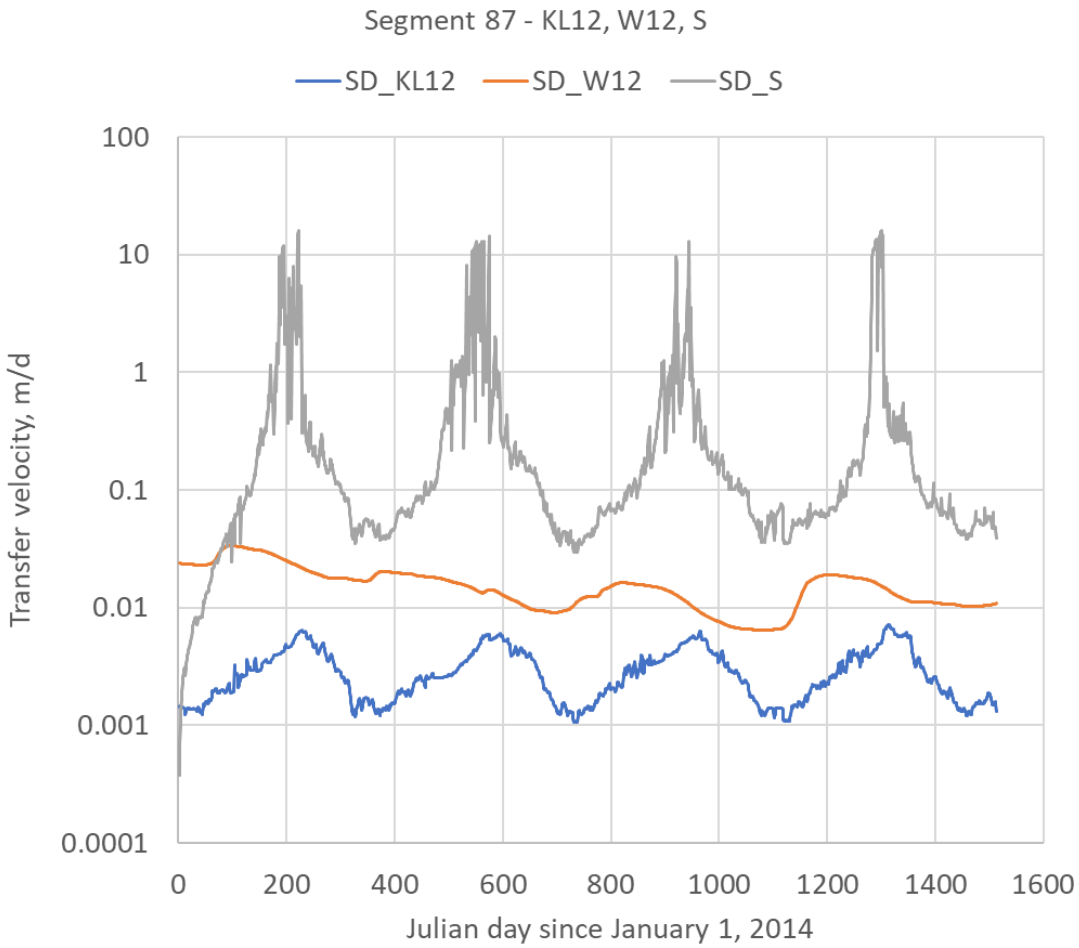

FIGURE 5. VARIATION OF SEDIMENT DIAGENESIS TRANSFER VELOCITIES AT A MODEL SEGMENT IN BROWNLEE RESERVOIR, ID/OR FOR THE BOTTOM LAYER.

Using these velocities from Figure 5, the Hg transfer velocity assuming 100% of the sediment diagenesis transfer velocity is shown for a couple model segments bottom layers in Brownlee Reservoir over a 4-year period in Figure 6.

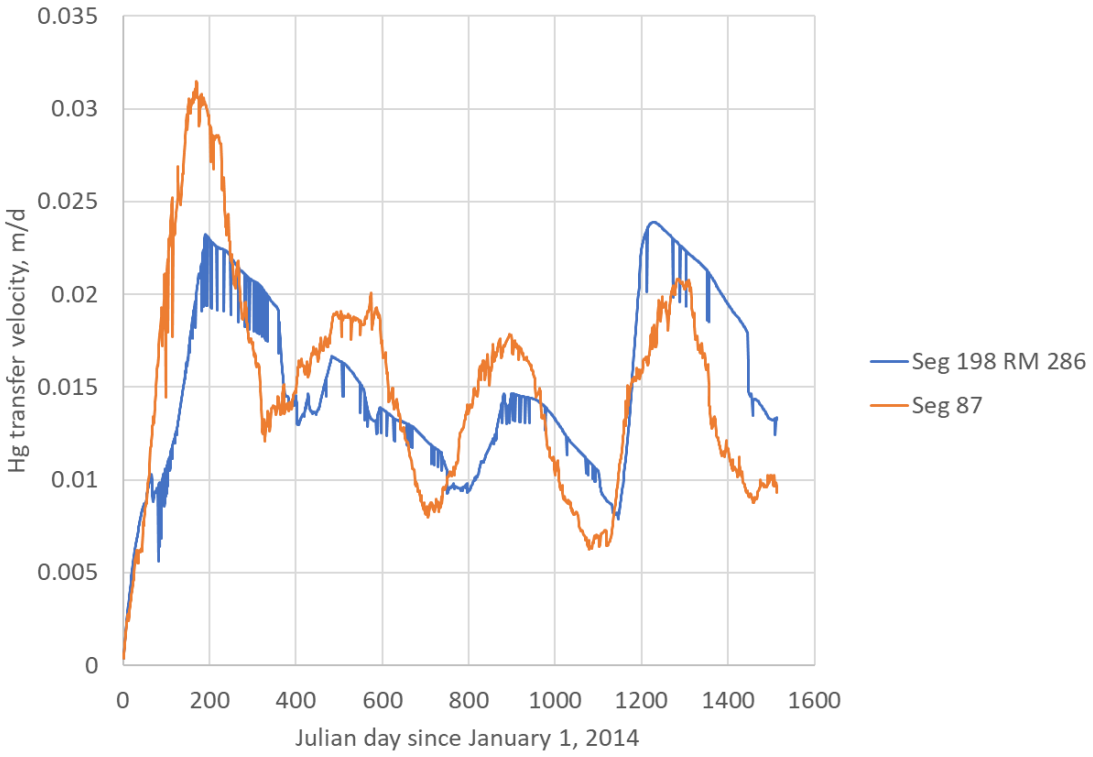

FIGURE 6. VARIATION OF HG SEDIMENT TRANSFER VELOCITIES AT A COUPLE SEGMENTS AT THE BOTTOM LAYERS OVER MULTIPLE YEARS SHOWING VARIATION IN TEMPERATURE AND SEDIMENT CONDITIONS.

4) Settling

Settling of algae, zooplankton, organic and inorganic suspended solids removes adsorbed Hg species in proportion to their bulk concentrations. The settling term of sorbed Hg for the surface layer (kt) is computed as

$$\underbrace{HgII \rightarrow Bed}_{settling} = -\frac{\left(v_{pom} f_{pom\text{-}Hg} + \sum_{n=1}^{NAL} v_{apn} f_{apn\text{-}Hg} + \sum_{n=1}^{NZOO} v_{zoopn} f_{zpn\text{-}Hg} + \sum_{n=1}^{NSS} v_{spn} f_{pn\text{-}Hg}\right) HgII(kt)}{h(kt)} \quad (16a)$$

Where h(kt) is the surface layer thickness (m), and (kt) is the array element at the surface.

The settling term of sorbed HgII for remaining layers below the surface layer for each layer k is shown in Figure 7 and is computed as

$$\underbrace{HgII \rightarrow Bed}_{settling} = \frac{\left(v_{pom} f_{pom\text{-}Hg} + \sum_{n=1}^{NAL} v_{apn} f_{apn\text{-}Hg} + \sum_{n=1}^{NZOO} v_{zoopn} f_{zpn\text{-}Hg} + \sum_{n=1}^{NSS} v_{spn} f_{pn\text{-}Hg}\right) (HgII(k-1) - HgII(k))}{h(k)} \quad (16b)$$

where

v_{pom} = settling velocity of POM (m d^{-1})
v_{apn} = settling velocity of algae group n (m d^{-1})
v_{zpn} = settling velocity of zooplankton group n (m d^{-1})
v_{spn} = settling velocity of inorganic solid group n (m d^{-1}).

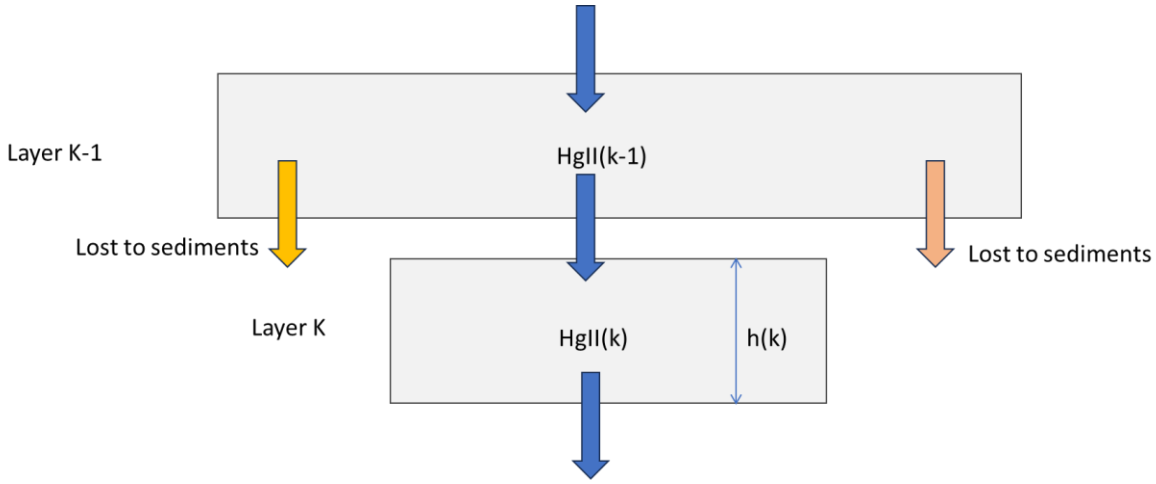

FIGURE 7. SCHEMATIC OF HGII SETTLING IN WATER COLUMN.

Methylmercury (MeHg):

The following six processes are simulated for the water column *MeHg*:

- Methylation
- Photodegradation
- Volatilization
- Biological Demethylation
- Settling of sorbed fractions
- Diffusion across the sediment-water interface

The internal source and sink rate equation for the total concentration of *MeHg* in the water column is stated as

$$\frac{d[MeHg]}{dt} = -\underbrace{MeHg \rightarrow Hg0}_{\text{photodegradation}} - \underbrace{MeHg \rightarrow HgII}_{\text{demethyation}} + \underbrace{HgII \rightarrow MeHg}_{\text{methylation}} - \underbrace{MeHg \rightarrow Bed}_{settling} + \underbrace{MeHg \leftrightarrow Bed}_{\text{diffusion}} + S_{atm\_dep\_MeHg} \quad (17)$$

where $S_{atm\_dep\_MeHg}$ is the atmospheric deposition source term for the surface layer only. Advective and dispersive fluxes in x and z within the water column are part of the CE-QUAL-W2 hydrodynamic modeling framework. Photodegradation is described in the section on

elemental Hg. Methylation and demethylation are described in the section on inorganic Hg (HgII).

1) Diffusion across the sediment-water interface

Sediment-water flux of *MeHg* is computed as:

$$\underbrace{MeHg \leftrightarrow Bed}_{\text{diffusion}} = \frac{v_m}{h}\left[\left(f_{d\text{-}MeHg2} + f_{doc\text{-}MeHg2}\right)\frac{MeHg_2}{\varphi} - \left(f_{d\text{-}MeHg} + f_{doc\text{-}MeHg}\right)MeHg\right] \quad (18)$$

2) Settling

The settling term of a sorbed Hg for a surface layer of height h(kt) is computed as:

$$\underbrace{MeHg \rightarrow Bed}_{settling} = -\frac{\left(v_{pom}f_{pom\text{-}Hg}+\sum_{n=1}^{NAL} v_{apn}f_{apn\text{-}Hg}++\sum_{n=1}^{NZOO} v_{zoopn}f_{zpn\text{-}Hg}+\sum_{n=1}^{NSS} v_{spn}f_{pn\text{-}Hg}\right)MeHg(kt)}{h(kt)} \quad (19a)$$

The settling term of a sorbed Hg for remaining layers of height h(k) below the surface layer is computed as:

$$\underbrace{MeHg \rightarrow Bed}_{settling} = \frac{\left(v_{pom}f_{pom\text{-}Hg}+\sum_{n=1}^{NAL} v_{apn}f_{apn\text{-}Hg}+\sum_{n=1}^{NZOO} v_{zoopn}f_{zpn\text{-}Hg}+\sum_{n=1}^{NSS} v_{spn}f_{pn\text{-}Hg}\right)(MeHg(k-1)-MeHg(k))}{h(k)}$$

(19b)

Active Sediment Layer Processes

An active Hg sediment layer and its relationship with the corresponding sediment diagenesis are shown in Figure 8. Two Hg species in the active sediment layer are modeled in W2: *HgII* and *MeHg*.

- *[HgII2],* concentration of total inorganic Hg with respect to a unit volume of total sediments (ng L^{-1})
- *[MeHg2],* concentration of total MeHg with respect to a unit volume of total sediments (ng L^{-1})

Currently, information from the sediment diagenesis model includes temperature, sediment diffusion velocity (v_m), organic solids in the sediment layer, and C turnover rate in the sediments for computation of methylation in the sediments.

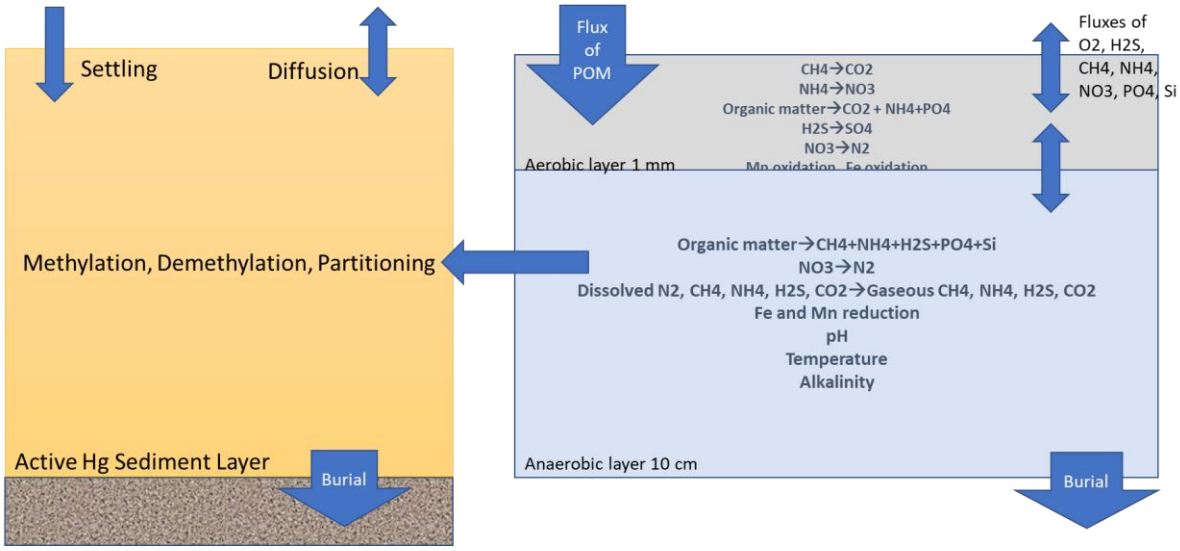

FIGURE 8. HG SEDIMENT LAYER DYNAMICS. FOR THE CURRENT MODEL RESUSPENSION IS NOT CONSIDERED.

Initial conditions of the state variables (HgII and MeHg) in ng/l, as well as sediment inorganic suspended solids in mg/l, were required for the active sediment layer.

HgII and *MeHg* can exist in the freely dissolved phase, DOC complexed phase, and attached to organic and inorganic solids in the sediment layer. The model will compute the following derived variables from the concentrations of total HgII and MeHg in sediment.

- $HgII2_d$, concentration of freely dissolved HgII in porewater(ng L^{-1})
- $HgII2_{doc}$, concentration of DOC complexed HgII in porewater (ng L^{-1})
- $HgII2_{pom}$, concentration of organic solid adsorbed HgII in sediment (ng L^{-1})
- $HgII2_{pt}$, total concentration of inorganic solids adsorbed HgII in sediment (ng L^{-1})
- $HgII2_{pts}$, total concentration of inorganic solids adsorbed HgII in sediment (ng g^{-1})
- $MeHg2_d$, concentration of dissolved MeHg in porewater (ng L^{-1})
- $MeHg2_{doc}$, concentration of DOC complexed MeHg in porewater (ng L^{-1})
- $MeHg2_{pom}$, concentration of organic solid adsorbed MeHg in sediment (ng L^{-1})
- $MeHg2_{pt}$, total concentration of inorganic solids adsorbed MeHg in sediment (ng L^{-1})
- $MeHg2_{pts}$, total concentration of inorganic solids adsorbed MeHg in sediment (ng g^{-1})

The total concentrations of *HgII* and *MeHg* within the sediment layer are computed in terms of mass per unit volume of water plus solids (ng L^{-1}). The following five processes are simulated for *HgII* and *MeHg* in the active sediment layer:

- Biological methylation
- Biological demethylation
- Settling of each non-living solid type

- Diffusion across the sediment-water interface
- Sediment deep burial (or erosion if settling is less than the sum of resuspension and decomposition.

Currently, resuspension of bed sediment is not included in the model.

1.2.1 Equilibrium partitioning and distribution of HgII and MeHg in the active sediment layer

Equilibrium partitioning of Hg species is handled in the same manner in the sediment layer as in the water column. The fractions associated with the dissolved phase in pore water, DOC complexed, and the solids adsorbed phases, are computed with considering the water content or porosity, φ.

$$f_{d2} = \frac{10^6 \varphi}{R_2} \quad (20a)$$

$$f_{doc2} = \frac{K_{doc2} \varphi \cdot [DOC2]}{R_2} \quad (20b)$$

$$f_{pom2} = \frac{K_{pom2}[POM2]}{R_2} \quad (20c)$$

$$f_{pn2} = \frac{K_{pn2}[ISS2_n]}{R_2} \quad (20d)$$

$$R_2 = 10^6 \varphi + K_{doc2} \varphi [DOC2] + K_{pom2}[POM2] + \sum_{n=1}^{NSS} K_{pn2}[ISS2_n] \quad (20e)$$

and

$$f_{d2} + f_{doc2} + + f_{pom2} + \sum_{n=1}^{NSS} f_{pn2} = 1 \quad (20f)$$

where

fd2 = Fraction of dissolved HgII or MeHg in sediment

fdoc2 = Fraction of DOC complexed HgII or MeHg in sediment

fpn2 = Fraction of solids adsorbed HgII or MeHg in sediment

Kdoc2 = HgII or MeHg equilibrium partition coefficient for sediment DOC (L kg^{-1})

Kpom2 = HgII or MeHg equilibrium partition coefficient for sediment POM (L kg^{-1})

Kpn2 = HgII or MeHg equilibrium partition coefficient for sediment solids (L kg^{-1})

DOC2 = Sediment dissolved organic carbon in pore water (mg L^{-1})

POM2 = Concentration of sediment POM (mg L^{-1})

$ISS2_n$ = Concentration of sediment solid "n" (mg L^{-1})

Dissolved and DOC complexed concentrations of *HgII and MeHg* in the sediment layer are calculated based on their mass relative to the total volume of solids and water. The porosity corrected concentrations in pore water are also computed. The multi-phase concentrations of *HgII* and *MeHg* in the sediment layer are computed as:

$$HgII2_d = f_{d\text{-}HgII2}[HgII2] \quad (21a)$$

$$HgII2_{doc} = f_{doc\text{-}HgII2}[HgII2] \quad (21b)$$

$$HgII2_{pom} = f_{pom\text{-}HgII2}[HgII2] \quad (21b)$$

$$HgII2_{pt} = \sum_{n=1}^{NSS} f_{pn\text{-}HgII2}[HgII2] \quad (21c)$$

$$HgII2_{pts} = 10^3 \frac{\sum_{n=1}^{NSS} f_{pn\text{-}HgII2}[HgII2]}{\sum_{n=1}^{NSS}[ISS2_n]} \quad (21d)$$

$HgII2_d$ and $HgII2_{doc}$ are computed based on the mass in the dissolved phase and DOC complexed phase per the sediment total volume. These concentrations are expressed based on the sediment pore water volume as:

$$HgII2_{dp} = \frac{HgII2_d}{\varphi} \quad (21e)$$

$$HgII2_{docp} = \frac{HgII2_{doc}}{\varphi} \quad (21f)$$

and

$$MeHg2_d = f_{d\text{-}MeHg2}[MeHg2] \quad (22a)$$

$$MeHg2_{doc} = f_{doc\text{-}MeHg2}[MeHg2] \quad (22b)$$

$$MeHg2_{pom} = f_{pom\text{-}MeHg2}[MeHg2] \quad (22b)$$

$$MeHg2_{pt} = \sum_{n=1}^{NSS} f_{pn\text{-}MeHg2}[MeHg2] \quad (22c)$$

$$MeHg2_{pts} = 10^3 \frac{\sum_{n=1}^{NSS} f_{pn\text{-}MeHg2}[MeHg2]}{\sum_{n=1}^{NSS}[ISS_{n2}]} \quad (22d)$$

Concentrations of $MeHg2_d$, $MeHg2_{doc}$ are expressed based on the sediment pore water volume as:

$$MeHg2_{dp} = \frac{MeHg2_d}{\varphi} \quad (22e)$$

$$MeHg2_{docp} = \frac{MeHg2_{doc}}{\varphi} \quad (22f)$$

Sediment Layer Internal Source and Sink Rate Equations for HgII, MeHg

Inorganic Hg (HgII)

The internal source and sink rate equation for the total concentration of *HgII* in the sediment layer is stated as

$$\frac{d[HgII2]}{dt} = \underbrace{V_s \frac{dHgII}{dz}}_{deposition} + \underbrace{MeHg2 \rightarrow HgII2}_{\text{demethyation}} - \underbrace{HgII2 \rightarrow MeHg2}_{\text{methylation}} - \underbrace{HgII \leftrightarrow HgII2}_{diffusion} - \underbrace{V_b \frac{dHgII2}{dz}}_{burial} \quad (23)$$

1) Methylation rate

As in the water column, the methylation rate in the sediments can be based on the rate of anoxic carbon turnover or not.

Carbon Turnover Rate Method

$$\underbrace{HgII2 \rightarrow MeHg2}_{\text{methylation}} = \left(k_{meth_{sed}} f_{d\text{-}HgII2} + k_{meth_{sdoc-sed}} f_{doc\text{-}HgII2} \right)[JOC2][HgII2] \quad (24a)$$

JOC2 is the organic C turnover rate in g/m^3/s in the sediments. This is computed as follows from the sediment diagenesis model:

$$JOC2 = \mu_{SD\_POC1} \theta_{POC1}^{(T_{sed}-20)} C_{SD\_POC1} + \mu_{SD\_POC2} \theta_{POC2}^{(T_{sed}-20)} C_{SD\_POC2}$$

where

μ_{SD_POC1}: first order sediment decay rate of labile particulate organic C (POC1, also termed POCG1 in sediment diagenesis model), 1/s, at 20°C

T_{sed}: sediment diagenesis temperature in anaerobic layer of sediment diagenesis model, °C

Θ_{POC1}: Arrhenius temperature correction factor for POC1

C_{SD_POC1}: concentration in the sediment diagenesis model of labile particulate organic C, g/m^3

μ_{SD_POC2}: first order sediment decay rate of refractory particulate organic C (POC2, also termed POCG2 in sediment diagenesis model), 1/s, at 20^{o}C

Θ_{POC2}: Arrhenius temperature correction factor for POC2

C_{SD_POC2}: concentration in the sediment diagenesis model of refractory particulate organic C, g/m^3

$K_{meth-sed}$ = $sediment$ methylation rate constant for HgII dissolved $\left(\frac{m^3}{g\ C}\right)$

$K_{meth-sdoc-sed}$ = $sediment$ methylation rate constant for HgII bound to DOC $\left(\frac{m^3}{g\ C}\right)$

If the sediment diagenesis model is not used, the model uses the C turnover rate from the first order sediment model as

$$JOC2 = \mu_{Sed1} C_{C-sediment}$$

where

μ_{Sed1}: first order sediment decay rate corrected by temperature, 1/s

$C_{C\text{-}sediment}$: C concentration in the first order sediment model, g/m^3

Methylation Not Based on Carbon Turnover

$$\underbrace{HgII2 \rightarrow MeHg2}_{\text{methylation}} = \left(k_{meth_{sed}} f_{d\text{-}HgII2} + k_{meth_{sdoc-sed}} f_{doc\text{-}HgII2} \right)[HgII2] \qquad (24b)$$

where

$K_{meth-sed}$ = $sediment$ methylation rate constant for HgII dissolved $\left(\frac{1}{s}\right)$ adjusted by temperature.

$K_{meth-sdoc-sed}$ =

$sediment$ methylation rate constant for HgII bound to DOC $\left(\frac{1}{s}\right)$adjusted by temperature.

Earlier the temperature dependence was based on carbon turnover rate dependencies, but in this approach the model user must specify the temperature dependence for the rate constants. An Arrhenius formulation is used to be compatible with earlier Hg studies. Hence, for demethylation the formula for adjusting temperature of the coefficient is the same as that for the water column, i.e., $k_T = k_{20}\theta^{T-20}$.

2) Demethylation rate

If methylation/demethylation are based on C turnover the equation used is

$$\underbrace{MeHg2 \rightarrow HgII2}_{\text{demethyation}} = \left(K_{demeth-sed} f_{d\text{-}MeHg} + K_{demeth-sdoc-sed} f_{doc\text{-}MeHg}\right)[JOC2][MeHg2] \quad (25a)$$

If not, then the equation used is

$$\underbrace{MeHg2 \rightarrow HgII2}_{\text{demethyation}} = \left(K_{demeth-sed} f_{d\text{-}MeHg} + K_{demeth-sdoc-sed} f_{doc\text{-}MeHg}\right)[MeHg2] \quad (25b)$$

where

$K_{demeth-sed}$ = *sediment de*methylation rate constant for HgII dissolved $\left(\frac{1}{s}\right)$ adjusted by temperature.

$K_{demeth-sdoc-sed}$ =

*sediment de*methylation rate constant for HgII bound to DOC $\left(\frac{1}{s}\right)$ adjusted by temperature.

The temperature adjustment is similar to the methylation temperature rate adjustment when it is not based on C turnover.

3) Diffusion rate across the sediment-water surface

$$\underbrace{HgII \leftrightarrow HgII2}_{diffusion} = \frac{v_m}{h2}\left[\left(f_{d\text{-}HgII2} + f_{doc\text{-}HgII2}\right)\frac{HgII2}{\varphi} - \left(f_{d\text{-}HgII} + f_{doc\text{-}HgII}\right)HgII\right] \quad (26)$$

4) Sediment burial rate

$$\underbrace{\frac{dHgII2}{dz}}_{burial} = \frac{1}{h2} v_b \left(f_{pom\text{-}HgII2} + \sum_{n=1}^{NSS} f_{pn\text{-}HgII2}\right) HgII2 \quad (27)$$

Methylmercury (MeHg):

The total sediment concentration of *MeHg* in the active layer is directly computed through solving the following mass balance equation.

$$\frac{d[MeHg2]}{dt} = \underbrace{V_s \frac{dMeHg2}{dz}}_{deposition} + \underbrace{HgII2 \rightarrow MeHg2}_{\text{methylation}} - \underbrace{MeHg2 \rightarrow HgII2}_{\text{demethyation}} -$$

$$\underbrace{MeHg \leftrightarrow MeHg2}_{diffusion} - \underbrace{V_b \frac{dMeHg2}{dz}}_{burial} \tag{28}$$

1) Diffusion rate across the sediment-water surface

$$\underbrace{MeHg \leftrightarrow MeHg2}_{diffusion} = \frac{v_m}{h2}\left[\left(f_{d-MeHg2} + f_{doc-MeHg2}\right)\frac{MeHg2}{\varphi} - \left(f_{d-MeHg} + f_{doc-MeHg}\right)MeHg\right] \tag{29}$$

2) Sediment burial rate

$$\underbrace{\frac{dMeHg2}{dz}}_{burial} = \frac{1}{h2} v_b \left(f_{pom-MeHg2} + \sum_{n=1}^{NSS} f_{pn-MeHg2}\right) MeHg2 \tag{30}$$

where

k_{meth_sed} = methylation rate constant $(m^3/g/s)$

k_{demeth_sed} = biological demethylation rate constant $(m^3/g/s)$

V_s = settling rate (m/s)

V_b = $burial$ rate (m/s)

Burial Velocity in Sediment Model

The model user can choose a fixed burial velocity or have it computed internally based on a mass balance of solids entering the sediment layer to those leaving the sediment layer. The internal computation makes the sediment layer solids content consistent over time. The internal burial velocity is computed for each sediment layer in cell k assuming no resuspension from

$$v_b(k) = \frac{\sum_n v_{sn} C_{ss-n}(k)}{\sum_n C_{ss-sed-n}(k)}$$

where

C_{ss-n} = concentration of inorganic solids of group "*n*" in water (g m^{-3})

$C_{ss-sed-n}$ = concentration of inorganic solids of group "*n*" in sediment bed (g m^{-3})

v_{sn} = settling velocity of solid "*n*" (m s^{-1})

v_b = sediment burial velocity (m s^{-1})

This rate of burial is assumed to be close to that of the organic solids.

Solids in Sediment Layer

The sediment layer consists of both inorganic solids and organic solids (particulate organic matter, POM) settled from the water column. These are used to compute partitioning in the sediment layer.

Inorganic Solids in Sediment Layer

The inorganic solids concentration in the sediment bed of thickness h2 is computed from the following mass balance for inorganic solids group n:

$$\frac{dC_{ss-sed-n}}{dt} = \frac{v_{sn}C_{ss-n} - v_b C_{ss-sed-n}}{h2}$$

Organic Solids in Sediment Layer

The organic solids concentration in the sediment bed is computed from the sediment diagenesis model as follows:

$$C_{POM-sed} = \frac{POCG1 + POCG2 + POCG3}{ORGC}$$

If the sediment diagenesis model is not used it computes it directly from

$$C_{POM-sed} = \frac{SEDC}{ORGC}$$

where

$C_{POM\text{-}sed}$ = concentration of organic solids in sediment bed (gm^{-3})

ORGC = C to organic matter ratio (typically 0.45)

SEDC = first order sediment model sediment C concentration (gm^{-3})

POCG1 = labile particulate organic C concentration from sediment diagenesis model (gm^{-3})

POCG2 = refractory particulate organic C concentration from sediment diagenesis model (gm^{-3})

POCG3 = inert particulate organic C concentration from sediment diagenesis model (gm^{-3})

Summary of Water Column and Sediment Model Parameters, Output Concentrations and Fluxes

Table 1 shows the water column model parameters used in the CE-QUAL-W2 model and the input units of the model. Internally, the model uses seconds rather than days.

Table 2 shows the bed sediment model parameters. Table 3 shows the Hg concentrations output by the model, and Table 4 shows the pathway fluxes output by the model.

TABLE 1. WATER COLUMN HG PARAMETERS

Symbol	Description	Units
Hg0		
$v_{v\text{-}Hg0}(T)$	Hg0 volatilization velocity	m d^{-1}
$Hg0_0$	Hg0 air concentration	ng L^{-1}
$K_{photoOxid}$	Hg0 photo-oxidation rate	d^{-1}
K_{ozid_1}	Oxidation rate constant	-
K_{ozid_2}	Oxidation rate constant	-
K_{ozid_3}	Oxidation rate constant	-
HgII		
$k_{doc\text{-}HgII}$	HgII equilibrium partition coefficient for DOC	L kg^{-1}
$K_{apn\text{-}HgII}$	HgII equilibrium partition coefficient for algae “n” (1 – NAL)	L kg^{-1}
$K_{pom\text{-}HgII}$	HgII equilibrium partition coefficient for organic solids	L kg^{-1}
$K_{pn\text{-}HgII}$	HgII equilibrium partition coefficient for inorganic solid “n” (1 – NSS)	L kg^{-1}
f_{pom}	fraction of instantaneous HgII binding sites on organic solids	-
f_{pn}	fraction of instantaneous HgII binding sites on inorganic solid “n”	-
$k_{ads-pom}$	HgII adsorption rate for organic solids	d^{-1}
$k_{des-pom}$	HgII desorption rate for organic solids	d^{-1}
k_{ads-pn}	HgII adsorption rate for inorganic solid “n”	d^{-1}
k_{des-pn}	HgII desorption rate for inorganic solid “n”	d^{-1}
$K_{reduction}$	HgII photoreduction rate	d^{-1}
$K_{meth-wat}$	HgII methylation rate constant	L mg^{-1}
$K_{meth-doc}$	DOC complexed HgII methylation rate constant	L mg^{-1}
MeHg		
$K_{doc\text{-}MeHg}$	MeHg equilibrium partition coefficient for DOC	L kg^{-1}
$K_{apn\text{-}MeHg}$	MeHg equilibrium partition coefficient for algae “n”	L kg^{-1}
$K_{pom\text{-}MeHg}$	MeHg equilibrium partition coefficient for organic solids	L kg^{-1}
$K_{pn\text{-}MeHg}$	MeHg equilibrium partition coefficients for inorganic solid “n”	L kg^{-1}
$K_{photoDeg}$	MeHg photo-degradation rate into Hg0	d^{-1}
$K_{demeth-wat}$	MeHg demethylation rate constant	L mg^{-1}
$K_{demeth-doc}$	DOC complexed MeHg demethylation rate constant	L mg^{-1}

TABLE 2. BED SEDIMENT HG PARAMETERS

Symbol	Description	Units
Global		
h_2	Sediment layer thickness	m
z_2	Sediment porewater diffusion layer thickness	cm
v_m	Sediment-water mass transfer coefficient	m d^{-1}
D_m	Molecular diffusivity	m^2 d^{-1}
ϕ	Sediment porosity	-
ρ	Sediment dry density	g cm^{-3}
v_b	Sediment burial velocity	m d^{-1}
HgII		
$k_{doc\text{-}HgII}$	HgII equilibrium partition coefficient for DOC	L kg^{-1}
$K_{pom\text{-}HgII}$	HgII equilibrium partition coefficient for organic solids	L kg^{-1}
$K_{pn\text{-}HgII}$	HgII equilibrium partition coefficient for inorganic solid "n" (1 – NSS)	L kg^{-1}
f_{pom}	fraction of instantaneous HgII binding sites on organic solids	-
f_{pn}	fraction of instantaneous HgII binding sites on inorganic solid "n" (1 – NSS)	-
$k_{ads-pom}$	HgII adsorption rate for organic solids	d^{-1}
$k_{des-pom}$	HgII desorption rate for organic solids	d^{-1}
k_{ads-pn}	HgII adsorption rate for inorganic solid "n"	d^{-1}
k_{des-pn}	HgII desorption rate for inorganic solid "n"	d^{-1}
$K_{meth-sed}$	HgII methylation rate constant	L mg^{-1}
$K_{meth-sdoc}$	DOC complexed HgII methylation rate constant	L mg^{-1}
MeHg		
$K_{doc\text{-}MeHg}$	MeHg equilibrium partition coefficient for DOC	L kg^{-1}
$K_{ap\text{-}MeHg}$	MeHg equilibrium partition coefficient for algae	L kg^{-1}
$K_{pom\text{-}MeHg}$	MeHg equilibrium partition coefficient for organic solids	L kg^{-1}
$K_{pn\text{-}MeHg}$	MeHg equilibrium partition coefficients for inorganic solid "n"	L kg^{-1}
$K_{demeth-sed}$	MeHg demethylation rate constant	L mg^{-1}
$K_{demeth-sdoc}$	DOC complexed MeHg demethylation rate constant	L mg^{-1}

TABLE 3. HG CONCENTRATIONS INCLUDED IN THE MODEL OUTPUTS.

Name	Definition	Units
Elemental Hg		
Hg0	Hg0 concentration in water	ng L^{-1}
Inorganic Hg		
HgII	Concentration of total HgII in water	ng L^{-1}

Name	Definition	Units
$HgII_d$	Concentration of dissolved HgII in water	ng L^{-1}
$HgII_{doc}$	Concentration of DOC complexed HgII in water	ng L^{-1}
$HgII_{ap}$	Total concentration of algae adsorbed HgII in water	ng L^{-1}
$HgII_{pom}$	Total concentration of POM adsorbed HgII in water	ng L^{-1}
$HgII_{pt}$	Total concentration of inorganic solids adsorbed HgII in water	ng L^{-1}
$HgII_{pts}$	Total concentration of inorganic solids adsorbed HgII in water	ng g^{-1}
$HgII2$	Concentration of total HgII in sediment	ng L^{-1}
$HgII2_{dp}$	Concentration of dissolved HgII in pore water	ng L^{-1}
$HgII2_{docp}$	Concentration of DOC complexed HgII in pore water	ng L^{-1}
$HgII2_{pom}$	Total concentration of POM adsorbed HgII in sediment	ng L^{-1}
$HgII2_{pt}$	Total concentration of inorganic solids adsorbed HgII in sediment	ng L^{-1}
$HgII2_{pts}$	Total concentration of inorganic solids adsorbed HgII in sediment	ng g^{-1}
Methymercury		
$MeHg$	Concentration of total MeHg in water	ng L^{-1}
$MeHg_d$	Concentration of dissolved MeHg in water	ng L^{-1}
$MeHg_{doc}$	Concentration of DOC complexed MeHg in water	ng L^{-1}
$MeHg_{ap}$	Total concentration of algae adsorbed MeHg in water	ng L^{-1}
$MeHg_{pom}$	Total concentration of POM adsorbed MeHg in water	ng L^{-1}
$MeHg_{pt}$	Total concentration of inorganic solids adsorbed MeHg in water	ng L^{-1}
$MeHg_{pts}$	Total concentration of inorganic solids adsorbed MeHg in water	ng g^{-1}
$MeHg2$	Concentration of total MeHg in sediment	ng L^{-1}
$MeHg2_{dp}$	Concentration of dissolved MeHg in pore water	ng L^{-1}
$MeHg2_{docp}$	Concentration of DOC complexed MeHg in pore water	ng L^{-1}
$MeHg2_{pom}$	Total concentration of POM adsorbed MeHg in sediment	ng L^{-1}
$MeHg2_{pt}$	Total concentration of inorganic solids adsorbed MeHg in sediment	ng L^{-1}
$MeHg2_{pts}$	Total concentration of inorganic solids adsorbed MeHg in sediment	ng g^{-1}

TABLE 4. HG PATHWAY FLUXES INCLUDED IN THE MODEL OUTPUTS.

Flux	Units
Hg0 volatilization	ng L^{-1} d^{-1}
Hg0 photo-oxidation into HgII in water	ng L^{-1} d^{-1}
HgII photo-reduction into Hg0 in water	ng L^{-1} d^{-1}
HgII methylation into MeHg in water	ng L^{-1} d^{-1}
HgII settling	ng L^{-1} d^{-1}
HgII sediment-water flux	ng L^{-1} d^{-1}
sediment HgII methylation into MeHg	ng L^{-1} d^{-1}

Flux	Units
HgII deposition	ng L^{-1} d^{-1}
HgII sediment-water flux	ng L^{-1} d^{-1}
Sediment HgII burial	ng L^{-1} d^{-1}
MeHg photo-degradation into Hg0 in water	ng L^{-1} d^{-1}
MeHg demethylation into HgII in water	ng L^{-1} d^{-1}
MeHg settling	ng L^{-1} d^{-1}
MeHg sediment-water flux	ng L^{-1} d^{-1}
sediment MeHg demethylation into HgII	ng L^{-1} d^{-1}
MeHg deposition	ng L^{-1} d^{-1}
Sediment MeHg burial	ng L^{-1} d^{-1}

Field Data used in the CE-QUAL-W2 Model

Field data in the Hells Canyon Complex was used for both boundary conditions as well as for in-reservoir model-data comparisons. Figure 9 shows the Brownlee model grid and locations of inflows and outflows. Figure 10 shows the Oxbow model grid and locations of inflows and outflows. Figure 11 shows the Hells Canyon model grid and locations of inflows and outflows.

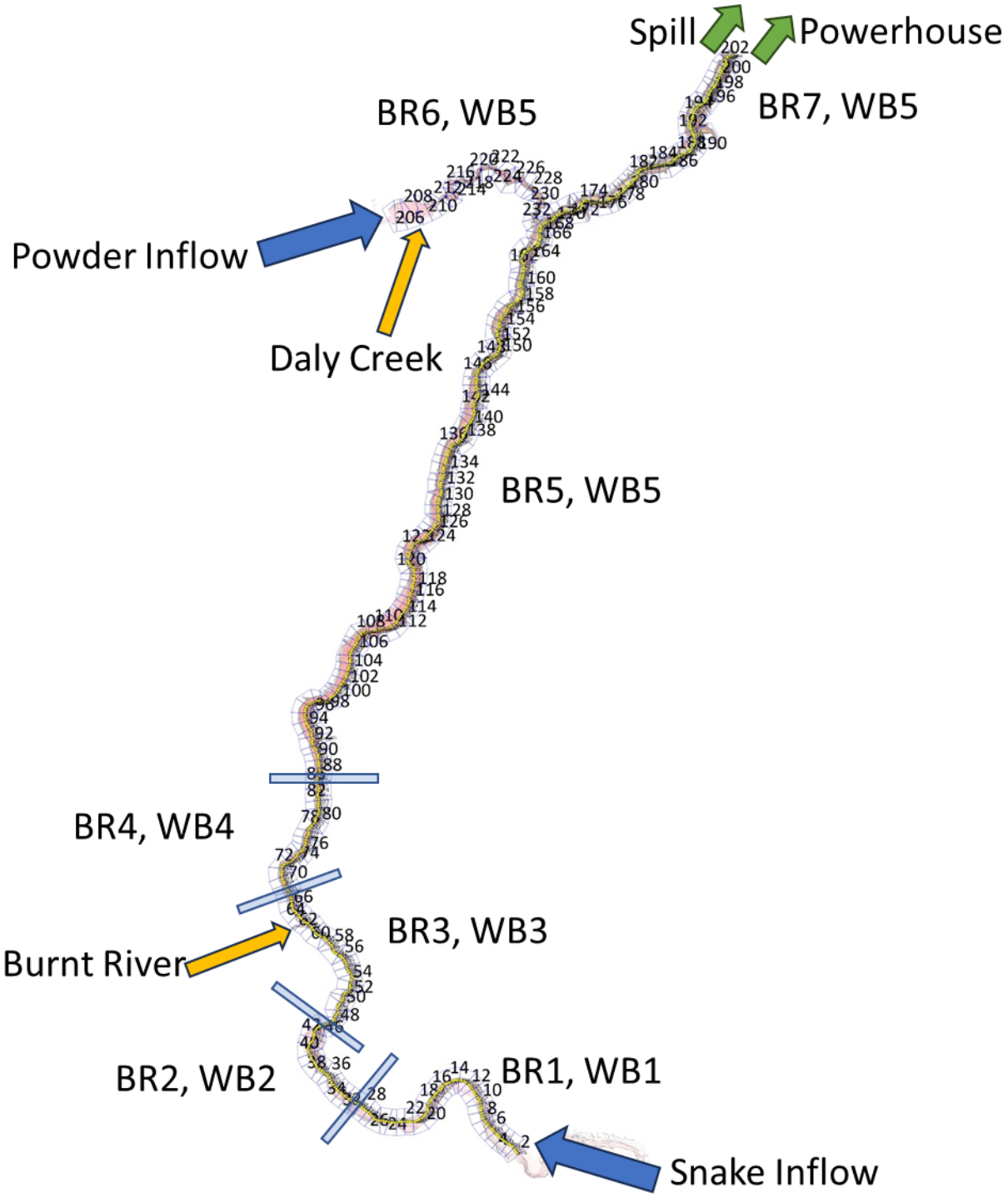

FIGURE 9. BROWNLEE MODEL GRID. WATER BODY (WB) 1, BRANCH (BR) 1: SEGMENTS 2-29; WB2 (BR2): SEGMENTS 32-42; WB3 (BR 3): SEGMENTS 45-66; WB 4 (BR 4): SEGMENTS 69-83; WB 5: BR 5: SEGMENTS 86-202 (AT DAM), BR 6 SEGMENTS 205-233 (POWDER ARM); BR 7: SEGMENTS 236-238 (INLET CHANNEL). SEGMENT SPACING IN MAINSTEM IS 500 M, IN POWDER ARM 503 M, AND IN INLET CHANNEL 60 M. LENGTH OF MAINSTEM IS 96.5 KM.

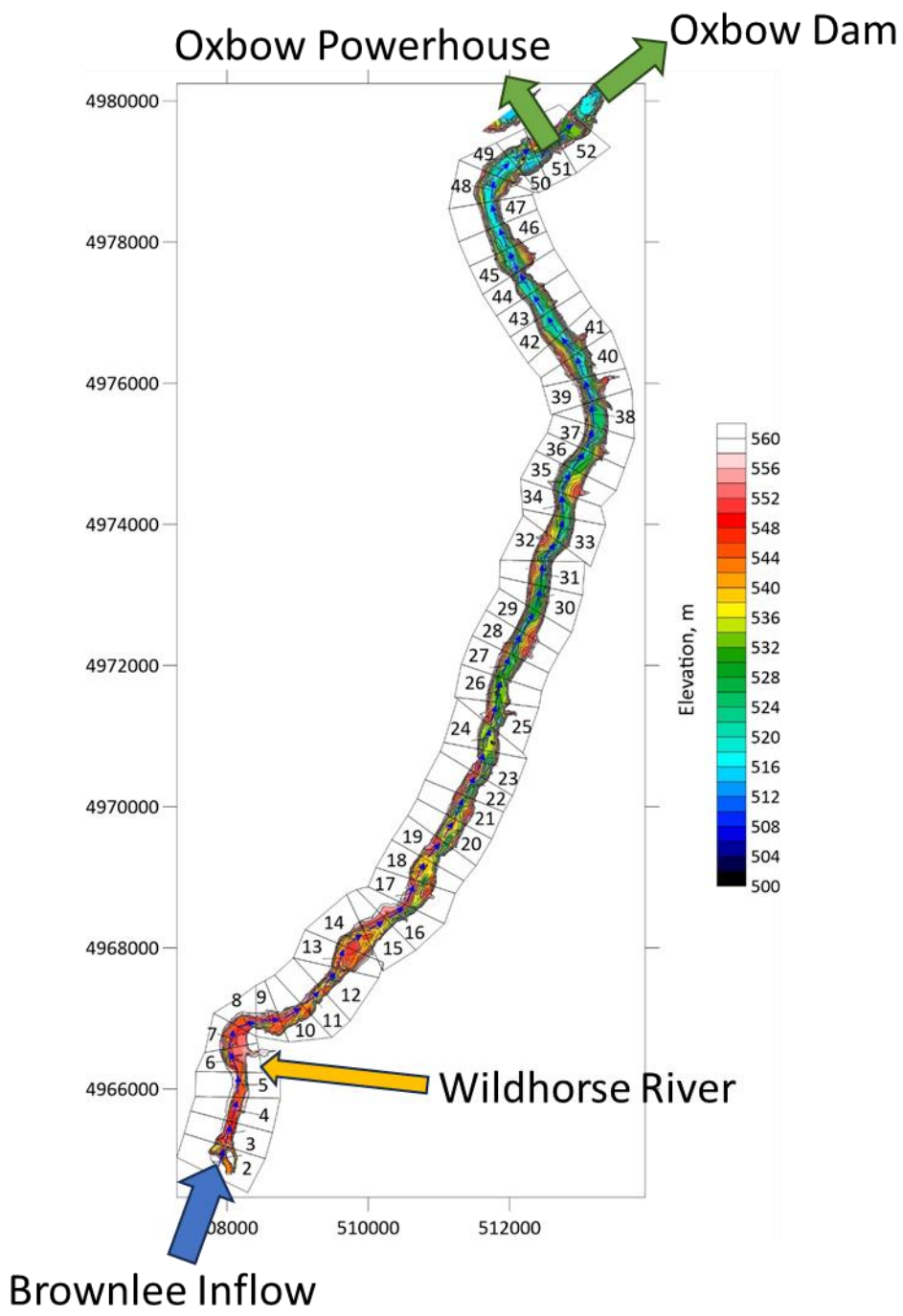

FIGURE 10. OXBOW MODEL GRID. SEGMENT SPACING IS 357 M. LENGTH OF MODEL DOMAIN IS 18.2 KM.

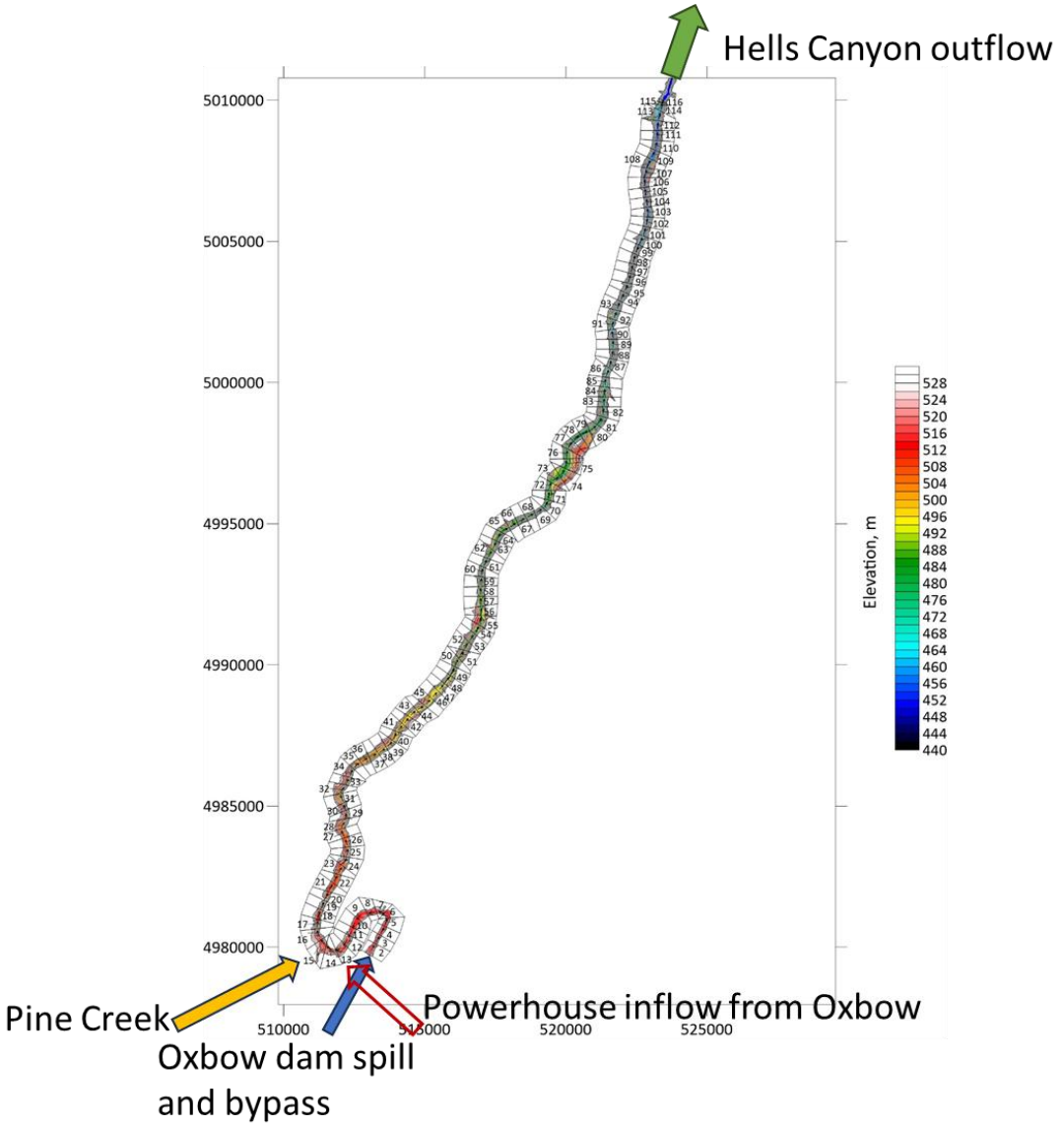

FIGURE 11. HELLS CANYON MODEL GRID. SEGMENT SPACING IS 351 M (EXCEPT FOR 3 SEGMENTS BEFORE THE DAM TO ACCOUNT FOR COFFERDAM). LENGTH OF MAINSTEM IS 39.6 KM.

Hg Sediment Initial Conditions

Sediment biogeochemical data published by USGS (Marvin-DiPasquale, et al., 2020) was used to develop some of the parameters for the mercury module for the three reservoirs: initial sediment porewater concentrations of HgII and MeHg. Table 5 lists the average values of shallow sediment (0-5 cm) pore water parameters during the sampling period of 2016-2017 for various river miles. River mile 248 corresponds to Hells Canyon Reservoir, and river miles 286-318 correspond to Brownlee Reservoir. HgII was estimated by subtracting the average MeHg from the average total Hg.

Table 5. Average values of mercury shallow sediment pore water parameters at various river miles for 2016-2017.

Average	RM 248	RM 286	RM 300	RM 310	RM 318	Total Avg
Total Hg (ng/l)	5.59	8.35	9.13	16.22	17.59	11.11
MeHg (ng/l)	1.62	2.77	3.38	1.81	1.45	2.34
HgII (ng/l) - Estimated	3.97	5.58	5.75	14.41	16.15	8.77

Atmospheric Deposition

The atmospheric deposition rates in CE-QUAL-W2 for a variable with a unit of g/m^3 (mg/l) are given in kg/km^2/year. For Hg, since the state variable is in units of $\mu g/m^3$ (ng/l), the atmospheric deposition rates are in units of mg/km^2/year. No direct measurements were made during this study, but a study by Buetel, et al. (2021) estimated for Total Hg dry deposition: 2.4 ± 1.4 $ng/m^2 \cdot h$ (21 $\mu g/m^2$/yr) and wet deposition of 7.0 ± 4.8 $ng/m^2 \cdot h$ (61 $\mu g/m^2$/yr) for Pullman, WA, USA. These seem to be very high considering other studies such as Zhang et al. (2019) who showed that annual averages in North America were 9.1 $\mu g/m^2$/yr for wet deposition and 6.4 $\mu g/m^2$/yr for dry deposition. Knightes et al. (2014) used a value of annual deposition of 10 $\mu g\ Hg/m^2$ /yr with 98.5% HgII and 1.5% MeHg in a watershed Hg model. Also, Wang et al. (2014) showed wet deposition flux of Total Hg of 28.7 ± 5.1 $\mu g/m^2$/yr in urban areas of Chongquin, China.

The atmospheric deposition file defined for each waterbody was as shown below:

$atm_deposition_wb1.csv		For Brownlee Reservoir
Atmospheric mass input	kg/km2/year [For Hg it is mg/km2/year]	
JDAY	Hg0	HgII
1	1	5000
4500	1	5000

Converting these values above for combined wet and dry deposition, these are 5 $\mu g/m^2$/yr for HgII and 0.001 $\mu g/m^2$/yr for Hg0.

Constituent Inputs

Constituent concentrations for the Snake River inflow to Brownlee Reservoir were developed using Idaho Power Company (IPC) and USGS (USGS, 2021) data. Battelle data (included in the USGS data set) was only used for Hg inputs until July 2014. Data were collected from sampling stations located at RM 345.6. Data was not available for Powder River, Eagle Creek, or Burnt River during the simulation period, so input concentrations for these rivers were either set equal to Snake River inflow concentrations or regressions were developed to estimate certain

parameters obtained by USGS and IPC. Regressions were created using either Snake River inflow concentrations of the same parameter or using tributary flows. The regressions that resulted in the best r-squared value were used for each site and for each parameter. Powder River input concentrations were calculated using a flow weighted average of Eagle Creek and Powder River concentrations near Richland, Oregon. Wildhorse River, Pine Creek, Daly Creek, and the distributed tributary concentrations were all set equal to flow weighted Powder River concentrations. Daily average flows for Snake River, Powder River, Burnt River, and Eagle Creek were calculated from the 15-minute input flows to use in the regressions and flow weighting. Table 6 lists all the tributaries in each model and segment location. Table 7 lists each of Hg constituents and methods to create the constituent inflow timeseries for the Snake River. Table 8 lists each of each of Hg constituents and the methods used to create the Hg constituent inflow timeseries for the Burnt River and Powder River. The regressions in Table 7 and Table 8 were originally determined from Harris (2022) but were later computed by PSU with updated USGS field data.

The following approach was used for processing data values for the input concentrations:

- USGS values with a "<" flag next to the reported value were halved when included in the inputs.
- IPC values with a "<" flag next to the reported value were halved when included in the inputs.
- Negative values and duplicates were removed.
- Any values of zero or "trace" were input as the minimum of (1) the lowest halved no detect ("<") value or (2) half of the lowest value observed (greater than zero).
- All other values were included as the value listed, including values flagged as suspect or estimates or were filtered in the laboratory prior to analysis. USGS values that were flagged with "< RL, estimate based on lowest standard" were also left at the value listed.
- Gaps in data measurements were linearly interpolated except for when regressions or daily output from a loading model were used as described in the tables below.
- For linearly interpolated inputs, if multiple values were recorded on the same day, the average value was used for the input.
- Daily concentration output from loading models based on measured concentration, discharge, season, and time, were used to develop key input constituents. Kalman estimates from Weighted Regressions on Time Discharge and Season (WRTDS, Naymik et al. 2023, Hirsch 2019, Hirsch and De Cicco 2015) were used for nutrients, algae and TSS. Loadflex composite estimates (Appling et al. 2015, Aulenbach and Hooper 2006), which are similar to WRTDS Kalman estimates, were used for DOC (Yoder et al. 2024 *accepted*) and Hg inputs (Baldwin et al. 2022).

-

Interpolation was used to fill gaps in the data values for creating the model input timeseries.

Table 6. Modeled HCC inflows for the 3 models: Brownlee, Oxbow, and Hells Canyon.

Tributary	**Model**	**Model Inflow Type, Number and Inflow Location**
Snake River	Brownlee	Branch 1 Inflow, Segment 2
Powder River	Brownlee	Branch 6 Inflow, Segment 205
Burnt River	Brownlee	Tributary #1, Segment 62
Daly Creek	Brownlee	Tributary #2, Segment 207
Brownlee Water Balance Inflow	Brownlee	Branch 5 Distributed Tributary
Brownlee Dam Spill	Oxbow	Branch 1 Inflow, Segment 2
Wildhorse River	Oxbow	Tributary #1, Segment 6
Brownlee Turbines	Oxbow	Tributary #2, Segment 2
Oxbow Dam Spill and Bypass	Hells Canyon	Branch 1 Inflow, Segment 2
Oxbow Turbines	Hells Canyon	Tributary #1, Segment 13
Pine Creek	Hells Canyon	Tributary #2, Segment 15

Table 7. Development of modeled constituent concentrations in Snake River inflows to Brownlee Reservoir. The constituent number is the number used in the CE-QUAL-W2 model.

#	**Constituent**	**Comments**
42	Hg0, ng/L	Set to constant 0.05
43	Hg(II), ng/L	Hg(II) was estimated from the sum of filtered and particulate HgII from USGS data and loadflex composite estimates were used for daily values (Baldwin et al. 2022): $$\Phi HgII_{model\ input} = \Phi HgII_{filt.data} + \Phi HgII_{part.data}$$ 3 spikes in Hg(II) were removed from the model inputs either during the loadflex analysis (6/19/2018) or during model calibration (6/27/2016 and 4/17/2018) because particulate Hg(II) particulate Hg(II) values were very high for unknown reasons and occurred with low associated TSS values. In the model, this condition translates to a large spikes in filtered Hg(II) concentrations which were not appropriate.
44	MeHg, ng/L	MeHg was estimated from the sum of filtered and particulate MeHg from USGS data and loadflex composite estimates were used for daily values (Baldwin et al. 2022):

#	Constituent	Comments
		$\Phi MeHg_{model\ input} = \Phi MeHg_{filt.data} + \Phi MeHg_{part.data}$ One spike in MeHg (12/29/2016) was removed from the model inputs through the loadflex analysis.

Table 8. Development of modeled constituent concentrations in the Burnt River and Powder River. Wildhorse River, Pine Creek, Daly Creek, and the distributed tributary concentrations were all set equal to flow weighted Powder River concentrations. The constituent number is the number used in the CE-QUAL-W2 model.

#	Constituent	Comments
42	Hg0, ng/L	Set to constant 0.05
43	Hg(II), ng/L	Burnt R., Powder R., and Eagle Cr. Hg(II) concentrations during the simulation period were estimated using a regression with Snake inflow HgII concentrations from USGS data (see Figure 12). Regressions were created using USGS HgII data available after the simulation period. Burnt River Regressions: $\Phi HgII_{unfilt} = \exp\left(0.889 + 0.760\left(ln\left(\Phi HgII_{Snake\ filt}\right)\right)\right) * 1.121$ Powder River Regressions: $\Phi HgII_{unfilt} = \exp\left(-0.109 + 0.323\left(ln\left(\Phi HgII_{Snake\ filt}\right)\right)\right) * 1.067$ Eagle Creek Regressions: $\Phi HgII_{unfilt} = \exp\left(-923 + 0.529\left(ln\left(\Phi HgII_{Snake\ unfilt}\right)\right)\right) * 1.071$ HgII model inputs used the unfilt (unfiltered) or total HgII as estimated from the regressions with Snake River data.
44	MeHg, ng/L	Burnt R., Powder R., and Eagle Cr. MeHg concentrations during the simulation period were estimated using a regression with Snake inflow MeHg concentrations from USGS data (see Figure 13). Regressions were created using USGS MeHg data available after the simulation period. Burnt River Regressions: $\Phi MeHg_{unfilt} = \exp\left(0.566 + 0.840\left(ln\left(\Phi MeHg_{Snake\ filt}\right)\right)\right) * 1.237$ Powder River Regressions: $\Phi MeHg_{unfilt} = \exp\left(-1.05 + 0.432\left(ln\left(\Phi MeHg_{Snake\ filt}\right)\right)\right) * 1.096$ Eagle Creek Regressions: $\Phi MeHg_{unfilt} = \exp\left(-2.75 + 0.483\left(ln\left(\Phi MeHg_{Snake\ filt}\right)\right)\right) * 1.103$

#	Constituent	Comments
		HgII model inputs used the unfilt (unfiltered) or total MHg as estimated from the regressions with Snake River data.

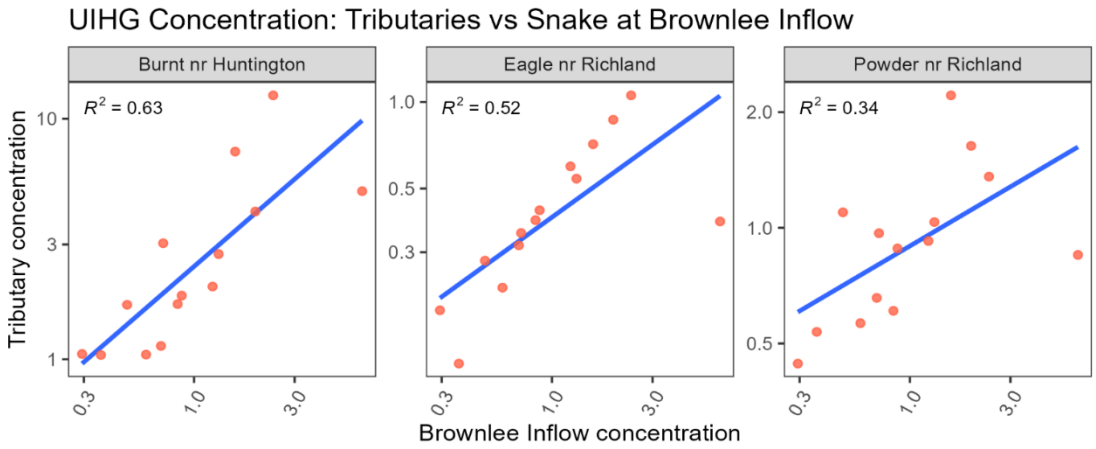

FIGURE 12. REGRESSION EQUATIONS FOR TRIBUTARY UNFILTERED INORGANIC HG CONCENTRATIONS BASED ON SNAKE RIVER CONCENTRATIONS FROM BALDWIN(2024).

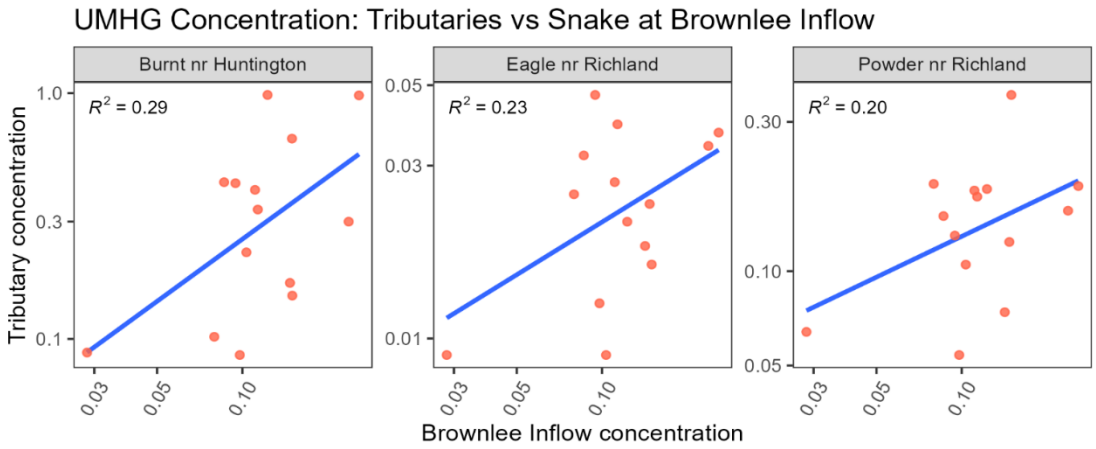

FIGURE 13. REGRESSION EQUATIONS FOR TRIBUTARY UNFILTERED MHG CONCENTRATIONS BASED ON SNAKE RIVER CONCENTRATIONS FROM BALDWIN(2024).

Constituent input concentrations for the Snake River inflow and tributaries are shown in Figure 14.

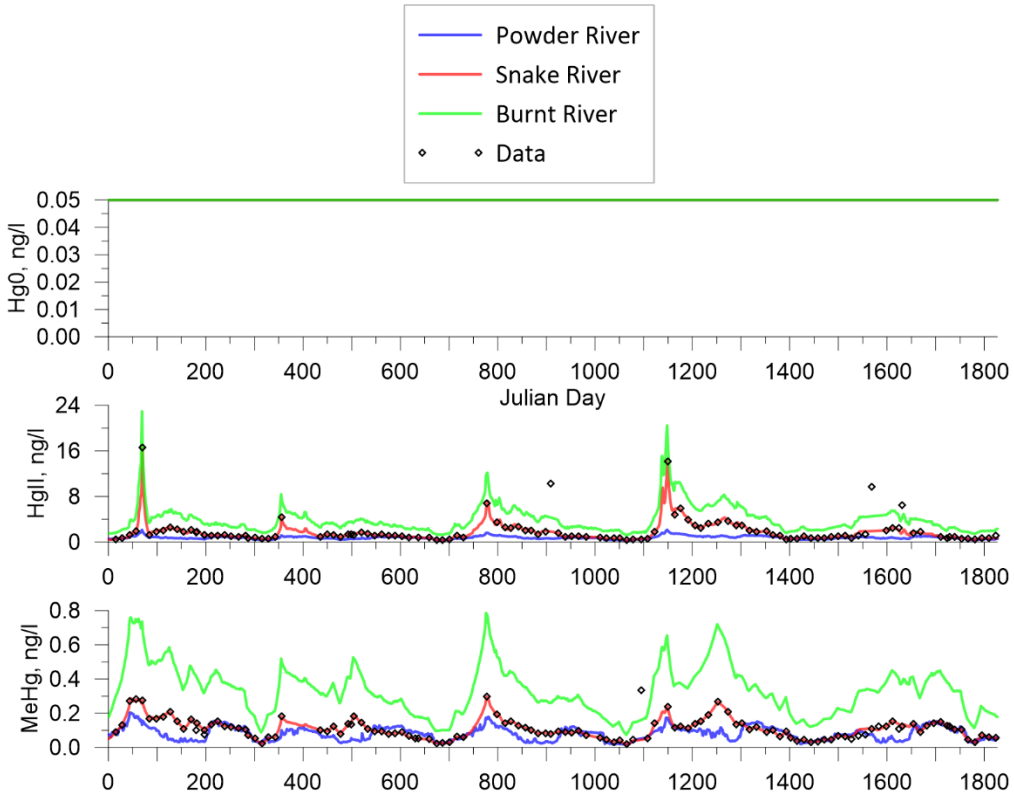

Figure 14. Constituent concentrations for Hg0, HgII, MeHg. Daly Creek, Brownlee Reservoir distributed tributary, Pine Creek, and Wildhorse River were set equal to Powder River concentrations.

Model-Data Comparisons in Hells Canyon Complex

The water quality and hydrodynamic CE-QUAL-W2 model for the Hells Canyon Complex was compared to field data and results were summarized in Garstecki et al., 2023. Model results were compared to vertical profile data, outflow data, and sediment porewater data from IPC and USGS for the three reservoirs. Model-data comparisons were made for temperature, dissolved oxygen, pH, dissolved organic carbon, particulate organic carbon, chlorophyll a, zooplankton, nitrate, ammonia, TKN, TN, TP, dissolved ortho-phosphorus, chloride, oxidized and reduced Fe and Mn, CH_4, H_2S, sulfate, and suspended solids. Table 9 lists the locations with data used for outflow and profile model comparisons, and Table 10 lists the locations with USGS data used for sediment and porewater model comparisons. Brownlee Reservoir profile data were collected between (and including) river miles 327.8 to 286, Oxbow Reservoir profile data were collected at river mile 273, and Hells Canyon Reservoir profile data were collected between (and including) river miles 263.3 to 247.9. The following approach was used for processing data values for water quality comparisons:

- USGS values with a "<" flag next to the reported value were shown in figures as "no detects" at half the value listed and were omitted from statistics calculations.

- IPC values with a "<" flag next to the reported value were shown in figures as "no detects" at half the value listed in figures and omitted from statistics calculations.
- Negative values and duplicates were removed.
- Any values of zero or "trace" were shown on figures as the minimum of (1) the lowest halved no detect ("<") value or (2) half of the lowest value observed (greater than zero) and omitted from the statistics calculations.
- Negative depths were converted to positive and USGS depths of "SW" were converted to 0.3m. However, these only applied to inflow/outflow locations where flow was well-mixed and depth was not used for generating comparisons.
- All other values were included as the value listed, including values flagged as suspect or estimates or were filtered in the laboratory prior to analysis. USGS values that were flagged with "< RL, estimate based on lowest standard" were also left at the value listed.

Table 9 and Table 10 also include Hg data that will be used for model-data comparisons.

Table 9. Data used for outflow and profile model comparisons in Wells et al. 2025 and for Hg model-data comparisons.

Parameter	Source	BR Pr	BR Out RM 283.9	OX Pr	OX Out RM 269.9	HC Pr	HC Out RM 247.6	HC Out RM 246.9	Notes
Dissolved Oxygen	IPC	X	X	-	X	X	X	-	
pH	IPC	X	-	-	-	X	-	-	
Chlorophyll a	IPC	X	X	-	-	-	-	X	Outliers of 801 ug/l and 288 ug/l removed.
Ammonia	IPC	X	X	-	-	-	-	X	
Nitrate	IPC	X	X	-	-	-	-	X	
Nitrate	USGS	X	X	X	X	X	-	X	
Total Kjeldahl Nitrogen	IPC	X	X	-	-	-	-	X	
Particulate Organic Nitrogen	USGS	X	X	X	X	X	-	X	Using particulate nitrogen from data.
Orthophosphate	IPC	X	X	-	-	-	-	X	
Orthophosphate	USGS	X	X	X	X	X	-	X	Using filter-passing phosphorus from data.
Total Phosphorus	IPC	X	X	-	-	-	-	X	

Parameter	Source	BR Pr	BR Out RM 283.9	OX Pr	OX Out RM 269.9	HC Pr	HC Out RM 247.6	HC Out RM 246.9	Notes
Total Inorganic Carbon	USGS	X	X	X	X	X	-	X	Using dissolved inorganic carbon from data.
Dissolved Organic Carbon	USGS	X	X	X	X	X	-	X	Using "Boulder" DOC data
Particulate Organic Carbon	USGS	X	X	X	X	X	-	X	
Chloride	USGS	X	X	X	X	X	-	X	
Sulfate	IPC	X	X	-	-	-	-	X	
Sulfate	USGS	X	X	X	X	X	-	X	
H2S	USGS	X	X	-	X	X	-	X	Using filter-passing inorganic sulfide from data.
Zooplankton	IPC, USGS	X	X	X	X	X	-	-	Using plankton biomass from IPC data for outflow comparisons, and zooplankton biomass from USGS data for profile comparisons.
Fe(II)	USGS	X	X	X	X	X	-	X	Using filtered Fe from data. Outlier of 277 ng/l at RM 300 removed.
FeOOH	USGS	X	X	-	X	X	-	X	Using particulate Fe from data.
Mn(II)	USGS	X	X	X	X	X	-	X	Using filtered Mn from data.
MnO2	USGS	X	X	-	X	X	-	X	Using particulate Mn from data.
Total Suspended Solids	USGS	X	X	X	X	X	-	X	
Total Suspended Solids	IPC	X	X	-	-	-	-	X	
Volatile Suspended Solids	IPC	-	X	-	-	-	-	X	Model predictions of POC compared to VSS data x 0.45 as an estimate of POC from VSS.
Hg(II), unfiltered, ng/l	USGS	X	X	X	X	X	-	X	Using sum of particulate and filtered HgII from data when both filtered and particulate data were available.
MeHg, unfiltered, ng/l	USGS	X	X	X	X	X	-	X	

Parameter	Source	BR Pr	BR Out RM 283.9	OX Pr	OX Out RM 269.9	HC Pr	HC Out RM 247.6	HC Out RM 246.9	Notes
Hg(II), particulate, ng/l	USGS	X	X	X	X	X	-	X	
MeHg, particulate, ng/l	USGS	X	X	X	X	X	-	X	
Hg(II), filtered, ng/l	USGS	X	X	X	X	X	-	X	
MeHg, filtered, ng/l	USGS	X	X	X	X	X	-	X	
Hg(II), particulate, ng/g	USGS	X	X	X	X	X	-	X	
MeHg, particulate, ng/g	USGS	X	X	X	X	X	-	X	

Pr: Profile; Out: Outflow

Table 10. USGS data available for sediment and porewater model comparisons. Shaded rows indicate data used for comparisons in Wells et al. (2025).

Parameter	Source	BR RM 318	BR RM 314	BR RM 310	BR RM 305	BR RM 300	BR RM 286	OX RM 273	HC RM 252	HC RM 248/ 248.1	Notes
Hg(II), particulate, ng/g	1	X	-	X	-	X	X	X	X	X	HgII estimated from HgTotal-MeHg when both were above MDL
MeHg, particulate, ng/g	1	X	-	X	-	X	X	X	X	X	
HgTotal, particulate, ng/g	1	X	-	X	-	X	X	X	X	X	
Hg(II), filtered, ng/l	2	X	-	X	-	X	X	-	-	X	HgII estimated from HgTotal-MeHg when both were above MDL
MeHg, filtered, ng/l	2	X	-	X	-	X	X	-	-	X	
HgTotal, filtered, ng/l	2	X	-	X	-	X	X	-	-	X	
Dissolved Organic Carbon	2	X	-	X	-	X	X	-	-	X	

Parameter	Source	BR RM 318	BR RM 314	BR RM 310	BR RM 305	BR RM 300	BR RM 286	OX RM 273	HC RM 252	HC RM 248/ 248.1	Notes
H2S	2	X	-	X	-	X	X	-	-	X	Using pore water sulfide from data.
Mn(II)	2	X	-	X	-	X	X	-	-	X	Using pore water manganese from data.
Fe(II)	2	X	-	X	-	X	X	-	-	X	Using pore water iron from data.
Orthophosphate	2	X	-	X	-	X	X	-	-	X	
Nitrate	2	X	-	X	-	X	X	-	-	X	
Sulfate	2	X	-	X	-	X	X	-	-	X	
Ammonia	2	X	-	X	-	X	X	-	-	X	
Hg(II), particulate, ng/g	3	-	-	X	-	X	X	X	-	X	HgII estimated from HgTotal-MeHg when both were above MDL
MeHg, particulate, ng/g	3	-	-	X	-	X	X	X	-	X	
HgTotal, particulate, ng/g	3	-	-	X	-	X	X	X	-	X	
Hg(II), unfiltered, ng/l	4	X	X	X	X	X	X	-	-	X	Unfiltered HgII estimated as sum of particulate and filtered HgII when both had data available.
Hg(II), particulate, ng/l	4	X	X	X	X	X	X	-	-	X	
Hg(II), filtered, ng/l	4	X	X	X	X	X	X	-	-	X	
Hg(II), particulate, ng/g	4	X	X	X	X	X	X	-	-	X	
MeHg, unfiltered, ng/l	4	X	X	X	X	X	X	-	-	X	
MeHg, particulate, ng/l	4	X	X	X	X	X	X	-	-	X	
MeHg, filtered, ng/l	4	X	X	X	X	X	X	-	-	X	
MeHg, particulate, ng/g	4	X	X	X	X	X	X	-	-	X	
HgTotal, unfiltered, ng/l	4	X	X	X	X	X	X	-	-	X	

Parameter	Source	BR RM 318	BR RM 314	BR RM 310	BR RM 305	BR RM 300	BR RM 286	OX RM 273	HC RM 252	HC RM 248/ 248.1	Notes
HgTotal, particulate, ng/l	4	X	X	X	X	X	X	-	-	X	
HgTotal, filtered, ng/l	4	X	X	X	X	X	X	-	-	X	
HgTotal, particulate, ng/g	4	X	X	X	X	X	X	-	-	X	
Chloride	4	X	X	X	X	X	X	-	-	X	
Dissolved Organic Carbon	4	X	X	X	X	X	X	-	-	X	
H2S	4	X	X	X	X	X	X	-	-	X	Using filter-passing inorganic sulfide from data.
MnO2	4	X	X	X	X	X	X	-	-	X	Using particulate Mn from data.
Mn(II)	4	X	X	X	X	X	X	-	-	X	Using filtered Mn from data.
FeOOH	4	X	X	X	X	X	X	-	-	X	Using particulate Fe from data.
Fe(II)	4	X	X	X	X	X	X	-	-	X	Using filtered Fe from data.
Orthophosphate	4	X	X	X	X	X	X	-	-	X	Using filter-passing phosphorus from data.
Nitrate	4	X	X	X	X	X	X	-	-	X	
Sulfate	4	X	X	X	X	X	X	-	-	X	
Total Suspended Solids	4	X	X	X	X	X	X	-	-	X	

(1) Shallow bulk sediment, (2) Shallow sediment porewater, (3) Sediment deep cores, (4) Samples taken within approximately one meter above the sediments

Typical Hg Parameters Values

Table 11 shows typical water column parameter values used in the Hg module in CE-QUAL-W2 many of which were suggested by Harris (2021). Table 12 shows typical Hg parameter values for the sediment model also many of which were suggested by Harris (2021). These values were used as starting points for the Hg model calibration.

TABLE 11. HG PARAMETERS FOR THE WATER COLUMN.

Symbol	Description	Typical values	Units
ANOX	Fraction of anoxic to oxic decay rate used in computing JPOC	0.01-0.1. Lee (1992) suggests though that the rates of oxic and anoxic decomposition could be of a similar order of magnitude. Lee (1992) showed that this ratio varies from 0.04 to 1 depending on the location and organic compound. In most cases though the oxic decay rate was much larger than the anoxic one.	[-]
	Hg0		
$Hg0_0$	Hg0 air concentration	1.5E-3 (=1.5 ng/m^3); Zhu et al. (2017) used 0.0	ng L^{-1}
K_{oxid_1}	Hg0 photo-oxidation rate constant	0.00188	unitless
K_{oxid_2}	Hg0 photo-oxidation rate constant	-0.73385	unitless
K_{oxid_3}	Hg0 photo-oxidation rate constant	2.0409	Unitless
k_{Hg0}	Hg0 volatilization velocity (currently calculated internally in the model so the model user cannot fix this rate)	6.2 (spring) to 11.6 (fall), Vette et al, (2002); Zhu et al. (2017) used 33 cm/hr	cm hr^{-1}
	HgII		
$HgII_{dry}$	HgII dry deposition rate	1.0	µg m^{-2} Yr^{-1}
$k_{doc\text{-}HgII}$	HgII equilibrium partition coefficient for DOC	4E6	L kg^{-1}
$K_{apn\text{-}HgII}$	HgII equilibrium partition coefficient for algae	4E6	L kg^{-1}
$K_{pom\text{-}HgII}$	HgII equilibrium partition coefficient for non-living organic solids	1E7	L kg^{-1}
$K_{pn\text{-}HgII}$	HgII equilibrium partition coefficient for inorganic solid group (silt, clay)	1E6	L kg^{-1}
$K_{reduction}$	HgII photoreduction rate constant into Hg0	0.003 (based on target rate of 30%/day at surface and 100 W PAR at surface)	m^2 W^{-1} d^{-1}
$K_{meth-wat}$	HgII methylation rate constant	EPA (2001) WASP application to Savannah River, Georgia used 1E-4 day^{-1} which is an overall rate compared to that computed in CE-QUAL-W2.	m^3/g C decomposed
K_{p_silt}	HgII equilibrium partition coefficient for DOC	2E4 EPA (2001) WASP application to Savannah River, Georgia; $10^{6.2}$ soil partition coefficient (Knightes et al., 2014)	L kg^{-1}

Symbol	Description	Typical values	Units
K_{p_sand}	HgII equilibrium partition coefficient for sand	1E4 EPA (2001) WASP application to Savannah River, Georgia; 10^4 soil partition coefficient (Knightes et al., 2014) ; Zhu et al. (2017) used 1E3	L kg^{-1}
K_{doc}	HgII equilibrium partition coefficient for silt	4E5 EPA (2001) WASP application to Savannah River, Georgia; Zhu et al. (2017) used 2E3	L kg^{-1}
	MeHg		
$MeHg_0$	MeHg air concentration *[This is not used currently in the model for volatilization of MeHg.]*	0.000015	ng L^{-1}
$K_{doc\text{-}MeHg}$	MeHg equilibrium partition coefficient for DOC	4E6	L kg^{-1}
$K_{apn\text{-}MeHg}$	MeHg equilibrium partition coefficient for algae	4E6	L kg^{-1}
$K_{pom\text{-}MeHg}$	MeHg equilibrium partition coefficient for non-living organic solids	1E7	L kg^{-1}
$K_{pn\text{-}MeHg}$	MeHg equilibrium partition coefficients for inorganic solid group (silt, clay)	1E6	L kg^{-1}
$K_{photoDeg}$	MeHg photo-degradation rate constant into Hg0	0.01 (based on target rate of 10%/day at surface and 100 W PAR at surface)	m^2 W^{-1} d^{-1}
$K_{demeth-wat}$	MeHg biological demethylation rate constant	EPA (2001) WASP application to Savannah River, Georgia used 1E-4 day^{-1} which is an overall rate compared to the rate computed by CE-QUAL-W2.	m^3/g C decomposed
K_{p_silt}	MeHg equilibrium partition coefficient for silt	4E5 EPA (2001) WASP application to Savannah River, Georgia; Zhu et al. (2017) used 1E3.	L kg^{-1}
K_{p_sand}	MeHg equilibrium partition coefficient for sand	1E3 EPA (2001) WASP application to Savannah River, Georgia; $10^{2.5}$ soil partition coefficient (Knightes et al., 2014) ; Zhu et al. (2017) used 0.5E3.	L kg^{-1}
K_{doc}	MeHg equilibrium partition coefficients for DOC	2E5 EPA (2001) WASP application to Savannah River, Georgia; 10^6 (Knightes et al., 2014)	L kg^{-1}

TABLE 12. HG PARAMETERS FOR THE BED SEDIMENT LAYER.

Symbol	Description	Typical values	Units
	HgII		
v_m	HgII sediment-water mass transfer coefficient (velocity) for dissolved mercury	3X10-6 to 0.03 cm/d A (bio)diffusion coefficient values from the literature range from 0.01 to 100 cm^2/yr (Boudreau, 1997; Lecroart et al., 2010).	cm/d
$k_{doc\text{-}HgII}$	HgII equilibrium partition coefficient for DOC	4e6	L kg^{-1}
$K_{pom\text{-}HgII}$	HgII equilibrium partition coefficient for non-living organic solids	1e7	L kg^{-1}
$K_{pn\text{-}HgII}$	HgII equilibrium partition coefficient for inorganic solid group (silt, clay)	1e6	L kg^{-1}
$K_{meth-sed}$	HgII methylation rate constant	Helmich et al. (2022) report a value of 0.04 d^{-1} ±0.03 d^{-1} for the overall decay rate for aquatic sediments which would be comparable to $K_{meth\text{-}sed}$JPOC2. EPA (2001) in a WASP application to Savannah River, Georgia used 2E-5 day^{-1} which is an overall rate. Knightes et al. (2014) used overall maximum rates at 15°C of between 0.001-0.01 day^{-1}	m^3/g C decomposed
	MeHg		
v_m	MeHg sediment-water transfer coefficient (velocity)	3X10-6 to 0.03 cm/d A (bio)diffusion coefficient values from the literature range from 0.01 to 100 cm^2/yr (Boudreau, 1997; Lecroart et al., 2010).	cm d^{-1}
$K_{doc\text{-}MeHg}$	MeHg equilibrium partition coefficient for DOC	4e6	L kg^{-1}
$K_{pom\text{-}MeHg}$	MeHg equilibrium partition coefficient for non-living organic solids	1e7	L kg^{-1}
$K_{pn\text{-}MeHg}$	MeHg equilibrium partition coefficients for inorganic solid group (silt, clay)	1e6	L kg^{-1}

Symbol	Description	Typical values	Units
$K_{demeth-sed}$	MeHg biological demethylation rate constant	Helmich et al. (2022) report a value of 0.5 d^{-1} to 1.8 d^{-1} for the overall decay rate for aquatic sediments which would be comparable to $K_{demeth-sed}$JPOC2. EPA (2001) in a WASP application to Savannah River, Georgia used 2E-5 day^{-1} which is an overall rate. Knightes et al. (2014) used overall maximum rates at 20°C of between 0.003-0.03 day^{-1}	m^3/g C decomposed

Effect of Temperature on Methylation and Demethylation

Most researchers have used the Arrhenius method of adjusting methylation and demethylations rates by temperature. A summary of some of these studies are shown in Table 13 for methylation and demethylation.

Most studies report values in terms of Q_{10}, which is defined as

$$Q_{10} = \left(\frac{k_2}{k_1}\right)^{\frac{10}{T_2 - T_1}}$$

TABLE 13. METHYLATION AND DEMETHYLATION RATES AFFECTED BY TEMPERATURE.

Description	Q10	Base temperature, oC	Reference	Comments
Methylation	1.14	15	Knightes et al. (2014)	
	1.17 to 1.4	20	Harris and Beals (2012)	Used for temperatures between 20 and 30°C. Microbial activity was much higher with Q10 values between 2.1-3.63
Demethylation	1.04	20	Knightes et al. (2014)	
			Harris and Beals (2012)	

Initial Assessment: Hg Model Predictions Compared to Field Data

A simulation was performed using the model described in Wells et al. (2025) with Hg with a set of model parameters that have not been calibrated. This initial assessment is to provide a baseline for further improvements in model parameter selection. The model was run from January 1, 2014 to December 31, 2018 and evaluated profiles and outlet concentrations of Hg in Brownlee, Oxbow and Hells Canyon.

Brownlee Reservoir

Parameter values for this Hg model results for Brownlee Reservoir are shown in Table 14.

TABLE 14. HG COEFFICIENTS USED IN THE INITIAL ASSESSMENT SIMULATION IN BROWNLEE RESERVOIR.

$Hg Module Control File w2_Hg.csv				
$Brownlee Reservoir				
$11/11/2021 SWells				
Global	0			
"Model sediment processes of HgII, MeHg below the water body"	.TRUE.			
"Model HgII and MeHg partitioning on DOC for equilibrium (1) or non-equilibrium (2)"	1	1		
"Model HgII and MeHg partitioning on POM for equilibrium (1) or non-equilibrium (2)"	1	1		
"Model HgII and MeHg partitioning on ISS (1 to NSS) for equilibrium (1) or non-equilibrium (2)"	1	1		
"Model HgII and MeHg equilibrium partitioning on algae (1 to NAL)"	1	1		
"Model HgII and MeHg equilibrium partitioning on zooplankton (1 to NZP)"	1	1		
"Number of regions for Hg parameters"	4			
"Starting segment for regions"	2	70	129	167
"Ending segment for regions"	69	128	166	239
Water_Column	Region 1	Region 2	Region 3	Region 4
"Air concentration of Hg0 (ng/L)"	0.0015	0.0015	0.0015	0.0015
"Hg0 volatilization velocity definded by user, m/d"	0.5	0.5	0.5	0.5
"Hg0 volatilization velocity temperature correction coefficient"	1.024	1.024	1.024	1.024
"Hg0 photo-oxidation rate constant 1"	0.00188	0.00188	0.00188	0.00188
"Hg0 photo-oxidation rate constant 2"	-0.73385	-0.73385	-0.73385	-0.73385
"Hg0 photo-oxidation rate constant 3"	2.0409	2.0409	2.0409	2.0409
"HgII molecular weight, g/mol"	271.52	271.52	271.52	271.52
"HgII equilibrium partition coefficient for DOC, L/kg"	1.20E+07	1.20E+07	1.20E+07	1.20E+07

"HgII equilibrium partition coefficient for POM, L/kg"	1.50E+07	1.50E+07	1.50E+07	1.50E+07
"HgII equilibrium partition coefficient for ISS, L/kg, ISS group #1"	1.20E+06	1.20E+06	1.20E+06	1.20E+06
"HgII equilibrium partition coefficient for ISS, L/kg, ISS group #2"	3.20E+06	3.20E+06	3.20E+06	3.20E+06
"HgII equilibrium partition coefficient for ISS, L/kg, ISS group #3"	5.20E+06	5.20E+06	5.20E+06	5.20E+06
"HgII equilibrium partition coefficient for ISS, L/kg, ISS group #4"				
"HgII equilibrium partition coefficient for ISS, L/kg, ISS group #5"				
"HgII equilibrium partition coefficient for algae, L/kg, NAL group #1"	1.20E+07	1.20E+07	1.20E+07	1.20E+07
"HgII equilibrium partition coefficient for algae, L/kg, NAL group #2"	1.20E+07	1.20E+07	1.20E+07	1.20E+07
"HgII equilibrium partition coefficient for algae, L/kg, NAL group #3"	1.20E+07	1.20E+07	1.20E+07	1.20E+07
"HgII equilibrium partition coefficient for algae, L/kg, NAL group #4"				
"HgII equilibrium partition coefficient for algae, L/kg, NAL group #5"				
"HgII equilibrium partition coefficient for zooplankton, L/kg, Zoo group #1"	1.00E+07	1.00E+07	1.00E+07	1.00E+07
"HgII equilibrium partition coefficient for zooplankton, L/kg, Zoo group #2"				
"HgII equilibrium partition coefficient for zooplankton, L/kg, Zoo group #3"				
"HgII equilibrium partition coefficient for zooplankton, L/kg, Zoo group #4"				
"HgII equilibrium partition coefficient for zooplankton, L/kg, Zoo group #5"				
"HgII photoreduction rate constant for dissolved phase, m2/W/d"	0.03	0.03	0.03	0.03
"HgII photoreduction rate for DOC complexed phase, m2/W/d"	0.03	0.03	0.03	0.03
"HgII methylation rate for dissolved phase, m3/gC"	0.1	0.1	0.1	0.1
"HgII methylation rate for DOC complexed phase, m3/gC"	0.1	0.1	0.1	0.1
"HgII sediment-water mass transfer velocity or release rate, cm/d or (ng/L/d/g-O2)"	-0.6	-0.6	-0.1	-0.1
"MeHg molecular weight, g/mol"	230.66	230.66	230.66	230.66
"MeHg equilibrium partition coefficient for DOC, L/kg"	1.50E+06	1.50E+06	1.50E+06	1.50E+06
"MeHg equilibrium partition coefficient for POM, L/kg"	1.80E+06	1.80E+06	1.80E+06	1.80E+06
"MeHg equilibrium partition coefficient for ISS, L/kg, ISS group 1"	1.00E+05	1.00E+05	1.00E+05	1.00E+05
"MeHg equilibrium partition coefficient for ISS, L/kg, ISS group 2"	2.00E+05	2.00E+05	2.00E+05	2.00E+05
"MeHg equilibrium partition coefficient for ISS, L/kg, ISS group 3"	3.00E+05	3.00E+05	3.00E+05	3.00E+05
"MeHg equilibrium partition coefficient for ISS, L/kg, ISS group 4"				

"MeHg equilibrium partition coefficient for ISS, L/kg, ISS group 5"				
"MeHg equilibrium partition coefficient for algae, L/kg, ALG group 1"	1.80E+06	1.80E+06	1.80E+06	1.80E+06
"MeHg equilibrium partition coefficient for algae, L/kg, ALG group 2"	1.80E+06	1.80E+06	1.80E+06	1.80E+06
"MeHg equilibrium partition coefficient for algae, L/kg, ALG group 3"	1.80E+06	1.80E+06	1.80E+06	1.80E+06
"MeHg equilibrium partition coefficient for algae, L/kg, ALG group 4"				
"MeHg equilibrium partition coefficient for algae, L/kg, ALG group 5"				
"MeHg equilibrium partition coefficient for zooplankton, L/kg, Zoo group 1"	3000000	3000000	3000000	3000000
"MeHg equilibrium partition coefficient for zooplankton, L/kg, Zoo group 2"				
"MeHg equilibrium partition coefficient for zooplankton, L/kg, Zoo group 3"				
"MeHg equilibrium partition coefficient for zooplankton, L/kg, Zoo group 4"				
"MeHg equilibrium partition coefficient for zooplankton, L/kg, Zoo group 5"				
"MeHg photo-degradation rate for dissolved phase, m2/W/d"	0.0003	0.0003	0.0003	0.0003
"MeHg photo-degradation rate for DOC complexed phase, m2/W/d"	0.0003	0.0003	0.0003	0.0003
"MeHg demethylation rate from dissolved phase, m3/gC"	8.00E-02	8.00E-02	8.00E-02	8.00E-02
"MeHg demethylation rate from DOC complexed phase, m3/gC"	8.00E-02	8.00E-02	8.00E-02	8.00E-02
"MeHg sediment-water mass transfer velocity or release rate, cm/d or (ng/L/d/g-O2)"	-0.6	-0.6	-0.1	-0.1
"MethDemethC: 1: use JOC (units:m3/gC); 2: no JOC link (units:1/d)"	2	2	2	2
"Methylation Q10 if MethDemethC ==2"	1.75	1.75	1.75	1.75
"Demethylation Q10 if MethDemethC==2"	2	2	2	2
Sediment_Layer	Region 1	Region 2	Region 3	Region 4
"Use user-defined sediment burial velocity"	.FALSE.			
"Sediment burial velocity, m/d"	1.00E-04	1.00E-04	1.00E-04	1.00E-04
"Active sediment layer thickness, m"	0.03	0.03	0.03	0.03
"Sediment porosity"	0.8	0.8	0.8	0.8
"Sediment dry density, g/cm3"	2.2	2.2	2.2	2.2
"HgII equilibrium partition coefficient for DOC, L/kg"	1.00E+08	1.00E+08	1.00E+08	1.00E+08
"HgII equilibrium partition coefficient for POM, L/kg"	1.00E+07	1.00E+07	1.00E+07	1.00E+07
"HgII equilibrium partition coefficient for ISS, L/kg, ISS group #1"	1.00E+06	1.00E+06	1.00E+06	1.00E+06
"HgII equilibrium partition coefficient for ISS, L/kg, ISS group #2"	3.00E+06	3.00E+06	3.00E+06	3.00E+06

"HgII equilibrium partition coefficient for ISS, L/kg, ISS group #3"	5.00E +06	5.00E +06	5.00E +06	5.00E +06
"HgII equilibrium partition coefficient for ISS, L/kg, ISS group #4"				
"HgII equilibrium partition coefficient for ISS, L/kg, ISS group #5"				
"HgII methylation rate for dissolved phase, m3/gC"	0.1	0.1	0.1	0.1
"HgII methylation rate for DOC complexed phase, m3/gC"	0.1	0.1	0.1	0.1
"MeHg equilibrium partition coefficient for DOC, L/kg"	1.00E +08	1.00E +08	1.00E +08	1.00E +08
"MeHg equilibrium partition coefficient for POM, L/kg"	1.00E +06	1.00E +06	1.00E +06	1.00E +06
"MeHg equilibrium partition coefficient for ISS, L/kg ISS group#1"	1.00E +05	1.00E +05	1.00E +05	1.00E +05
"MeHg equilibrium partition coefficient for ISS, L/kg ISS group#2"	2.00E +05	2.00E +05	2.00E +05	2.00E +05
"MeHg equilibrium partition coefficient for ISS, L/kg ISS group#3"	3.00E +05	3.00E +05	3.00E +05	3.00E +05
"MeHg equilibrium partition coefficient for ISS, L/kg ISS group#4"				
"MeHg equilibrium partition coefficient for ISS, L/kg ISS group#5"				
"MeHg demethylation rate from dissolved phase, m3/gC or 1/day"	0.08	0.08	0.08	0.08
"MeHg demethylation rate from DOC complexed phase, m3/gC or 1/day"	0.08	0.08	0.08	0.08
Sediment_Initial_Conditions	Region 1	Region 2	Region 3	Region 4
"Number of regions for initial conditions"	4			
"Starting segment for initial conditions"	2	70	129	167
"Ending segment for initial conditions"	69	128	166	239
"Sediment concentration of total HgII ng/L"	6000	7250	9000	10000
"Sediment concentration of total MeHg ng/L"	400	400	500	500
"Sediment concentration of ISS, mg/L, ISS group #1"	49000	49000	49000	49000
"Sediment concentration of ISS, mg/L, ISS group #2"	50000	50000	50000	50000
"Sediment concentration of ISS, mg/L, ISS group #3"	52000	52000	52000	52000
"Sediment concentration of ISS, mg/L, ISS group #4"				
"Sediment concentration of ISS, mg/L, ISS group #5"				
Hg flux output file	Region 1	Region 2	Region 3	Region 4
"Number of regions for Hg fluxes"	4			
"Time interval for fluxes in days"	30			
"Starting segment for Hg flux output"	2	70	129	167
"Ending segment for Hg flux output"	69	128	166	239

Table 15 shows error statistics for Brownlee model-data outflow comparisons. Figure 15 and Figure 16 show model predicted HgII and MHg outflow comparisons to field data. Table 16 shows model-data error statistics for Brownlee profile comparisons of HgII and MHg.

Appendix C shows profile comparisons for HgII and MHg compared to field data. Table 17 shows water quality statistics for sediment and porewater concentrations of Hg.

Table 15. Water quality error statistics for Brownlee Reservoir outflow for HgII and MHg.

Parameter	Model Average	# of data	ME	MAE	RMSE	MAE/Model Average
MeHg - filtered (ng/l)	0.072	119	0.025	0.040	0.053	0.556
MeHg - particulate (ng/l)	0.047	122	0.019	0.029	0.037	0.617
MeHg - unfiltered (ng/l)	0.119	122	0.045	0.063	0.081	0.529
Hg(II) - filtered (ng/l)	0.456	124	0.071	0.145	0.210	0.318
Hg(II) - particulate (ng/l)	0.293	120	-0.018	0.206	0.535	0.703
Hg(II) - unfiltered (ng/l)	0.749	120	0.057	0.255	0.550	0.340
MeHg - particulate (ng/g)	21.91	65	8.185	12.183	15.736	0.556
Hg(II) - particulate (ng/g)	93.836	63	15.208	56.186	74.965	0.599

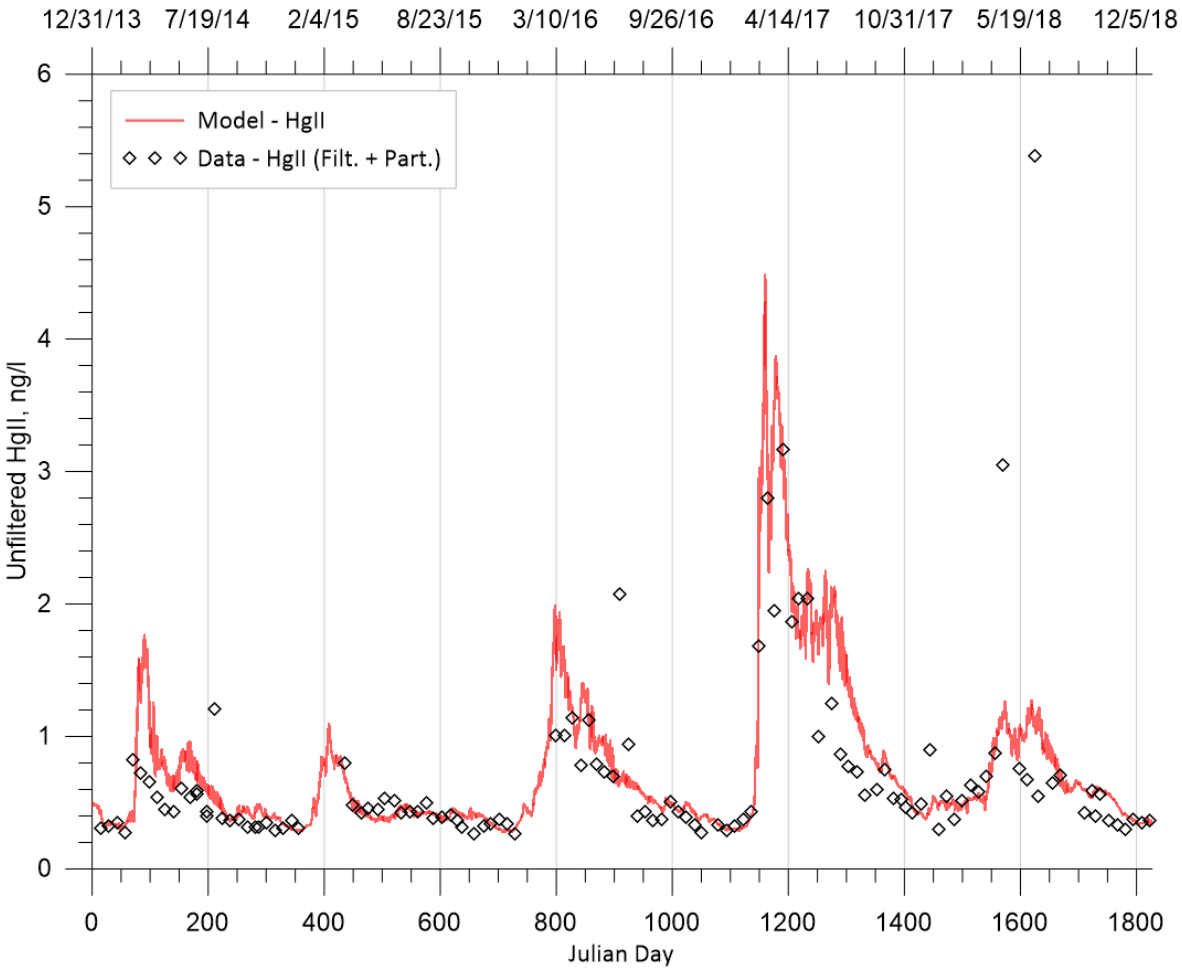

FIGURE 15. BROWNLEE RESERVOIR MODEL OUTFLOW HGII.

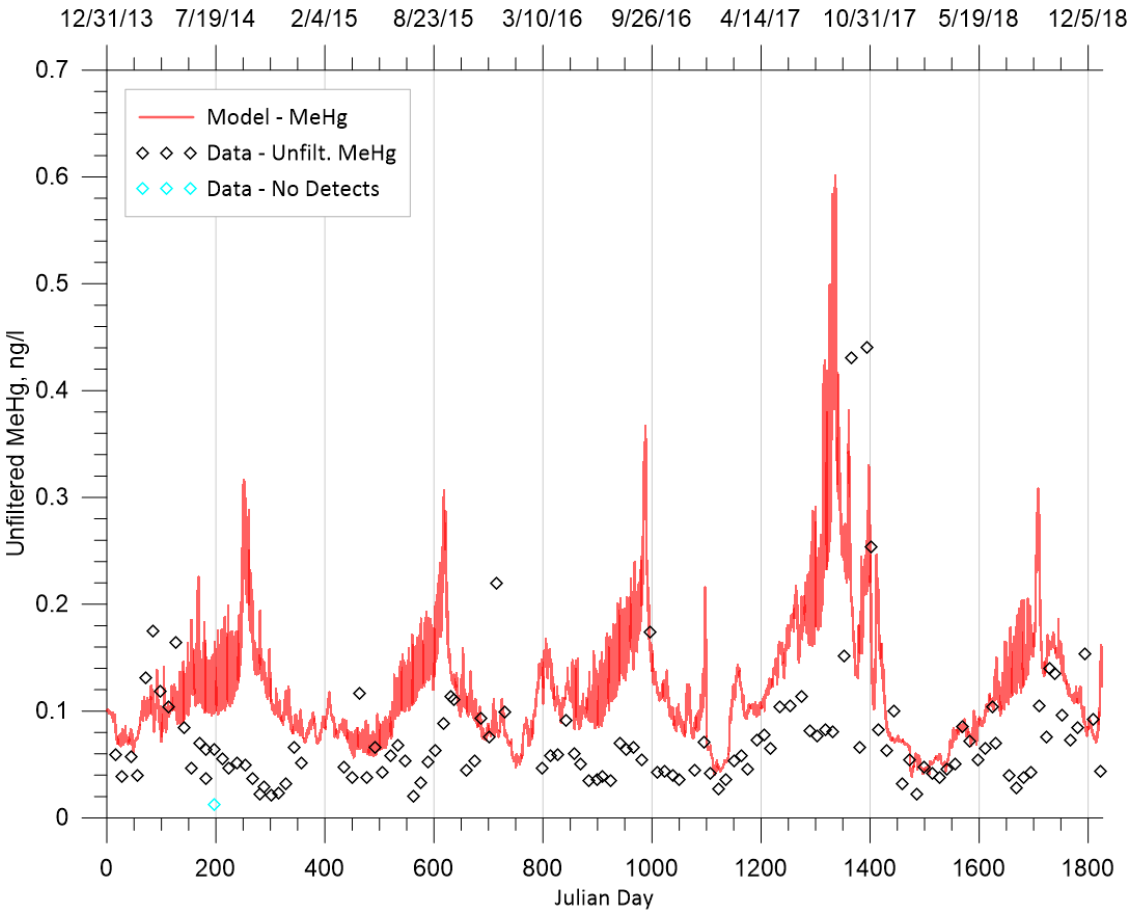

FIGURE 16. BROWNLEE RESERVOIR MODEL OUTFLOW MEHG.

Table 16. Water quality error statistics for Brownlee Reservoir vertical profiles for HgII and MHg.

Parameter	# of Profiles	# of Data	ME	MAE	RMSE
Particulate HgII_w (ng/l)	138	590	0.054	0.326	0.359
Particulate HgII_s (ng/g)	93	381	-55.625	102.370	124.452
Particulate MeHg_w (ng/l)	143	608	-0.007	0.066	0.091
Particulate MeHg_s (ng/g)	98	395	-26.461	37.153	55.810
Dissolved HgII (ng/l)	143	617	-0.025	0.186	0.219
Dissolved MeHg (ng/l)	139	574	-0.077	0.144	0.213

Table 17. Water quality error statistics for Brownlee Reservoir sediment and porewater comparisons for Hg.

Parameter	Model Average	# of Data	ME	MAE	RMSE
HgII - sediment (ng/g)	52.863	42	-4.736	9.172	12.660
MeHg - sediment (ng/g)	3.634	42	0.583	1.539	2.068
HgII - porewater (ng/l)	3.945	14	-4.690	9.689	14.438
MeHg - porewater (ng/l)	3.642	14	2.458	2.468	2.970
HgII - bottom of water column - part. (ng/l)	0.704	57	-3.663	3.804	6.975
HgII - bottom of water column - filt. (ng/l)	0.443	49	-0.767	0.952	2.234
HgII - bottom of water column - part. (ng/g)	104.603	54	-116.674	179.303	485.257
MeHg - bottom of water column - part. (ng/l)	0.160	57	-0.352	0.433	0.807
MeHg - bottom of water column - filt. (ng/l)	0.183	58	-0.169	0.296	0.562
MeHg - bottom of water column - part. (ng/g)	34.015	54	-16.711	56.160	212.930

Oxbow Reservoir

Table 18 shows error statistics for Oxbow model-data outflow comparisons. Figure 17 and Figure 18 show model predicted HgII and MHg outflow comparisons to field data. Table 19 shows model-data error statistics for Oxbow profile comparisons of HgII and MHg. Appendix C shows profile comparisons for HgII and MHg compared to field data.

Table 18. Water quality error statistics for Oxbow Reservoir outflow.

Parameter	Model Average	# of data	ME	MAE	RMSE	MAE/Model Average
MeHg - filtered (ng/l)	0.000	115	-0.049	0.049	0.060	N/A
MeHg - particulate (ng/l)	0.100	118	0.076	0.077	0.103	0.770
MeHg - unfiltered (ng/l)	0.246	121	0.177	0.178	0.204	0.724
Hg(II) - filtered (ng/l)	0.364	124	-0.018	0.107	0.163	0.294

Parameter	Model Average	# of data	ME	MAE	RMSE	MAE/Model Average
Hg(II) - particulate (ng/l)	0.221	118	-0.081	0.158	0.349	0.715
Hg(II) - unfiltered (ng/l)	0.585	118	-0.094	0.176	0.365	0.301
MeHg - particulate (ng/g)	45.594	61	36.444	36.444	41.586	0.799
Hg(II) - particulate (ng/g)	73.591	62	-10.492	47.612	61.612	0.647

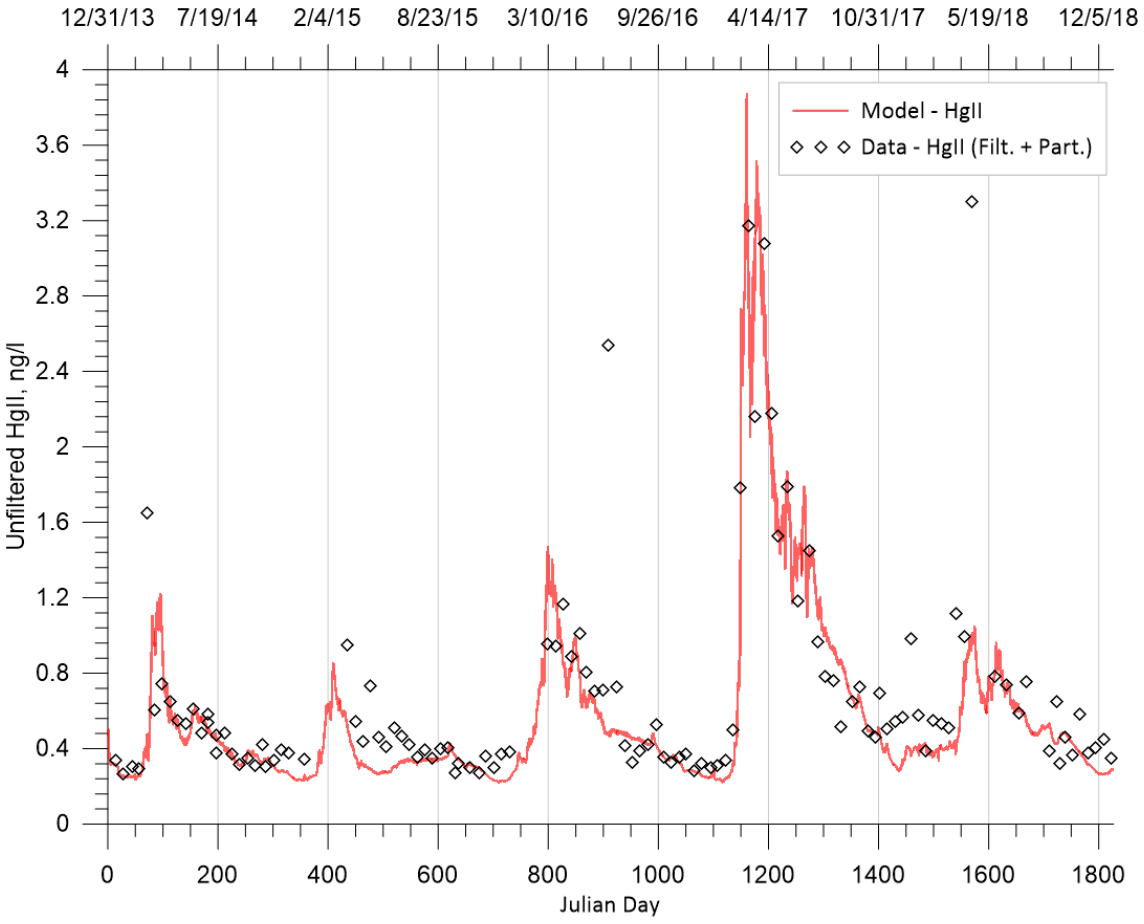

FIGURE 17. OXBOW RESERVOIR MODEL OUTFLOW HGII COMPARED TO DATA.

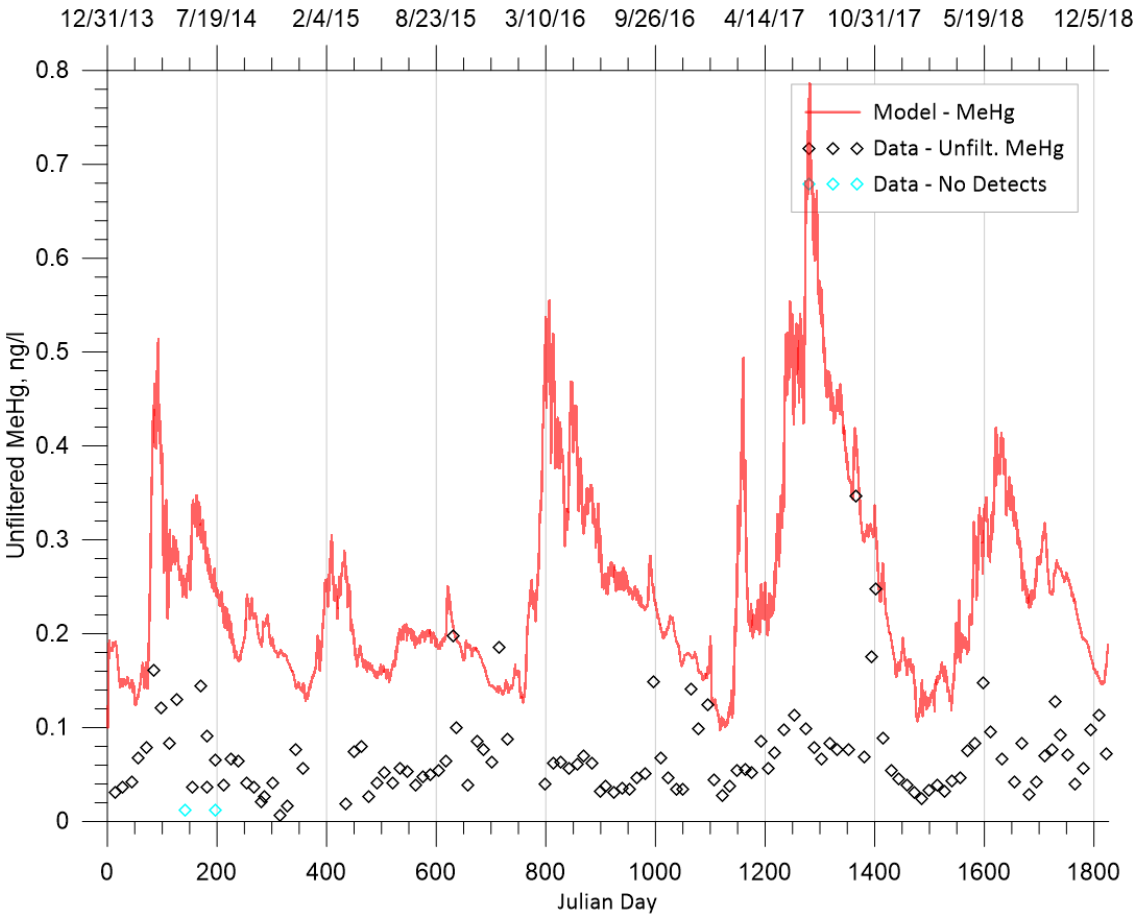

FIGURE 18. OXBOW RESERVOIR MODEL OUTFLOW MEHG COMPARED TO DATA.

Table 19. Water quality error statistics for Oxbow Reservoir vertical profiles.

Parameter	# of Profiles	# of Data	ME	MAE	RMSE
HgII (ng/l)	4	17	-0.083	0.094	0.126
MeHg (ng/l)	4	17	0.037	0.173	0.262
Particulate HgII_w (ng/l)	4	17	-0.067	0.067	0.074
Particulate HgII_s (ng/g)	3	14	-44.745	45.218	57.683
Particulate MeHg_w (ng/l)	4	17	0.023	0.033	0.035
Particulate MeHg_s (ng/g)	3	14	19.860	25.449	26.331
Dissolved HgII (ng/l)	4	17	-0.016	0.083	0.100
Dissolved MeHg (ng/l)	4	16	0.012	0.138	0.228

Hells Canyon Reservoir

Table 20 shows error statistics for Oxbow model-data outflow comparisons. Table 21 shows model-data error statistics for Oxbow profile comparisons of HgII and MHg. Appendix C shows profile comparisons for HgII and MHg compared to field data. Table 22 shows water quality statistics for sediment and porewater concentrations of Hg.

Table 20. Water quality error statistics for Hells Canyon Reservoir outflow.

Parameter	Model Average	# of data	ME	MAE	RMSE	MAE/Model Average
MeHg - filtered (ng/l)	0.000	104	-0.042	0.042	0.054	N/A
MeHg - particulate (ng/l)	0.081	116	0.058	0.059	0.079	0.728
MeHg - unfiltered (ng/l)	0.230	221	0.132	0.142	0.165	0.617
Hg(II) - filtered (ng/l)	0.375	120	0.020	0.131	0.242	0.349
Hg(II) - particulate (ng/l)	0.188	112	-0.131	0.170	0.353	0.904
Hg(II) - unfiltered (ng/l)	0.562	112	-0.092	0.161	0.357	0.286
MeHg - particulate (ng/g)	43.015	60	35.103	35.106	39.720	0.816
Hg(II) - particulate (ng/g)	71.828	56	-21.658	47.664	68.274	0.664

Table 21. Water quality error statistics for Hells Canyon Reservoir vertical profiles.

Parameter	# of Profiles	# of Data	ME	MAE	RMSE
HgII (ng/l)	38	180	-0.198	0.272	0.372
MeHg (ng/l)	38	180	-0.245	0.503	0.756
Particulate HgII_w (ng/l)	38	182	-0.222	0.252	0.330
Particulate HgII_s, (ng/g)	16	89	-62.352	95.644	108.399
Particulate MeHg_w (ng/l)	38	180	-0.027	0.112	0.153
Particulate MeHg_s (ng/g)	16	87	30.036	44.423	51.571

Parameter	# of Profiles	# of Data	ME	MAE	RMSE
Dissolved HgII (ng/l)	38	181	0.017	0.168	0.200
Dissolved MeHg (ng/l)	38	178	-0.418	0.418	0.710

Table 22. Water quality error statistics for Hells Canyon Reservoir sediment and porewater comparisons.

Parameter	Model Average	# of Data	ME	MAE	RMSE
HgII - sediment (ng/g)	57.212	8	-13.231	21.792	26.587
MeHg - sediment (ng/g)	0.216	8	-2.264	2.264	2.552
HgII - porewater (ng/l)	1.022	2	-4.759	5.726	7.445
MeHg - porewater (ng/l)	36.762	3	41.986	41.986	48.449
HgII - bottom of water column - part. (ng/l)	7.863	6	-2.530	7.177	11.033
HgII - bottom of water column - filt. (ng/l)	101.663	6	166.328	166.328	185.131
HgII - bottom of water column - part. (ng/g)	0.217	6	-96.701	96.701	109.646
MeHg - bottom of water column - part. (ng/l)	91.104	6	165.969	165.969	168.579
MeHg - bottom of water column - filt. (ng/l)	0.472	6	0.680	0.680	0.691
MeHg - bottom of water column - part. (ng/g)	0.160	6	-5.620	5.620	6.002

Summary

This report summarizes the development of the Mercury model in CE-QUAL-W2 for the Hells Canyon complex (Brownlee Reservoir, Oxbow Reservoir, and Hells Canyon Reservoir) on the Snake River. The CE-QUAL-W2 model framework provides for horizontal and vertical advection and dispersion. The report describes the following:

- Hg module in CE-QUAL-W2 including state variables: Hg0 (elemental mercury), HgII (inorganic mercury), and MeHg (methylmercury). The model uses equilibrium partitioning of HgII and MeHg on solids. These solids include inorganic suspended solids, organic solids (refractory organic matter, RPOM, and labile particulate organic matter, LPOM), algae, and zooplankton. The Hg model was divided into a water column model and a bed sediment model and included these processes:
    - Water Column processes: photoreduction, photo-oxidation, photodegradation, volatilization, methylation, demethylation, diffusion to and from the sediment layer, and settling
    - Sediment processes: diffusion to and from the sediment bed, burial, methylation, demethylation
- Hg Bed Sediment Dynamics including its connection to the CE-QUAL-W2 sediment diagenesis model. The Hg sediment model uses temperature, organic solids concentrations, diffusion rates between the water and bed, and C turnover rates.

The report also describes the location of field data used for boundary conditions and for internal model-data comparisons. The process for computing time series of Hg0, HgII, and MeHg was described.

Also, a table was presented with model coefficient suggestions for calibration.

An initial assessment of the model calibration for HgII and MeHg was presented as a baseline for further improvements in the model, not as a finished calibration. Model-data error statistics were provided for profiles, outflows from the dams and in the sediment.

Appendix A presents a detailed overall of how to use the CE-QUAL-W2 Hg model and what input files and output files are required. Appendix B presents a section on non-equilibrium sorption if that is to be used in the future. Appendix C shows model coefficients used in the preliminary Hg model results. Appendix D shows profile model-data comparisons in Brownlee, Oxbow and hells Canyon as an initial assessment.

Next steps in refining the Hg model within CE-QUAL-W2 could include the following:

- Add partitioning onto particulate Fe and Mn in the Hg algorithm. Currently partitioning onto solids did not include partitioning onto FeOOH and MnO_2.
- Continue to improve methylation/demethylation processes by accounting for processes that may be important in Brownlee Reservoir. This may include age of anoxia of a water cell, NO_3-N concentrations, and/or SO_4 concentrations. The age of

anoxia was explored in some preliminary model simulations, such as shown in Figure 19 showing the increasing age of anoxia with depth near Brownlee dam.

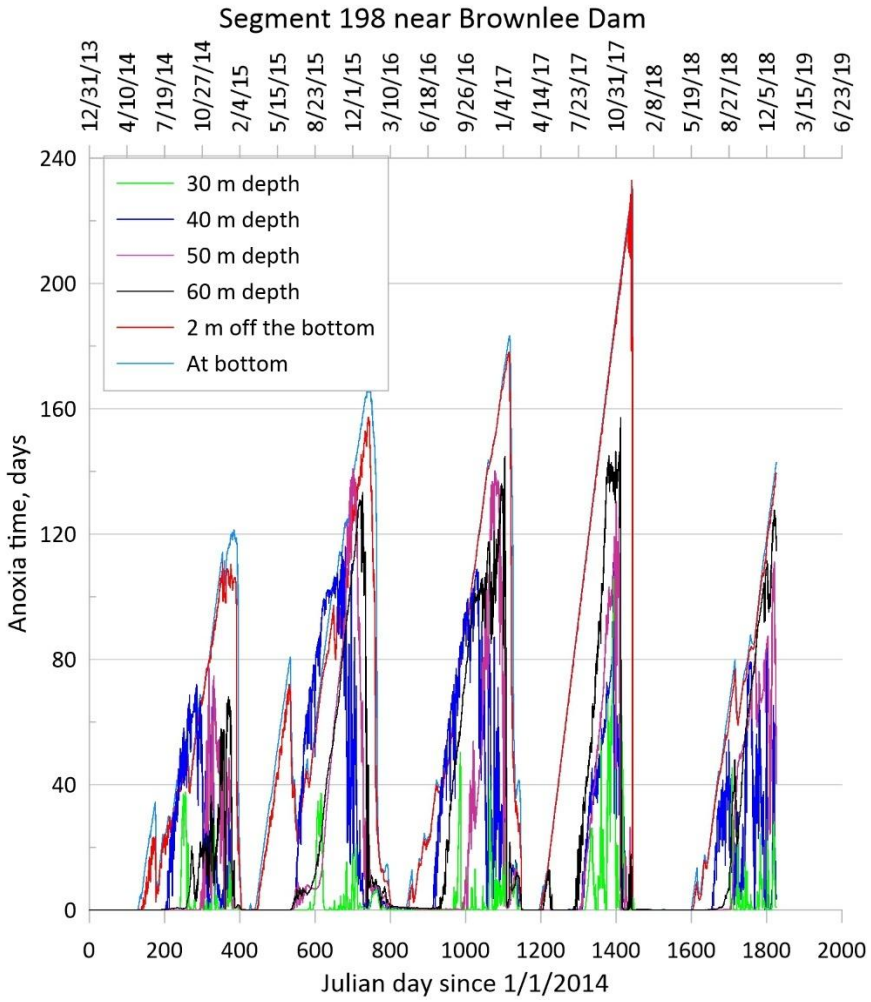

FIGURE 19. AGE OF ANOXIA IN BROWNLEE RESERVOIR AT SPECIFIC VERTICAL DEPTHS BETWEEN 2014-2018.

References

Appling, A. P., Leon, M.C., McDowell, W.H. 2015. Reducing Bias and Quantifying Uncertainty in Watershed Flux Estimates: The R Package Loadflex. Ecosphere, 6, pp 1-25.

Aulenback, B.T., Hooper, R.P. 2006. The Composite Method: An Improved Method for Stream-Water Solute Load Estimation. Hydrol. Processes. 20, pp. 3029-3047.

Baldwin, A.K., C.A. Eagles-Smith, J.J. Willacker, B.A. Poulin, D.P. Krabbenhoft, J. Naymik, M.T. Tate, D. Bates, N. Gastelecutto, C. Hoovestol, and C. Larsen. 2022. In-reservoir physical

processes modulate aqueous and biological methylmercury export from a seasonally anoxic reservoir. Environ Sci Technol. 56(19):13751–13760. doi:10.1021/acs.est.2c03958.

Beutel, M.W.; DeSilva, L.; Amegbletor, L. 2021. Direct Measurement of Mercury Deposition at Rural and Suburban Sites in Washington State, USA. Atmosphere 2021, 12, 35. https://doi.org/10.3390/atmos12010035

Boudreau BP. 1997. Diagenetic Models and Their Implementation: Modelling Transport and Reactions in Aquatic Sediments. Springer, Berlin/Heidelberg, Germany. 414 p.

EPA . 2001. TMDL for Total Mercury in Fish Tissue Residue in the Middle and Lower Savannah River Watershed, EPA Region 4, February 28, 2001.

Harris, R, and Beals, C. 2012. Effects of Climate Change On Mercury Cycling and Bioaccumulation in the Great Lakes Region, Great Lakes Atmospheric Deposition (GLAD) Program 2009 GLAD Program Contract 09-05, Prepared for the U.S. Environmental Protection Agency, October 2012.

Harris, R., Hutchinson, D., and Beals, D. 2020. "Application of the Dynamic Mercury Cycling Model (D-MCM) to the South River, Virginia," Final Report Prepared for: Nancy R. Grosso DuPont Corporate Remediation Group, E. I. du Pont de Nemours and Company Wilmington, Delaware, April 21, 2020.

Harris, R. 2022. Personal communication.

Helmrich, Stefanie; Vlassopoulos, Dimitri; Alpers, Charles N.; O'Day, Peggy A. 2022. "Critical review of mercury methylation and methylmercury demethylation rate constants in aquatic sediments for biogeochemical modeling," Critical Reviews in Environmental Science and Technology, doi: 10.1080/10643389.2021.2013073.

Hirsch RM. 2019. Making WRTDS_K flux estimates: U.S. Geological Survey Exploration and Graphics for RivEr Trends (EGRET); [cited 4 Nov 2020]. Available from http://usgsr.github.io/EGRET/articles/Making%20 WRTDS_K%20flux%20estimates.html.

Hirsch RM, De Cicco LA. 2015. User guide to Exploration and Graphics for RivEr Trends (EGRET) and dataRetrieval: R packages for hydrologic data (version 2.0, Feb 2015): U.S. Geological Survey Techniques and Methods 4-A10; 104 p.

Knightes, C., Golden, H., Journey, C., Davis, G., Conrads, P., Marvin-DiPasquale, M., Brigham, M., Bradley, P. 2014. Mercury and methylmercury stream concentrations in a Coastal Plain watershed: A multi-scale simulation analysis, Environmental Pollution, Volume 187, 2014, Pages 182-192, https://doi.org/10.1016/j.envpol.2013.12.026.

Lee, Cindy. 1992. "Controls on organic carbon preservation: The use of stratified water bodies to compare intrinsic rates of decomposition in oxic and anoxic systems," Geochimica

et Cosmochimica Acta, Volume 56, Issue 8, 1992, Pages 3323-3335, doi.org/10.1016/0016-7037(92)90308-6.

Marvin-DiPasquale, M., Agee, J.L., Kakouros, E., Kieu, L.H., Arias, M.R., Baesman, S.M., Poulin, B.A., Antweiler, R.C., Fuller, C.C., Tate, M.T., and Krabbenhoft, D.P., 2020, Biogeochemical Data for Mercury and other Constituents in Surface Sediment and Deep Cores from the Hells Canyon Reservoir Complex, Idaho and Oregon 2014-2018: U.S. Geological Survey data release, https://doi.org/10.5066/P9L4XCD0.

Mill, T., W. R. Mabey, D. C. Bomberger, T. W. Chou, D. G. Hendrey, and J. H. Smith. 1982. Laboratory protocols for evaluating the fate of organic chemicals in air and water. EPA-600/3-82-022. Athens, GA.: U.S. Environmental Protection Agency, Environmental Research Laboratory.

Naymik J., Larsen C.A., Myers R., Hoovestol C., Gastelecutto N., and Bates, D. 2023. Long-term trends in inflowing chlorophyll a and nutrients and their relation to dissolved oxygen in a large western reservoir, Lake and Reservoir Management, DOI: 10.1080/10402381.2022.2160395

Sanemasa, I. 1975. “The Solubility of Elemental Mercury in Vapor in Water,” Bulletin of the Chemical Society of Japan, 48 (6), 1795-1798.

Senlin Zhu, Zhonglong Zhang, Dušan Žagar. 2018. Mercury transport and fate models in aquatic systems: A review and synthesis. Science of The Total Environment, 15 October 2018.

Wang, Y., Peng, Y., Wang, D., Zhang, C. 2014. Wet deposition fluxes of total mercury and methylmercury in core urban areas, Chongqing, China, Atmospheric Environment, Volume 92, 2014, Pages 87-96.

Wells, S., Garstecki, B., Berger, C., Naymik, J. 2025. “Hells Canyon Complex CE-QUAL-W2 Water Quality Model Development and Calibration,” Department of Civil and Environmental Engineering, Portland State University, Portland, OR.

Wells, S. A., editor. 2024. "CE-QUAL-W2: A two-dimensional, laterally averaged, hydrodynamic and water quality model, version 4.5, user manual parts 1-5," Department of Civil and Environmental Engineering, Portland State University, Portland, OR.

Yoder, A.M., Baldwin, A., Marvin-DiPasquale, M., Poulin, B. A., Naymik, J., Krabbenhoft, D. P. 2024 *accepted*. Longitudinal and seasonal changes of organic matter sources through a semi-arid river-reservoir system. Journal of Geophysical Research – Biogeosciences.

Zhang, Z. and Johnson, B. 2016. Aquatic Contaminant and Mercury Simulation Modules Developed for Hydrologic and Hydraulic Models, Environmental Quality Technology Research Program ERDC/EL TR-16-8, Environmental Laboratory U.S. Army Engineer Research and Development Center 3909 Halls Ferry Road Vicksburg, MS.

Zhang, L., Zhou, P., Cao, S., and Zhao, Y. 2019. Atmospheric mercury deposition over the land surfaces and the associated uncertainties in observations and simulations: a critical review, Atmos. Chem. Phys., 19, 15587–15608, https://doi.org/10.5194/acp-19-15587-2019.

Zhu, S., Zhang, Z., Liu, X. 2017. Enhanced Two Dimensional Hydrodynamic and Water Quality Model (CE-QUAL-W2) for Simulating Mercury Transport and Cycling in Water Bodies, *Water*, 2017, 9, 643; doi:10.3390/w9090643

Appendix A: Implementation of Hg Model in CE-QUAL-W2

This Appendix describes how to turn use the Hg module in CE-QUAL-W2. The required input files described below are in the Excel macro-enabled worksheet as separate tabs that can be written out as input files to the CE-QUAL-W2 model. This section assumes familiarity with the CE-QUAL-W2 model and its User manual (Wells, 2024).

Input File: w2_con.csv

The Hg module in CE-QUAL-W2 can be turned ON/OFF by following these steps:

1. In the w2_con.csv tab, turn ON HG

w2_con.csv file format	CE-QUAL-W2 Version		4.5						
	Control File version		4.5	w2_con45.csv					
TITLE C	**Title comments: next 10 lines**								
Any comment - this is written only to the SNP file	"CE-QUAL-W2 Model / Version 4.5"								
:s.	"Brownlee Reservoir"								
tied to the name of the tab	"2014-2018"								
	"5 WB model/ 7 branches"								
	"Hg Module Zhong Zhang"								
	""								
:ttom) Export to CSV file	"Scott Wells, Chris Berger, Bernadel Garstecki"								
	""								
	""								
	""								
GRID/NPROC/CLOSE DIALOG BOX	**NWB**	NBR	IMX	KMX	NPROC	CLOSEC			
	5	7	239	102	1	OFF			
IN/OUTFLOW	**NTR**	NST	NIW	NWD	NGT	NSP	NPI	NPU	
	2	0	0	0	6	0	0	0	
CONSTITUENTS	**NGC**	NSS	NAL	NEP	NBOD	NMC	NZP		
	3	1	3	1	0	0	1		
MISCELLANEOUS	**NDAY**	SELECTC	HABTATC	ENVIRPC	AERATEC	INITUWL	ORGCC	SED_DIAG	HG
	400	OFF	OFF	OFF	OFF	OFF	OFF	ON	ON

NDAY	SELECTC	HABTATC	ENVIRPC	AERATEC	INITUWL	ORGCC	SED_DIAG	HG
400	OFF	OFF	OFF	OFF	OFF	OFF	ON	ON

2. In the w2_con.csv tab, make sure that Hg0, Hg2, and MeHg are active constituents.

CST - Concentration State variables and initial conditions		CNAME2 Short na	CNAME Long name
	1	TDS	"TDS, g/m^3 "
	2	Gen1-Tr	"Tracer, g/m^3 "
	3	Gen2-Cnd	"Conductivity, uS/cm "
	4	Gen3-Cl	"Chloride, mg/l "
	5	ISS1	"ISS, g/m^3 "
	6	ISS2	"ISS, g/m^3 "
	7	WaterAge	"Age, days "
	8	Bacteria	"Bacteria, col/100ml "
	9	DGP	"Dissolved Gas Pressure,atm "
	10	N2	"N2 dissolved gas, mg/l "
	11	H2S	"H2S, dissolved gas, mg S/l "
	12	CH4	"CH4 dissolved gas, mg C/l "
	13	SO4	"SO4 dissolved, mg S/l "
	14	FEII	"Reduced FE(II), mg/l "
	15	FEOOH	"Oxidized FeOOH, mg/l "
	16	MnII	"Reduced Mn(II), mg Fe/l "
	17	MnO2	"Oxidized MnO2, mg Mn/l
	18	PO4	"Phosphate, gP/m^3"
	19	NH4	"Ammonium, gN/m^3 "
	20	NO3	"Nitrate-Nitrite, gN/m^3 "
	21	DSI	"Dissolved silica, g/m^3 "
	22	PSI	"Particulate silica, g/m^3 "
	23	LDOM	"Labile DOM, g/m^3 "
	24	RDOM	"Refractory DOM, g/m^3 "
	25	LPOM	"Labile POM, g/m^3 "
	26	RPOM	"Refractory POM, g/m^3 "
	27	ALG1	"Algae1, g/m^3 "
	28	ALG2	"Algae2, g/m^3 "
	29	ALG3	"Algae3, g/m^3 "
	30	DO	"Dissolved oxygen, g/m^3 "
	31	TIC	"Inorganic carbon, g/m^3 "
	32	ALK	"Alkalinity, g/m^3 "
	33	ZOO1	"Zoo1, g/m^3 "
	34	LDOM-P	"LDOM P, mg/m^3 "
	35	RDOM-P	"RDOM P, mg/m^3 "
	36	LPOM-P	"LPOM P, mg/m^3 "
	37	RPOM-P	"RPOM P, mg/m^3 "
	38	LDOM-N	"LDOM N, mg/m^3 "
	39	RDOM-N	"RDOM N, mg/m^3 "
	40	LPOM-N	"LPOM N, mg/m^3 "
	41	RPOM-N	"RPOM N, mg/m^3 "
	42	MICROCYSTIN	"Microcystin, g/m^3"
	43	CYLINDROSPERM	"Clindrospermopsin, g/m^3"
	44	ANATOXIN-A	"Anatoxin-A, g/m^3"
	45	SAXITOXIN	"Saxitoxin, g/m^3"
	46	Hg0	"Hg0, ng/L"
	47	HgII_total	"HgII total, ng/L"
	48	MeHg_total	"MeHg total, ng/L"

3. Specify which input files have these as inputs including atmospheric deposition.

CNAME2 Short na	CNAME Long name	CAC Active	FMTC Fort	CMULT Output N	C2I(JW)-init	C2I(JW)-in	C2I(JW)-in	C2I(JW)-in	C2I(JW)-in	CPRWBC(JW	CPRWBC(JW)-prin	CPRWBC(JW)-print	CPRWBC(JW	CPRWBC(JW	C_ATM_DE	C_ATM_DE	C_ATM_DE	C_ATM_DE	C_ATM_DE
TDS	"TDS, g/m^3 "	OFF	(F10.3)	1	70	70	70	70	70	OFF	OFF	OFF	OFF	OFF	OFF	OFF	OFF	OFF	OFF
Gen1-Tr	"Tracer, g/m^3 "	OFF	(g10.3)	1	0	0	0	0	0	OFF	OFF	OFF	OFF	OFF	OFF	OFF	OFF	OFF	OFF
Gen2-Cnd	"Conductivity, uS/cm "	OFF	(g10.3)	1	58	58	58	58	58	OFF	OFF	OFF	OFF	OFF	OFF	OFF	OFF	OFF	OFF
Gen3-Cl	"Chloride, mg/l "	ON	(g10.3)	1	19	19	19	19	19	ON	ON	ON	ON	ON	OFF	OFF	OFF	OFF	OFF
ISS1	"ISS, g/m^3 "	ON	(F10.3)	1	1.5	1.5	1.5	1.5	1.5	ON	ON	ON	ON	ON	OFF	OFF	OFF	OFF	OFF
ISS2	"ISS, g/m^3 "	ON	(F10.3)	1	1.5	1.5	1.5	1.5	1.5	ON	ON	ON	ON	ON	OFF	OFF	OFF	OFF	OFF
WaterAge	"Age, days "	ON	(F10.3)	1	0	0	0	0	0	ON	ON	ON	ON	ON	OFF	OFF	OFF	OFF	OFF
Bacteria	"Bacteria, col/100ml "	OFF	(F10.3)	1	0	0	0	0	0	OFF	OFF	OFF	OFF	OFF	OFF	OFF	OFF	OFF	OFF
DGP	"Dissolved Gas Pressure,atm "	OFF	(F10.3)	1	0	0	0	0	0	OFF	OFF	OFF	OFF	OFF	OFF	OFF	OFF	OFF	OFF
N2	"N2 dissolved gas, mg/l "	OFF	(F10.3)	1	0	0	0	0	0	OFF	OFF	OFF	OFF	OFF	OFF	OFF	OFF	OFF	OFF
H2S	"H2S, dissolved gas, mg S/l "	ON	(F10.3)	1	0	0	0	0	0	ON	ON	ON	ON	ON	OFF	OFF	OFF	OFF	OFF
CH4	"CH4 dissolved gas, mg C/l "	ON	(F10.3)	1	0	0	0	0	0	ON	ON	ON	ON	ON	OFF	OFF	OFF	OFF	OFF
SO4	"SO4 dissolved, mg S/l "	ON	(F10.3)	1	56	56	56	56	56	ON	ON	ON	ON	ON	OFF	OFF	OFF	OFF	OFF
FEII	"Reduced FE(II), mg/l "	ON	(F10.3)	1	0	0	0	0	0	ON	ON	ON	ON	ON	OFF	OFF	OFF	OFF	OFF
FEOOH	"Oxidized FeOOH, mg/l "	ON	(F10.3)	1	0.2	0.2	0.2	0.2	0.2	ON	ON	ON	ON	ON	OFF	OFF	OFF	OFF	OFF
MnII	"Reduced Mn(II), mg Fe/l "	ON	(F10.3)	1	0	0	0	0	0	ON	ON	ON	ON	ON	OFF	OFF	OFF	OFF	OFF
MnO2	"Oxidized MnO2, mg Mn/l "	ON	(F10.3)	1	0.28	0.28	0.28	0.28	0.28	ON	ON	ON	ON	ON	OFF	OFF	OFF	OFF	OFF
PO4	"Phosphate, gP/m^3"	ON	(F10.3)	1	0.045	0.045	0.045	0.045	0.045	ON	ON	ON	ON	ON	OFF	OFF	OFF	OFF	OFF
NH4	"Ammonium, gN/m^3 "	ON	(F10.3)	1	0.03	0.03	0.03	0.03	0.03	ON	ON	ON	ON	ON	OFF	OFF	OFF	OFF	OFF
NO3	"Nitrate-Nitrite, gN/m^3 "	ON	(F10.3)	1	2	2	2	2	2	ON	ON	ON	ON	ON	OFF	OFF	OFF	OFF	OFF
DSI	"Dissolved silica, g/m^3 "	OFF	(F10.3)	1	0	0	0	0	0	OFF	OFF	OFF	OFF	OFF	OFF	OFF	OFF	OFF	OFF
PSI	"Particulate silica, g/m^3 "	OFF	(F10.3)	1	0	0	0	0	0	OFF	OFF	OFF	OFF	OFF	OFF	OFF	OFF	OFF	OFF
LDOM	"Labile DOM, g/m^3 "	ON	(F10.3)	1	3	3	3	3	3	ON	ON	ON	ON	ON	OFF	OFF	OFF	OFF	OFF
RDOM	"Refractory DOM, g/m^3 "	ON	(F10.3)	1	3	3	3	3	3	ON	ON	ON	ON	ON	OFF	OFF	OFF	OFF	OFF
LPOM	"Labile POM, g/m^3 "	ON	(F10.3)	1	0.5	0.5	0.5	0.5	0.5	ON	ON	ON	ON	ON	OFF	OFF	OFF	OFF	OFF
RPOM	"Refractory POM, g/m^3 "	ON	(F10.3)	1	0.5	0.5	0.5	0.5	0.5	ON	ON	ON	ON	ON	OFF	OFF	OFF	OFF	OFF
ALG1	"Algae1, g/m^3 "	ON	(F10.3)	1	0.005	0.005	0.005	0.005	0.005	ON	ON	ON	ON	ON	OFF	OFF	OFF	OFF	OFF
ALG2	"Algae2, g/m^3 "	ON	(F10.3)	1	0.005	0.005	0.005	0.005	0.005	ON	ON	ON	ON	ON	OFF	OFF	OFF	OFF	OFF
ALG3	"Algae3, g/m^3 "	ON	(F10.3)	1	0.005	0.005	0.005	0.005	0.005	ON	ON	ON	ON	ON	OFF	OFF	OFF	OFF	OFF
DO	"Dissolved oxygen, g/m^3 "	ON	(F10.3)	1	10.7	10.7	10.7	10.7	10.7	ON	ON	ON	ON	ON	OFF	OFF	OFF	OFF	OFF
TIC	"Inorganic carbon, g/m^3 "	ON	(F10.3)	1	5.92	5.92	5.92	5.92	5.92	ON	ON	ON	ON	ON	OFF	OFF	OFF	OFF	OFF
ALK	"Alkalinity, g/m^3 "	ON	(F10.3)	1	22	22	22	22	22	ON	ON	ON	ON	ON	OFF	OFF	OFF	OFF	OFF
ZOO1	"Zoo1, g/m^3 "	ON	(F10.3)	1	0.001	0.001	0.001	0.001	0.001	ON	ON	ON	ON	ON	OFF	OFF	OFF	OFF	OFF
LDOM-P	"LDOM P, mg/m^3 "	ON	(F10.3)	1	0.003	0.003	0.003	0.003	0.003	ON	ON	ON	ON	ON	OFF	OFF	OFF	OFF	OFF
RDOM-P	"RDOM P, mg/m^3 "	ON	(F10.3)	1	0.003	0.003	0.003	0.003	0.003	ON	ON	ON	ON	ON	OFF	OFF	OFF	OFF	OFF
LPOM-P	"LPOM P, mg/m^3 "	ON	(F10.3)	1	0.0005	0.0005	0.0005	0.0005	0.0005	ON	ON	ON	ON	ON	OFF	OFF	OFF	OFF	OFF
RPOM-P	"RPOM P, mg/m^3 "	ON	(F10.3)	1	0.0005	0.0005	0.0005	0.0005	0.0005	ON	ON	ON	ON	ON	OFF	OFF	OFF	OFF	OFF
LDOM-N	"LDOM N, mg/m^3 "	ON	(F10.3)	1	0.06	0.06	0.06	0.06	0.06	ON	ON	ON	ON	ON	OFF	OFF	OFF	OFF	OFF
RDOM-N	"RDOM N, mg/m^3 "	ON	(F10.3)	1	0.06	0.06	0.06	0.06	0.06	ON	ON	ON	ON	ON	OFF	OFF	OFF	OFF	OFF
LPOM-N	"LPOM N, mg/m^3 "	ON	(F10.3)	1	0.01	0.01	0.01	0.01	0.01	ON	ON	ON	ON	ON	OFF	OFF	OFF	OFF	OFF
RPOM-N	"RPOM N, mg/m^3 "	ON	(F10.3)	1	0.01	0.01	0.01	0.01	0.01	ON	ON	ON	ON	ON	OFF	OFF	OFF	OFF	OFF
MICROCYSTIN	"Microcystin, g/m^3"	OFF	(g10.3)	1	0	0	0	0	0	OFF	OFF	OFF	OFF	OFF	OFF	OFF	OFF	OFF	OFF
CYLINDROSPERM	"Clindrospermopsin, g/m^3"	OFF	(g10.3)	1	0	0	0	0	0	OFF	OFF	OFF	OFF	OFF	OFF	OFF	OFF	OFF	OFF
ANATOXIN-A	"Anatoxin-A, g/m^3"	OFF	(g10.3)	1	0	0	0	0	0	OFF	OFF	OFF	OFF	OFF	OFF	OFF	OFF	OFF	OFF
SAXITOXIN	"Saxitoxin, g/m^3"	OFF	(g10.3)	1	0	0	0	0	0	OFF	OFF	OFF	OFF	OFF	OFF	OFF	OFF	OFF	OFF
Hg0	"Hg0, ng/L"	ON	(f10.4)	1	0.05	0.05	0.05	0.05	0.05	ON	ON	ON	ON	ON	ON	ON	ON	ON	ON
HgII_total	"HgII total, ng/L"	ON	(f10.4)	1	5	5	5	5	5	ON	ON	ON	ON	ON	ON	ON	ON	ON	ON
MeHg_total	"MeHg total, ng/L"	ON	(f10.4)	1	0.1	0.1	0.1	0.1	0.1	ON	ON	ON	ON	ON	OFF	OFF	OFF	OFF	OFF

4. If atmospheric deposition is used, make sure this is turned ON in the control file w2_con.csv.

	AtmDep				
ATMOSPHERIC DEPOSITION	WB1	WB2	WB3	WB4	WB5
Atm_DepositionC - turn ON/OFF mass loading (kg/km2/year) for each water body	ON	ON	ON	ON	ON
Atm_Deposition_Interpolation - Interpolate between values ON/OFF	ON	ON	ON	ON	ON

5. KDO (half-saturation concentration of DO required for oxic decomposition) is now a function of waterbody and new variable AANOX (fraction of aerobic decay rate). These are variables that affect methylation and demethylation.

SED CO2	WB1	WB2	WB3	WB4	WB5
CO2R Sediment carbon dioxide release rate, fraction of sediment oxygen demand	0.5	0.5	0.5	0.5	0.5
	O2LIMIT				
OXYGEN Limit	WB1	WB2	WB3	WB4	WB5
O2 LIMIT KDO, Dissolved oxygen half-saturation constant or concentration at which	0.2	0.2	0.2	0.2	0.2
AANOX, ratio of anoxic to oxic carbon decomposition rate (0 - 1)	0.1	0.1	0.1	0.1	0.1
	SODRATES				

6. In the tab w2_Hg.csv, adjust model coefficients for Hg. Make sure you select the output file and click the button for exporting this file. This file is described in the next section.

Input file: w2_Hg.csv

This is located in the Excel spreadsheet under the tab by that name as shown below:

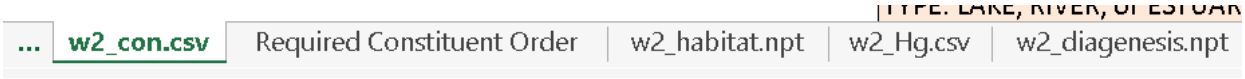

This file contains the following input variables which are described in this report.

Global				
"Model sediment processes of HgII, MeHg below the water body"	.TRUE.			.TRUE. or .FALSE.
"Model HgII and MeHg partitioning on DOC for equilibrium (1) or non-equilibrium (2)"	1	1		Set equal to 1 for activation, 0 to turn OFF
"Model HgII and MeHg partitioning on POM for equilibrium (1) or non-equilibrium (2)"	1	1		Set equal to 1 for activation, 0 to turn OFF
"Model HgII and MeHg partitioning on ISS (1 to NSS) for equilibrium (1) or non-equilibrium (2)"	1	1		Set equal to 1 for activation, 0 to turn OFF
"Model HgII and MeHg equilibrium partitioning on algae (1 to NAL)"	1	1		Set equal to 1 for activation, 0 to turn OFF
"Model HgII and MeHg equilibrium partitioning on zooplankton (1 to NZP)"	1	1		
"Number of regions for Hg parameters"	2			Set equal to 1 for activation, 0 to turn OFF
"Starting segment for regions"	1	120		
"Ending segment for regions"	120	239		
Water_Column	Region 1	Region 2	Region 3	Region 4
"Air concentration of Hg0 (ng/L)"	0.0015	0.0015		
"Hg0 volatilization velocity definded by user, m/d"	1.5	1.5		1.5 to 2.8 m/day
"Hg0 volatilization velocity temperature correction coefficient"	1.024	1.024		
"Hg0 photo-oxidation rate constant 1"	0.00188	0.00188		
"Hg0 photo-oxidation rate constant 2"	-0.73385	-0.73385		
"Hg0 photo-oxidation rate constant 3"	2.0409	2.0409		
"HgII molecular weight, g/mol"	271.52			
"HgII equilibrium partition coefficient for DOC, L/kg"	4.00E+05	4.00E+05		100000
"HgII equilibrium partition coefficient for POM, L/kg"	1.00E+05	1.00E+05		

"HgII equilibrium partition coefficient for ISS, L/kg, ISS group #1"	1.00E+04	1.00E+04		1000 for sand up to 100000 (silt)
"HgII equilibrium partition coefficient for ISS, L/kg, ISS group #2"	1.00E+04	1.00E+04		If more than 5 ISS groups add lines
"HgII equilibrium partition coefficient for ISS, L/kg, ISS group #3"				
"HgII equilibrium partition coefficient for ISS, L/kg, ISS group #4"				
"HgII equilibrium partition coefficient for ISS, L/kg, ISS group #5"				
"HgII equilibrium partition coefficient for algae, L/kg, NAL group #1"	1.00E+05	1.00E+05		If more than 5 Algae groups add lines
"HgII equilibrium partition coefficient for algae, L/kg, NAL group #2"	1.00E+05	1.00E+05		
"HgII equilibrium partition coefficient for algae, L/kg, NAL group #3"	1.00E+05	1.00E+05		
"HgII equilibrium partition coefficient for algae, L/kg, NAL group #4"				
"HgII equilibrium partition coefficient for algae, L/kg, NAL group #5"				
"HgII equilibrium partition coefficient for zooplankton, L/kg, Zoo group #1"	250000	250000		
"HgII equilibrium partition coefficient for zooplankton, L/kg, Zoo group #2"				
"HgII equilibrium partition coefficient for zooplankton, L/kg, Zoo group #3"				
"HgII equilibrium partition coefficient for zooplankton, L/kg, Zoo group #4"				
"HgII equilibrium partition coefficient for zooplankton, L/kg, Zoo group #5"				
"HgII photoreduction rate for dissolved phase, m2/W/d"	0.003	0.003		
"HgII photoreduction rate for DOC complexed phase, m2/W/d"	0.003	0.003		
"HgII methylation rate for dissolved phase, m3/gC"	10	10		
"HgII methylation rate for DOC complexed phase, m3/gC"	0.1	0.1		0
"HgII sediment-water mass transfer velocity or release rate, cm/d or (ng/L/d/g-O2)" If a minus value, the model uses this as a multiplier using the sediment diagenesis rate, i.e., ABS(HGIITransferVelocity)*SedimentDiageneis computed velocity. Hence a "-1.2" would be 1.2 X the predicted sediment diagenesis transfer velocity.	0.03	0.03		3E-6 to 0.03 cm/d range

"MeHg molecular weight, g/mol"	230.66	230.66		
"MeHg equilibrium partition coefficient for DOC, L/kg"	4.00E+05	4.00E+05		200000
"MeHg equilibrium partition coefficient for POM, L/kg"	1.00E+05	1.00E+05		
"MeHg equilibrium partition coefficient for ISS, L/kg, ISS group 1"	1.00E+04	1.00E+04		100 for sand up to 1e6 (silt)
"MeHg equilibrium partition coefficient for ISS, L/kg, ISS group 2"				100 for sand up to 1e6 (silt)
"MeHg equilibrium partition coefficient for ISS, L/kg, ISS group 3"				If more than 5 ISS groups add more lines
"MeHg equilibrium partition coefficient for ISS, L/kg, ISS group 4"				
"MeHg equilibrium partition coefficient for ISS, L/kg, ISS group 5"				
"MeHg equilibrium partition coefficient for algae, L/kg, ALG group 1"	1.00E+05	1.00E+05		
"MeHg equilibrium partition coefficient for algae, L/kg, ALG group 2"	1.00E+05	1.00E+05		
"MeHg equilibrium partition coefficient for algae, L/kg, ALG group 3"	1.00E+05	1.00E+05		If more than 5 NAL add more lines
"MeHg equilibrium partition coefficient for algae, L/kg, ALG group 4"				
"MeHg equilibrium partition coefficient for algae, L/kg, ALG group 5"				
"MeHg equilibrium partition coefficient for zooplankton, L/kg, Zoo group 1"	250000	250000		
"MeHg equilibrium partition coefficient for zooplankton, L/kg, Zoo group 2"				
"MeHg equilibrium partition coefficient for zooplankton, L/kg, Zoo group 3"				
"MeHg equilibrium partition coefficient for zooplankton, L/kg, Zoo group 4"				
"MeHg equilibrium partition coefficient for zooplankton, L/kg, Zoo group 5"				
"MeHg photo-degradation rate for dissolved phase, m2/W/d"	0.01	0.01		
"MeHg photo-degradation rate for DOC complexed phase, m2/W/d"	0.01	0.01		
"MeHg demethylation rate from dissolved phase, m3/gC"	0.1	0.1		
"MeHg demethylation rate from DOC complexed phase, m3/gC"	0.1	0.1		
"MeHg sediment-water mass transfer velocity or release rate, cm/d or (ng/L/d/g-O2)" If a minus value, the model uses this as a multiplier using the sediment diagenesis rate, i.e.,	0.01	0.01		3E-6 to 0.03 cm/d range

ABS(MEHGTransferVelocity)*SedimentDiageneis computed velocity. Hence a "-1.2" would be 1.2 X the predicted sediment diagenesis transfer velocity.				
"MethDemethC: 1: use C turnover rate (units:m3/gC); 2: use fixed rate (units:1/d)" If the value is "1" – both the water column and sediment use a C turnover based rate. If "2", they are decoupled from C turnover rates.	2	2		Applies to sediment also
"Methylation Q10 if MethDemethC ==2" This is the temperature dependence in the water column and sediment if Meth/Demth are not based on C turnover.	1.2	1.2		Applies to sediment also
"Demethylation Q10 if MethDemethC==2" This is the temperature dependence in the water column and sediment if Meth/Demth are not based on C turnover.	1.4	1.4		Applies to sediment also
Sediment_Layer	Region 1	Region 2	Region 3	Region 4
"Use user-defined sediment burial velocity"	.FALSE.			
"Sediment burial velocity, m/d"	1.00E-04	1.00E-04		
"Active sediment layer thickness, m"	0.1	0.1		
"Sediment porosity"	0.8	0.8		
"Sediment dry density, g/cm3"	2.7	2.7		
"HgII equilibrium partition coefficient for DOC, L/kg"	4.00E+05	4.00E+05		
"HgII equilibrium partition coefficient for POM, L/kg"	1.00E+05	1.00E+05		
"HgII equilibrium partition coefficient for ISS, L/kg, ISS group #1"	1.00E+05	1.00E+05		Add more lines if NSS > 5
"HgII equilibrium partition coefficient for ISS, L/kg, ISS group #2"	1.00E+05	1.00E+05		
"HgII equilibrium partition coefficient for ISS, L/kg, ISS group #3"				
"HgII equilibrium partition coefficient for ISS, L/kg, ISS group #4"				
"HgII equilibrium partition coefficient for ISS, L/kg, ISS group #5"				
"HgII methylation rate for dissolved phase, m3/gC"	20	20		
"HgII methylation rate for DOC complexed phase, m3/gC"	0	0		
"MeHg equilibrium partition coefficient for DOC, L/kg"	4.00E+05	4.00E+05		
"MeHg equilibrium partition coefficient for POM, L/kg"	1.00E+05	1.00E+05		
"MeHg equilibrium partition coefficient for ISS, L/kg ISS group#1"	1.00E+05	1.00E+05		Add more lines if NSS>5
"MeHg equilibrium partition coefficient for ISS, L/kg ISS group#2"	1.00E+05	1.00E+05		

"MeHg equilibrium partition coefficient for ISS, L/kg ISS group#3"				
"MeHg equilibrium partition coefficient for ISS, L/kg ISS group#4"				
"MeHg equilibrium partition coefficient for ISS, L/kg ISS group#5"				
"MeHg demethylation rate from dissolved phase, m3/gC or 1/day". The choice of units is based on specifying MethDemethC. If =1, then units are m3/gC. If =2 then units are 1/day.	1	1		
"MeHg demethylation rate from DOC complexed phase, m3/gC or 1/day". The choice of units is based on specifying MethDemethC. If =1, then units are m3/gC. If =2 then units are 1/day.	0	0		
Sediment_Initial_Conditions	Region 1	Region 2	Region 3	Region 4
"Number of regions for initial conditions"	2			
"Starting segment for initial conditions"	1	67		
"Ending segment for initial conditions"	66	239		
"Sediment concentration of total HgII ng/L"	200	1000		
"Sediment concentration of total MeHg ng/L"	100	200		
"Sediment concentration of ISS, mg/L, ISS group #1"	100	1000		Add more lines if NSS>5
"Sediment concentration of ISS, mg/L, ISS group #2"	100	1000		
"Sediment concentration of ISS, mg/L, ISS group #3"				
"Sediment concentration of ISS, mg/L, ISS group #4"				
"Sediment concentration of ISS, mg/L, ISS group #5"				
Sediment flux output file	Region 1	Region 2	Region 3	Region 4
"Number of regions for sediment fluxes"	4			
"Time interval for fluxes in days"	30			
"Starting segment for sediment flux output"	1	67	91	140
"Ending segment for sediment flux output"	66	90	139	239

Output Files Produced by the Hg Model

Flux output files for Hg processes include the time series files, flux output files, and spreadsheet profile files. In addition, the Hg variables are part of the W2_Post post-processor for visualizing contours, animations, profiles, and time series.

Time series files for water column and Hg sediment bed

These files are turned ON when a tsr file is defined in the main control file w2_con.csv. Hence, if the tsr file for the water column was ***tsr_37_seg154.csv***, then there would be 2 additional files produced: ***tsr_37_seg154_BedHg.csv*** (for the sediment bed) and ***tsr_37_seg154_Hg.csv*** (for the water column). See the CE-QUAL-W2 User Manual (Wells, 2024) on how to turn ON the tsr file output.

Output for the water column includes the following (instantaneous values):

JDAY
HgIId(ng/L)
HgIIdoc(ng/L)
HgIIpom(ng/L)
HgIIp1(ng/L)
HgIIp2(ng/L)
HgIIap1(ng/L)
HgIIap2(ng/L)
HgIIap3(ng/L)
HgIIzp1(ng/L)
HgIIpt(ng/L)
HgIIpts(ng/g)
MeHgd(ng/L)
MeHgdoc(ng/L)
MeHgpom(ng/L)
MeHgp1(ng/L)
MeHgp2(ng/L)
MeHgap1(ng/L)
MeHgap2(ng/L)
MeHgap3(ng/L)
MeHgzp1(ng/L)
MeHgpt(ng/L)
MeHgpts(ng/g)
THg(ng/L)
Hg0 volatilization(ng/L/d)
Hg0 oxidation(ng/L/d)
HgII reduction(ng/L/d)
HgII methylation(ng/L/d)
HgII settling(ng/L/d)
HgII sediment transfer(ng/L/d)
MeHg degradation(ng/L/d)
MeHg demethylation(ng/L/d)

MeHg settling(ng/L/d)
MeHg sediment transfer(ng/L/d)
JOC(gC/m3/d)

Output for the sediment bed includes the following (instantaneous values):

JDAY
BedHgII(ng/L)
BedHgIId(ng/L)
BedHgIIdoc(ng/L)
BedHgIIpom(ng/L)
BedHgIIp1(ng/L)
BedHgIIp2(ng/L)
BedHgIIpt(ng/L)
BedHgIIpts(ng/g)
BedMeHg(ng/L)
BedMeHgd(ng/L)
BedMeHgdoc(ng/L)
BedMeHgpom(ng/L)
BedMeHgp1(ng/L)
BedMeHgp2(ng/L)
BedMeHgpt(ng/L)
BedMeHgpts(ng/g)
BedTHg(ng/L)
BedISS1(mg/L)
BedISS2(mg/L)
BedHgII methylation(ng/L/d)
BedHgII burial(ng/L/d)
BedHgII settling accumulation(
BedMeHg demethylation(ng/L/d)
BedMeHg burial(ng/L/d)
BedMeHg settling accumulation(
JOC2(gC/m3/d)

Also, the original tsr file includes the Hg0, HgII, and MeHg concentrations and all derived variables that are active. Those that can be activated are:

PHgIIw "Particulate HgII-w, ng/L"
PHgIIs "Particulate HgII-s, ng/g"
PMeHgw "Particulate MeHg-w, ng/L"
PMeHgs "Particulate MeHg-s, ng/g"
DissHgII "Dissolved HgII + HgIIDOC, ng/L"
DissMeHg "Dissolved MeHg + MeHgDOC, ng/L"
HgIIAlgTot "HgII on all algae, ng/L"
HgIIZooTot "HgII on all zooplankton, ng/L"

HgIIISSTot "HgII on all inorganic SS, ng/L"
HgIIPOMTot "HgII on all POM, ng/L"
Methylation "Methylation rate, ng/L/d"
Demethylation "Demethylation rate, ng/L/d"
MeHgAlgTot "MeHg on all algae, ng/L"
MeHgZooTot "MeHg on all zooplankton, ng/L"
MeHgISSTot "MeHg on all inorganic SS, ng/L"
MeHgPOMTot "MeHg on all POM, ng/L"
JOC "C turnover rate, gC/m3/d'

Spreadsheet output file

The spreadsheet output file is described in the CE-QUAL-W2 User Manual (Wells, 2024). This file includes profiles of all model state variables including Hg0, HgII, and MeHg as well as profiles of the Hg fluxes and JOC (the C turnover used in the methylation rate equation) for the water column and sediment bed.

For the water column, besides Hg0, HgII, and MeHg, the fluxes include:

Hg0 volatilization(ng/L/d)
Hg0 oxidation(ng/L/d)
HgII reduction(ng/L/d)
HgII methylation(ng/L/d)
HgII settling(ng/L/d)
HgII sediment transfer(ng/L/d)
MeHg degradation(ng/L/d)
MeHg demethylation(ng/L/d)
MeHg settling(ng/L/d)
MeHg sediment transfer(ng/L/d)
MeHg sediment transfer(ng/L/d)
JOC(gC/m3/d)

For the sediment bed, besides HgII, and MeHg, the fluxes include:

BedHgII methylation(ng/L/d)
BedHgII burial(ng/L/d)
BedHgII settling accumulation(
BedMeHg demethylation(ng/L/d)
BedMeHg burial(ng/L/d)
BedMeHg settling accumulation(ng/L/d)
JOC2(gC/m3/d)

Flux File Output

If Flux Output is On in the main control file, w2_con.csv, then Hg flux rates are output in a file that includes average flux rates over time period defined in the input file. Specification of these fluxes is made in the W2_Hg.csv file under sediment fluxes.

Withdrawal Output Files

If the withdrawal output (WDO) file is specified in the main control file, all Hg state variables (Hg0, HgII, and MeHg) are written out for any withdrawal as well as all derived variables that are ON. These currently include:

PHgIIw "Particulate HgII-w, ng/L"
PHgIIs "Particulate HgII-s, ng/g"
PMeHgw "Particulate MeHg-w, ng/L"
PMeHgs "Particulate MeHg-s, ng/g"
DissHgII "Dissolved HgII + HgIIDOC, ng/L"
DissMeHg "Dissolved MeHg + MeHgDOC, ng/L"
HgIIAlgTot "HgII on all algae, ng/L"
HgIIZooTot "HgII on all zooplankton, ng/L"
HgIIISSTot "HgII on all inorganic SS, ng/L"
HgIIPOMTot "HgII on all POM, ng/L"
Methylation "Methylation rate, ng/L/d"
Demethylation "Demethylation rate, ng/L/d"
MeHgAlgTot "MeHg on all algae, ng/L"
MeHgZooTot "MeHg on all zooplankton, ng/L"
MeHgISSTot "MeHg on all inorganic SS, ng/L"
MeHgPOMTot "MeHg on all POM, ng/L"
JOC "C turnover rate, gC/m3/d'

Appendix B: Non-equilibrium Partitioning

A future addition to this model may include non-equilibrium sorption of *HgII* onto organic and inorganic solids in the water column and active sediment layer is included in the Hg module. Under non-equilibrium partitioning, the concentrations of dissolved and adsorbed phases of *HgII* are simulated separately.

Water Column:

Three state variables are simulated for *HgII* species in the water column:

- $HgII_d$, concentration of dissolved HgII in water (ng L^{-1})
- $HgII_{pom2}$, kinetic (strongly bound) concentration of organic solid adsorbed HgII in water (ng L^{-1})
- $HgII_{pn2}$, kinetic (strongly bound) concentration of inorganic solid "n" adsorbed HgII in water (ng L^{-1}) (n = 1 to NSS)

Note: Both boundary and initial conditions of concentrations of above state variables ($HgII_d$, $HgII_{pom2}$ and $HgII_{pn2}$) are required.

Organic and inorganic solids attached *HgII* are simulated with two sites: exchangeable (fast) and kinetic (rate-limited) kinetics. The concentration of attached *HgII* consists of an exchangeable (fast) sorption and the other associated with kinetic (rate-limited) sorption rate constraint parts.

$$[HgII_{pom}] = [HgII_{pom1}] + [HgII_{pom2}] \quad (2.1a)$$

$$[HgII_p] = \sum_1^{NSS}\{[HgII_{pn1}] + [HgII_{pn2}]\} \quad (2.1b)$$

1) POM attached component of *HgII*:

Using the linear isotherm previously described, exchangeable concentration of organic solid adsorbed HgII in water is determined by:

$$[HgII_{pom1}] = 10^{-6} f_{pom} K_{pom-HgII} [POM][HgII_d] \quad (2.2)$$

Where

f_{pom} is the fraction of exchange sites on organic solids assumed to be at equilibrium.

The source and sink rate equation for the POM attached kinetic component is stated as:

$$\frac{d[HgII_{pom2}]}{dt} = -\underbrace{\frac{dHgII_{pom2}}{dz}}_{settling} + \underbrace{\frac{dHgII_{pom2}}{dt}}_{sorption} \quad (2.3)$$

Where

$$\underbrace{\frac{dHgII_{pom2}}{dt}}_{sorption} = k_{ads}\left(\frac{HgII_{pom1}}{f_{pom}} - \frac{HgII_{pom2}}{(1-f_{pom})}\right) \quad for \quad \frac{HgII_{pom1}}{f_{pom}} > \frac{HgII_{pom2}}{(1-f_{pom})} \quad (2.4a)$$

$$\underbrace{\frac{dHgII_{pom2}}{dt}}_{sorption} = k_{des}\left(\frac{HgII_{pom1}}{f_{pom}} - \frac{HgII_{pom2}}{(1-f_{pom})}\right) \quad for \quad \frac{HgII_{pom1}}{f_{pom}} < \frac{HgII_{pom2}}{(1-f_{pom})} \quad (2.4b)$$

2) Inorganic solids attached component of *HgII*:

Exchangeable concentration of inorganic solid group n adsorbed HgII in water

$$[HgII_{pn1}] = 10^{-6} f_{pn} K_{pn-HgII} [ISS_n] \quad (2.5)$$

Where f_{pn} is the fraction of exchange sites on inorganic solid group n assumed to be at equilibrium.

The source and sink rate equation for the inorganic solid group n attached kinetic component:

$$\frac{d[HgII_{pn2}]}{dt} = -\underbrace{\frac{dHgII_{pn2}}{dz}}_{settling} + \underbrace{\frac{dHgII_{pn2}}{dt}}_{sorption} \quad (2.6)$$

where

$$\underbrace{\frac{dHgII_{pn2}}{dt}}_{sorption} = k_{ads}\left(\frac{HgII_{pn1}}{f_{pn}} - \frac{HgII_{pn2}}{(1-f_{pn})}\right) \quad for \quad \frac{HgII_{pn1}}{f_{pn}} > \frac{HgII_{pn2}}{(1-f_{pn})} \quad (2.7a)$$

$$\underbrace{\frac{dHgII_{pn2}}{dt}}_{sorption} = k_{des}\left(\frac{HgII_{pn1}}{f_{pn}} - \frac{HgII_{pn2}}{(1-f_{pn})}\right) \quad for \quad \frac{HgII_{pom1}}{f_{pn}} < \frac{HgII_{pn2}}{(1-f_{pn})} \quad (2.7b)$$

3) Dissolved phase, DOC complexed and algae attached phase of *HgII*:

$$R\ \frac{d[HgII_d]}{dt} = -\underbrace{HgII \rightarrow Hg0}_{\text{photoreduction}} + \underbrace{Hg0 \rightarrow HgII}_{\text{photo-oxidation}} - \underbrace{HgII \rightarrow MeHg}_{\text{methylation}} + \underbrace{MeHg \rightarrow HgII}_{\text{demethyation}} + \underbrace{HgII \leftrightarrow Bed}_{\text{diffusion}} - \underbrace{\frac{dHgII_{ap}}{dz}}_{settling} - \underbrace{\frac{dHgII_{pom1}}{dz}}_{settling} - \sum_1^N \underbrace{\frac{dHgII_{pn1}}{dz}}_{settling} - \underbrace{\frac{dHgII_{pom2}}{dt}}_{sorption} - \sum_1^N \underbrace{\frac{dHgII_{pn2}}{dt}}_{sorption} \quad (2.8)$$

$$R = 1 + 10^{-6}\sum_{n=1}^{NAL} K_{apn-HgII}[A_{pn}] + 10^{-6}K_{doc-HgII}[DOC] + 10^{-6}f_{pom}K_{pom-HgII}[POM] + \sum_{n=1}^{NSS} 10^{-6}f_{pn}K_{pn-HgII}[ISS_n] \quad (2.9)$$

Eq. 2.3, 2.6, and 2.8 will be solved to get $HgII_d$, $HgII_{pom2}$, $HgII_{pn2}$.

The concentration of the total (unfiltered) HgII in the water column is

$$[HgII] = R[HgII_d] + [HgII_{pom2}] + \sum_1^{NSS}[HgII_{pn2}] \quad (2.10)$$

Active Sediment Layer

Three state variables are simulated for *HgII* species in the active sediment layer:

- $HgII2_d$, concentration of dissolved HgII in porewater (ng L^{-1})
- $HgII2_{pom2}$, kinetic (slow) concentration of organic solid adsorbed HgII in sediment (ng L^{-1})
- $HgII2_{pn2}$, kinetic (slow) concentration of inorganic solid "n" adsorbed HgII in water (ng L^{-1}) (n = 1 to N)

Note: Only initial conditions of concentrations of above state variables ($HgII2_d$, $HgII2_{pom2}$ and $HgII2_{pn2}$) are required for the active sediment layer.

1) POM attached kinetic component of *HgII*:

$$\frac{d[HgII2_{pom2}]}{dt} = \underbrace{\frac{dHgII}{dz}}_{deposition} - \underbrace{\frac{dHgII2_{pom2}}{dz}}_{burial} + \underbrace{\frac{dHgII2_{pom2}}{dt}}_{sorption} \quad (2.11)$$

Where

$$\underbrace{\frac{dHgII2_{pom2}}{dt}}_{sorption} = k_{ads}\left(\frac{HgII2_{pom1}}{f_{pom}} - \frac{HgII2_{pom2}}{(1-f_{pom})}\right) \quad for \quad \frac{HgII2_{pom1}}{f_{pom}} > \frac{HgII2_{pom2}}{(1-f_{pom})}$$

(2.12a)

$$\underbrace{\frac{dHgII2_{pom2}}{dt}}_{sorption} = k_{des}\left(\frac{HgII2_{pom1}}{f_{pom}} - \frac{HgII2_{pom2}}{(1-f_{pom})}\right) \quad for \quad \frac{HgII2_{pom1}}{f_{pom}} < \frac{HgII2_{pom2}}{(1-f_{pom})}$$

(2.12b)

2) inorganic solids attached *HgII*:

$$\frac{d[HgII2_{pn2}]}{dt} = \underbrace{\frac{dHgII}{dz}}_{deposition} - \underbrace{\frac{dHgII2_{pn2}}{dz}}_{burial} + \underbrace{\frac{dHgII2_{pn2}}{dt}}_{sorption} \qquad (2.13)$$

where

$$\underbrace{\frac{dHgII2_{pn2}}{dt}}_{sorption} = k_{ads}\left(\frac{HgII2_{pn1}}{f_{pn}} - \frac{HgII2_{pn2}}{(1-f_{pn})}\right) \quad for \quad \frac{HgII2_{pn1}}{f_{pn}} > \frac{HgII2_{pn2}}{(1-f_{pn})} \qquad (2.14a)$$

$$\underbrace{\frac{dHgII2_{pn2}}{dt}}_{sorption} = k_{des}\left(\frac{HgII2_{pn1}}{f_{pn}} - \frac{HgII2_{pn2}}{(1-f_{pn})}\right) \quad for \quad \frac{HgII2_{pn1}}{f_{pn}} < \frac{HgII2_{pn2}}{(1-f_{pn})} \qquad (2.14b)$$

3) dissolved phase of *HgII*:

$$R2\frac{d\,[HgII2_d]}{dt} = \underbrace{MeHg2 \rightarrow HgII2}_{\text{demethyation}} - \underbrace{HgII2 \rightarrow MeHg2}_{\text{methylation}} - -\underbrace{HgII \leftrightarrow HgII2}_{diffusion} + \underbrace{\frac{dHgII_{ap}}{dz}}_{deposition} +$$

$$\underbrace{\frac{dHgII_{pom1}}{dz}}_{deposition} + \sum_1^N \underbrace{\frac{dHgII_{pn1}}{dz}}_{deposition} - \underbrace{\frac{dHgII_{2pom2}}{dt}}_{sorption} - \sum_1^N \underbrace{\frac{dHgII2_{pn2}}{dt}}_{sorption} \qquad (2.15)$$

$$R2 = 1 + 10^{-6}K_{doc\text{-}HgII}[DOC2] + 10^{-6}f_{pom}K_{pom-HgII}[POM2] + \sum_{n=1}^{NSS} 10^{-6}f_{pn}K_{pn-HgII}[ISS2_n]$$

(2.16)

The concentration of the total (unfiltered) HgII in the active sediment layer is

$$[HgII2] = R2[HgII_{2d}] + +\left[HgII2_{pom2}\right] + \sum_{1}^{NSS}\left[HgII2_{pn2}\right] \quad (2.17)$$

Appendix C – Vertical Profiles of HgII and MeHg in Brownlee, Oxbow, and Hells Canyon Reservoirs

-see Appendix C external file